UNIVERSIDADE FEDERAL DE SANTA CATARINA
CENTRO TECNOLÓGICO
PROGRAMA DE PÓS-GRADUAÇÃO EM ENGENHARIA DE ALIMENTOS

Maria Jaízia dos Santos Alves

Estabilização de compostos bioativos da própolis usando nanopartículas de amido: uma alternativa para fortificação de balas de gelatina

Florianópolis-SC
2023

Maria Jaízia dos Santos Alves

Estabilização de compostos bioativos da própolis usando nanopartículas de amido: uma alternativa para fortificação de balas de gelatina

Tese submetida ao Programa de Pós-graduação em Engenharia de Alimentos da Universidade Federal de Santa Catarina para obtenção do título de doutora em engenharia de alimentos.
Orientador: Prof. Dr. Germán Ayala Valencia
Coorientador: Profª. Drª. Alcilene Rodrigues Monteiro Fritz

Florianópolis-SC
2023

Ficha de identificação da obra elaborada pelo autor,
através do Programa de Geração Automática da Biblioteca Universitária da UFSC.

Alves, Maria Jaízia dos Santos
Estabilização de compostos bioativos da própolis usando nanopartículas de amido: uma alternativa para fortificação de balas de gelatina / Maria Jaízia dos Santos Alves ; orientador, Germán Ayala Valencia, coorientadora, Alcilene Rodrigues Monteiro Fritz, 2023.
171 p.

Tese (doutorado) - Universidade Federal de Santa Catarina, Centro Tecnológico, Programa de Pós-Graduação em Engenharia de Alimentos, Florianópolis, 2023.

Inclui referências.

1. Engenharia de Alimentos. 2. Compostos bioativos. 3. Nanopartículas. 4. Amidos. 5. Balas funcionais. I. Valencia, Germán Ayala. II. Fritz, Alcilene Rodrigues Monteiro. III. Universidade Federal de Santa Catarina. Programa de Pós-Graduação em Engenharia de Alimentos. IV. Título.

Maria Jaízia dos Santos Alves

Estabilização de compostos bioativos da própolis usando nanopartículas de amido: uma alternativa para fortificação de balas de gelatina

O presente trabalho em nível de Doutorado foi avaliado e aprovado, em 25 de agosto de 2023, pela banca examinadora composta pelos seguintes membros:

Prof.ª Izabel Cristina Freitas Moraes, Drª
USP

Prof. Cristiano José de Andrade , Dr.
UFSC

Prof. Marcelo Lanza, Dr.
UFSC

Certificamos que esta é a versão original e final do trabalho de conclusão que foi julgado adequado para obtenção do título de Doutora em Engenharia de Alimentos.

Documento assinado digitalmente
Jaciane Lutz Ienczak
Data: 20/11/2023 14:40:01-0300
CPF: ***.280.630-**
Verifique as assinaturas em https://v.ufsc.br

Coordenação do Programa de Pós-Graduação

Documento assinado digitalmente
German Ayala Valencia
Data: 16/11/2023 19:48:03-0300
CPF: ***.731.718-**
Verifique as assinaturas em https://v.ufsc.br

Prof. Germán Ayala Valencia, Dr.
Orientador

Florianópolis, 2023.

Dedico este trabalho inteiramente à minha amada família.

Muito obrigada

AGRADECIMENTOS

Agradeço a Deus pelo seu imenso amor, por me sustentar em todos os momentos de fraqueza, desespero e angústia, e me conduzir até aqui. Agradeço pelo dom da vida, pelas bênçãos e vitórias recebidas.

Aos meus pais, pelo amor incondicional, carinho, compreensão, por serem meus maiores exemplos de força, determinação e fé. Agradeço por estarem ao meu lado em todos os momentos, sobretudo, nos momentos difíceis, por me ajudar e incentivar sempre. Sem vocês na minha vida... nos meus dias, eu não conseguiria! Muito obrigada!

Ao meu irmão, Genilson, por ser simplesmente o meu tudo! Obrigada por me apoiar e me incentivar a ir sempre mais longe.

Ao meu namorado, por todo o seu amor, apoio, companheirismo, compreensão e paciência ao longo desta longa caminhada. Por estar sempre ao meu lado me ajudando a vencer os obstáculos ao longo desse caminho. Meu anjo, sempre!

Ao meu orientador, professor Germán Ayala Valencia, pelo apoio ao longo da construção deste trabalho, pela confiança e por seus ensinamentos que foram essenciais para o meu crescimento profissional. Você é inspiração, exemplo de professor e de ser humano.

Agradeço à Professora Alcilene R Monteiro pela orientação, paciência, disponibilidade e a gentileza em ensinar e, por todas as contribuições dadas ao longo do trabalho.

Aos queridos amigos do LIEB e PROFI, agradeço por toda a colaboração e ajuda recebida, pela amizade e descontração na rotina do laboratório. Vocês tornaram essa caminhada menos dolorosa.

À Jussara, Alexandre, Pedro, meus queridos IC's, obrigada pela dedicação e empenho no trabalho, e por fazer parte desta história.

Agradeço a UFSC e ao PPGEAL por essa grande oportunidade, e a CAPES e CNPq pelo suporte financeiro.

E a todos aqueles, que de alguma forma contribuíram para que este sonho fosse concretizado, os meus sinceros agradecimentos.

It's not that I'm so smart, it's just that I stay with problems longer.

Albert Einstein

RESUMO

A própolis é uma resina natural constituída de diversos compostos e elevada concentração em polifenóis com propriedades benéficas à saúde, como a atividade antioxidante e antimicrobiana. No entanto, sua aplicação em produtos alimentícios é limitada devido à sua baixa solubilidade em água e baixa biodisponibilidade. Nesse sentido, a estabilização de compostos bioativos da própolis pela técnica de nanoprecipitação antissolvente usando amidos como material de parede surge como alternativa para preservar as propriedades bioativas, aumentar a hidrossolubilidade, e minimizar os efeitos sensoriais negativos. Assim, este trabalho teve como objetivo produzir nanopartículas de amido com cristalinidade do tipo A (amido de mandioca) e do tipo B (amido de batata) para estabilizar os compostos bioativos da própolis, utilizando a técnica de nanoprecipitação antissolvente, bem como caracterizar as propriedades físico-químicas das nanopartículas e aplicá-las em alimentos usando balas de gelatina como modelo. Para alcançar o objetivo, a pesquisa foi realizada em etapas conforme apresentado a seguir. **Capítulo três:** as nanopartículas de amido de batata e de mandioca foram produzidas a partir de diferentes concentrações de etanol/água; **capítulo quatro:** extratos de própolis (EP) marrom foram produzidos em diferentes concentrações de etanol/água homogeneizado em banho ultrassônico, e caracterizados quanto ao conteúdo de fenólicos totais e atividade antioxidante (ABTS, DPPH). Adicionalmente, estudou-se a estabilização dos compostos bioativos da própolis em nanopartículas de amido, o efeito da concentração da fase orgânica nas propriedades físico-químicas das nanopartículas de amido/própolis produzidas por nanoprecipitação antissolvente. O EP marrom na concentração de etanol/água (96:04, v/v) foi o que apresentou maior concentração de compostos fenólicos (27,63±1,17). As nanopartículas foram caracterizadas quanto a morfologia, propriedades térmicas, físico-química e funcionais. Os resultados mostraram que as nanopartículas obtidas apresentaram distribuição bimodal com tamanho de partícula inferior a 600 nm. Além disso, as nanopartículas apresentaram estrutura amorfa e alta solubilidade em água a 30 ºC (S>69%) e a 90 ºC (S>80%). A concentração de etanol utilizada na solução hidroetanólica acidificada afetou a eficiência de recuperação e as propriedades físico-químicas das nanopartículas de amido, como tamanho de partícula e carga superficial. A espectroscopia no infravermelho com transformada de Fourier (FTIR) e a difração de Raios-X (DRX) confirmaram a estabilização do extrato de própolis, com eficiência de estabilização de >54, 91%. Neste capítulo, embora os compostos bioativos da própolis tenham sido estabilizados nos amidos, mas esses nanomateriais não apresentaram atividade antimicrobiana. **Capítulo cinco:** EP verde na concentração de etanol/água (96:04, v/v), a qual apresentou os melhores resultados no capítulo 4, foi utilizada para o estudo da atividade antimicrobiana e estudo de

digestibilidade *in vitro*. O EP apresentou atividade antimicrobiana frente a bactéria Gram-positiva *Litéria monocytogenes* com concentração mínima inibitória (CMI) de 0,5 mg/mL e concentração mínima bactericida (CMB) de 1,0 mg/mL. Já as nanopartículas apresentaram concentração mínima inibitória de variando de 500 mg/mL a 750 mg/mL. Além disso, as nanopartículas apresentaram liberação dos compostos bioativos durante a digestão *in vitro*, com valores para os compostos fenólicos entre 25,48 e 27,71 mg de EAG/g de nanopartículas. **Capítulo seis:** foi realizado a aplicação das nanopartículas de amido carregadas com EP verde na produção de balas à base de gelatina. Nesta etapa, as balas foram analisadas quanto suas propriedades físico-químicas, perfil de textura e estabilidade dos compostos bioativos durante 60 dias de armazenamento. As balas apresentaram estabilidade na cor, nos compostos fenólicos totais, e no perfil de textura durante o armazenamento. A partir dos resultados obtido pode-se concluir que os amidos utilizados como material de parede foram eficazes para estabilizar os compostos bioativos do EP. Essas nanopartículas possuem atividades antimicrobiana e antioxidantes e podem ser utilizadas para fortificação de alimentos, tendo como modelo balas de gelatina.

Palavras-chave: Compostos bioativos. Nanopartículas. Amidos. Balas funcionais

ABSTRACT

Propolis is a natural resin made up of several compounds and a high concentration of polyphenols with beneficial health properties, such as antioxidant and antimicrobial activity. However, its application in food products is limited due to its low water solubility and low bioavailability. In this sense, the stabilization of propolis bioactive compounds by the antisolvent nanoprecipitation technique using starches as a wall material appears as an alternative to preserve the bioactive properties, increase water solubility, and minimize negative sensory effects. Thus, this work aimed to produce starch nanoparticles with crystallinity type A (cassava starch) and type B (potato starch) to stabilize the bioactive compounds of propolis, using the technique of antisolvent nanoprecipitation, as well as to characterize the properties physical-chemical nanoparticles and apply them to food using gelatin candies as a model. To achieve the objective, the research was carried out in stages as shown below. **Chapter three:** potato and cassava starch nanoparticles were produced from different concentrations of ethanol/water; **chapter four:** extracts of brown propolis (EP) were produced in different concentrations of ethanol/water homogenized in an ultrasonic bath and characterized in terms of total phenolic content and antioxidant activity (ABTS, DPPH). Additionally, the stabilization of propolis bioactive compounds in starch nanoparticles, the effect of the concentration of the organic phase on the physicochemical properties of starch/propolis nanoparticles produced by antisolvent nanoprecipitation were studied. The brown EP in the ethanol/water concentration (96:04, v/v) showed the highest concentration of phenolic compounds (27.63±1.17). The nanoparticles were characterized in terms of morphology, thermal, physical-chemical and functional properties. The results showed that the obtained nanoparticles presented a bimodal distribution with a particle size smaller than 600 nm. In addition, the nanoparticles showed an amorphous structure and high solubility in water at 30 ºC (S>69%) and 90 ºC (S>80%). The ethanol concentration used in the acidified hydroethanolic solution affected the recovery efficiency and the physicochemical properties of the starch nanoparticles, such as particle size and surface charge. Fourier Transform Infrared Spectroscopy (FTIR) and X-Ray Diffraction (XRD) confirmed the stabilization of the propolis extract, with a stabilization efficiency of >54.91%. In this chapter, although the bioactive compounds of propolis were stabilized in starches, but these nanomaterials did not show antimicrobial activity. **Chapter five:** Green PE at ethanol/water concentration (96:04, v/v), which showed the best results in chapter 4, was used for the study of antimicrobial activity and in vitro digestibility study. EP showed antimicrobial activity against the Gram-positive bacterium *Literia monocytogenes* with a minimum inhibitory concentration (MIC) of 0.5 mg/mL and a minimum bactericidal

concentration (MBC) of 1.0 mg/mL. The nanoparticles, on the other hand, presented a minimum inhibitory concentration ranging from 500 mg/mL to 750 mg/mL. In addition, the nanoparticles released bioactive compounds during in vitro digestion, with values for phenolic compounds between 25.48 and 27.71 mg of EAG/g of nanoparticles. **Chapter six:** the application of starch nanoparticles loaded with green EP in the production of gelatin-based candies was carried out. At this stage, the candies were analyzed for their physicochemical properties, texture profile and stability of bioactive compounds during 60 days of storage. The candies showed stability in color, total phenolic compounds, and texture profile during storage. From the results obtained, it can be concluded that the starches used as wall material were effective in stabilizing the bioactive compounds of the EP. These nanoparticles have antimicrobial and antioxidant activities and can be used for food fortification, using gelatin candy as a model.

Keywords: Bioactive compounds. Nanoparticles. potato and cassava starches, Functional candies.

LISTA DE FIGURAS

LISTA DE TABELAS

LISTA DE ABREVIATURAS E SIGLAS

ABTS - 2,2′-azino-bis (3-etilbenzotiazolina-6-ácido sulfônico)

AB - Amido de batata

ANOVA - Análise de variância

AM - Amido de mandioca

CFT – Compostos fenólicos totais

DMEM - Dulbecco's Modified Eagle's Medium

DMSO - Dimetilsulfóxido

DMEM - Meio de cultura, do inglês Dulbecco modification of Minimum Essential Media

DPPH - 2,2-difenil-1-picril-hidrazil

DSC - Calorimetria exploratória diferencial

DTA - Térmica Diferencial

EAG - Equivalente em ácido gálico

EC3G - Equivalente de cianidina-3-glicosídeo

EEP - Extrato etanólico da própolis

EP - Extrato de própolis

FTIR - Espectroscopia de infravermelho por transformada de fourier

HPLC-DAD-MS - Cromatografia líquida de alta eficiência acoplada à detecção de arranjo de diodos e espectrometria de massa

LPS - Lipopolissacarídeo

MET - Microscopia Eletrônica de Transmissão

MTT - 3-(4,5 dimetiltiazol-2- il) - 2,5-difenil tetrazol

NPA - Nanopartículas de amido

NMA – Nanomateriais de amido

NPs - Nanopartículas

ST - Sólidos totais

SST - Sólidos solúveis totais

TGA - Análise termogravimétrica

SUMÁRIO

DIAGRAMA CONCEITUAL

O quê?
- Estabilizar os compostos bioativos da própolis pela técnica de nanoprecipitação antissolvente usando amidos, de batata e de mandioca, como material de parede.
Por quê?
- A aplicação de compostos bioativos extraídos da própolis é limitada devido a fatores como baixa estabilidade química e baixa solubilidade em meio aquoso; - A estabilização dos extratos de própolis proporcionará aumento da solubilidade em água, maior estabilidade dos compostos bioativos, possibilitando liberação dos compostos bioativos, e assim melhor eficiência das atividades biológicas; - A nanoprecipitação é uma técnica que visa a proteção, assegurando a estabilidade e liberação de compostos ativos; - O amido é um polissacarídeo abundante, barato, não tóxico, biodegradável e biocompatível, que tem sido amplamente utilizado em diferentes aplicações alimentícias devido a facilidade de obtenção; - Uso em produtos alimentícios.
O que já foi feito?
- Encapsulamento de extrato de própolis por nanoprecipitação usando outros materiais de paredes (quitosana, goma arábica, proteínas do arroz, proteínas da ervilha, proteína da soja, ciclodextrinas, zeína, alginato); - Encapsulamento de extrato de própolis por outras técnicas como spray drying, liofilização, coacervação complexa, gelificação iônica; - Aplicação de extrato da própolis em alimentos como hambúrguer, peixes e em filmes para embalagem.
Hipóteses?
- É possível produzir nanopartículas de amido e estabilizar compostos bioativos da própolis nessas nanopartículas; - A concentração do etanol acidificado e a cristalinidade do amido (tipo A, tipo B) podem influenciar nas propriedades físico-químicas e de encapsulamento das nanopartículas produzidas por nanoprecipitação; - A nanoprecipitação do extrato de própolis com amido proporcionará maior solubilidade em meio aquoso e liberação gastrointestinal in vitro; - As nanopartículas apresentam atividades antimicrobiana contra a *Listeria monocytogenes*; - As propriedades funcionais das nanopartículas são preservadas quando aplicadas em balas de gelatina.
Metodologia experimental
- A estabilização dos compostos bioativos da própolis pela técnica de nanoprecipitação utilizando polissacarídeos (amido de batata e de mandioca); - Estudo de digestibilidade das nanopartículas de própolis em modelo de digestão *in vitro*; - A aplicação das nanopartículas de contendo compostos bioativos da própolis em balas de gelatina.
Respostas
- A influência da concentração do etanol acidificado e da cristalinidade do amido nas propriedades físico-químicas e de encapsulamento das nanopartículas de própolis; - Obtenção de nanopartículas de própolis à base de amidos (amido de batata, amido de mandioca) que promovam a proteção, solubilidade em meio aquoso, boa estabilidade e liberação intestinal *in vitro*; - Nanopartículas de amido contendo extratos de própolis como fonte de compostos fenólicos; - Balas a base de gelatina com nanopartículas de própolis como fonte de compostos fenólicos.

APRESENTAÇÃO DA ESTRUTURA DA TESE DE DOUTORADO

Esta tese de doutorado está estruturada em capítulos e apresentada da seguinte maneira:

- Capítulo 1. INTRODUÇÃO E OBJETIVOS

- Capítulo 2. REVISÃO BIBLIOGRÁFICA

Metodologia e Resultados

A metodologia de cada etapa do trabalho e seus respectivos resultados e discussão serão apresentadas em capítulos, na forma de artigos, como descrito abaixo.

As referências bibliográficas de todos os capítulos da tese de doutorado estão apresentadas no final do documento.

- Capítulo 3.

Impact of the acidified hydroethanolic concentration on the physicochemical properties of starch nanoparticles produced by anti-solvent precipitation.

Este capítulo será apresentado inglês, na forma de artigo científico.

- Capítulo 4.

Antioxidant nanoparticles based on starch and the phenolic compounds from propolis extract: Production and physicochemical properties.

Este capítulo será apresentado inglês, na forma de artigo científico.

- Capítulo 5.

Starch nanoparticles containing phenolic compounds from green propolis: characterization and evaluation of antioxidant, antimicrobial and digestibility properties.

Este capítulo será apresentado inglês, na forma de artigo científico.

- Capítulo 6.

Gelatin candies architected with active starch nanoparticles containing phenolic compounds from propolis extract

Este capítulo será apresentado inglês, na forma de artigo científico.

- Capítulo 7.

Conclusão geral e sugestões de trabalhos futuros

- Capítulo 8.

REFERÊNCIAS

CAPÍTULO 1

INTRODUÇÃO E OBJETIVOS

1 INTRODUÇÃO

A própolis é um material resinoso e heterogêneo produzido pelas abelhas a partir de substâncias coletadas em partes de plantas. Este composto possui teores significativos de flavonoides e ácidos fenólicos (ALMUHAYAWI, 2020; ANDRADE et al., 2017, 2018), sendo utilizado mundialmente na medicina tradicional, indústrias farmacêutica, cosmética e alimentícia devido às suas propriedades antibacterianas, antifúngicas, anti-inflamatórias, anti-sépticas, antiproliferativas, anticarcinogênicas e antioxidantes (PASUPULETI et al., 2017; SFORCIN, 2016; TORETI et al., 2013; XAVIER et al., 2017).

Devido suas propriedades funcionais e/ou ativas pode ser utilizada na formulação ou conservação de alimentos. Porém, o uso da própolis como ingrediente alimentar ainda é limitado devido à sua baixa solubilidade em água, seu metabolismo rápido e sua instabilidade físico-química e biológica. Consequentemente, apresenta baixa biodisponibilidade, além do forte sabor e aroma que podem alterar as propriedades organolépticas dos alimentos (BODINI et al., 2013; NORI et al., 2011). Dessa forma, alguns pesquisadores têm relatado o encapsulamento da própolis como uma alternativa para mascarar sabores/aromas, mantendo as propriedades organolépticas em salame tipo italiano (BERNARDI et al., 2013a), hambúrguer de peixe (SPINELLI et al., 2015), hambúrguer de carne (REIS et al., 2017), pudim, queijo Minas Frescal (JANSEN-ALVES et al., 2018) e filé de peixe (PIEDRAHÍTA MÁRQUEZ; FUENMAYOR; SUAREZ MAHECHA, 2019). Contudo, ainda são poucos os trabalhos que realizam a etapa de aplicação das nanopartículas/micropartículas/emulsões com aplicação em sistemas alimentícios.

Além disso, o encapsulamento de própolis pode proteger sua bioatividade e aumentar sua solubilidade em água. Nesse sentido, vários trabalhos de pesquisa relataram o encapsulamento de própolis usando diferentes técnicas, secagem por *spray drying* (ANDRADE et al., 2018; BUSCH et al., 2017; CATCHPOLE et al., 2018), liofilização (ZHANG et al., 2018), coacervação complexa (NORI et al., 2011; ONBAS et al., 2016) e gelificação iônica (ONG et al., 2017).

Outra alternativa para encapsular a própolis é por meio do método de precipitação com antissolvente. Neste método, duas fases são utilizadas: uma fase aquosa contendo uma macromolécula solúvel em água, e uma fase orgânica contendo o composto ativo. Em seguida, a macromolécula é precipitada pelo gotejamento da fase orgânica, sendo que o composto ativo é estabilizado durante sua precipitação (MARTÍNEZ RIVAS et al., 2017; QIN et al., 2016). A vantagem dessa técnica é o baixo custo, uso de baixas temperatura ou temperatura ambiente,

menor risco de contaminação da amostra, não há necessidade de grandes quantidades de solventes tóxico (ASCHENBRENNER et al., 2013) e não necessita de um agente emulsificante, como em outros métodos (por exemplo, nanoemulsões) (CAICEDO CHACON et al., 2023b).

Estudos mostraram que o amido e seus derivados são bons candidatos para produzir nanopartículas (NPs), tendo sido usado recentemente como macromolécula solúvel em água pelo método de precipitação antissolvente para estabilizar resveratrol (AHMAD; GANI, 2021), curcumina (ACEVEDO-GUEVARA et al., 2018), silibinina (QIU et al., 2020), piroxicam (BHATIA; ROHILLA, 2020) e antocianinas (ESCOBAR-PUENTES et al., 2020; LIMA et al., 2021). O amido é uma macromolécula natural considerada a mais importante fonte de energia alimentar encontrada nas plantas. Esta macromolécula é formada por amilose e amilopectina, sendo armazenada na forma de grânulos com diferentes tamanhos de partícula, variando entre 2 e 100 μm (DUFRESNE, 2014; DULARIA et al., 2019). Os grânulos de amido têm estruturas cristalinas que fornecem padrões de difração de raios-X específicos, sendo classificados como A (por exemplo, amidos de cereais e tubérculos), B (por exemplo, amidos de tubérculos, frutas e caule) e tipo C (por exemplo, amidos vegetais e de raiz). Particularmente, as estruturas do tipo C podem ser consideradas como a mistura de cristais do tipo A e B (PÉREZ-MASIÁ et al., 2015).

A própolis estabilizada em amidos por precipitação antissolvente surge como uma alternativa para preservar as propriedades bioativas e aumentar a solubilidade da própolis em água. Além disso, na literatura revisada (de 2017 a 2023), não foram encontrados estudos sobre essa abordagem.

Neste contexto, esta pesquisa teve como objetivo estabilizar os compostos bioativos do extrato de própolis através do processo de nanoprecipitação antissolvente, utilizando amidos como material de parede, além de caracterizar as nanopartículas obtidas e avaliar seu perfil de liberação em condições gastrointestinais simuladas, após sua aplicação em balas de gelatina.

1.1 OBJETIVOS

1.1.1 Objetivo Geral

Este trabalho tem como objetivo produzir nanopartículas carregadas com os compostos bioativos da própolis pelo método de precipitação antissolvente utilizando duas fontes de amidos, batata e mandioca, visando sua estabilização e aplicação em balas de gelatina.

1.1.2 Objetivos Específicos

- Obter e caracterizar os extratos de própolis marrom e verde com diferentes concentrações etanólicas quanto aos compostos fenólicos totais e atividade antioxidante;
- Produzir nanopartículas de amido de batata e de mandioca usando diferentes concentrações de etanol acidificado pela técnica de nanoprecipitação antissolvente;
- Caracterizar as principais propriedades físico-químicas das nanopartículas;
- Obter e caracterizar nanopartículas de amido carregadas com extrato de própolis marrom e verde com diferentes concentrações de etanol acidificado pela técnica de nanoprecipitação antissolvente utilizando amido de batata e amido de mandioca;
- Estudar a digestibilidade gastro-intestinal *in vitro* dos compostos fenólicos e antioxidantes das nanopartículas;
- Estudar a atividade antimicrobiana das nanopartículas contra *Listeria monocytogenes;*
- Produzir balas de gelatina fortificadas com nanopartículas de amido com e sem extrato de própolis;
- Estudar as propriedades mecânicas (dureza, gomosidade, mastigabilidade) das balas de gelatinas fortificadas nanopartículas de amido com e sem extrato de própolis, e verificar a estabilidade durante o armazenamento;
- Avaliar a degradação dos compostos bioativos da própolis nas balas de gelatina em função do tempo de armazenamento.

CAPÍTULO 2

REVISÃO DE LITERATURA

2 REFERENCIAL TEÓRICO

Este segundo capítulo tem como objetivo apresentar uma revisão de literatura atual sobre este tema de tese, apresentando o crescente interesse no uso da técnica de nanoprecipitação antissolvente para o encapsulamento de compostos bioativos, destacando o uso de amidos como material encapsulante. Assim, obtendo e apresentando um panorama do desenvolvimento desta área nos últimos anos. Além disso, são apresentadas as características da própolis, composição, benefícios à saúde, os diversos compostos que estão presentes em extratos de própolis, as técnicas e os materiais de parede que têm sido utilizados para encapsular os compostos bioativos da própolis e aplicações desses materiais em alimentos.

O conteúdo faz parte de um artigo de revisão intitulado “Food Applications of Starch Nanomaterials: A Review” publicado na revista Starch. De acordo com as regras de assinatura da Wiley, os autores se reservam o direito de incluir o artigo em uma tese, desde que não seja publicado comercialmente. Além disso, foi publicado um capítulo de livro intitulado “Applications in food products” no livro Biopolymeric Nanomaterials da Elsevier.

2.1 PRÓPOLIS: CARACTERÍSTICAS GERAIS

A própolis é uma substância resinosa produzida pelas abelhas a partir de diversas fontes vegetais, como das flores e exsudatos, com intuito de vedação, assepsia, forro, impermeabilização de água ou proteção contra crescimento de micro-organismos e fungos nas colmeias. É um material duro e quebradiço em temperaturas abaixo de 25 °C e torna-se macio, flexível, pegajoso ou muito pegajoso entre 25 °C e 45 °C (ALVARENGA et al., 2021).

A própolis crua deve ser purificada para remover o material ceroso e preservar a fração de polifenóis, considerados os mais significativos para os efeitos antioxidantes. Os métodos mais comuns de extração são: maceração (AUGUSTO-OBARA et al., 2019; PETER et al., 2019; WOŹNIAK et al., 2019), maceração combinada com ultrassom (ESCRICHE; JUAN-BORRÁS, 2018), soxhlet (SHARAF; EL-NAGGAR, 2018), micro-ondas (MAŠEK et al., 2018), fluido supercrítico (altas pressões) (BISCAIA; FERREIRA, 2009; MONROY et al., 2017), e banho de ultrassom (ANDRADE et al., 2017; DEMBOGURSKI et al., 2018; SEIBERT et al., 2019). Tais métodos apresentam variação de parâmetros como, por exemplo, temperatura, tempo, proporção amostra-solvente e tipo de solvente. No que diz respeito à capacidade antioxidante e as inúmeras atividades biológicas desses extratos, destaca-se os extratos obtidos

pela extração por ultrassom. GargourI et al. (2019) estudou os compostos fenólicos na própolis tunisiana, comparando o solvente convencional e os procedimentos assistidos por ultrassom, ambos utilizando etanol 80%, e os resultados dos teores de fenólicos totais e flavonoides foram mais eficientes por ultrassom.

Os solventes mais utilizados para a extração são: água, etanol, metanol, clorofórmico, hexano, éter etílico (MARTINOTTI; RANZATO, 2015; MELLO; HUBINGER, 2012; MELLO; PETRUS; HUBINGER, 2010). Dentre esses, o etanol é o mais utilizado por se obter de extratos com baixo teor de cera e mais ricos em compostos bioativos, pela elevada solubilidade da própolis no etanol (MARTINOTTI; RANZATO, 2015; MELLO; HUBINGER, 2012; MELLO; PETRUS; HUBINGER, 2010). Além disso, o etanol não é tóxico e também pode ser facilmente removido após a extração, caso o extrato de própolis seja usado como ingrediente alimentar (GARGOURI et al., 2019).

2.1.1 Composição e propriedades biológicas da Própolis

Em geral a própolis bruta é composta de resinas (50–60%), cera (30–40%), óleos essenciais (5–10%), pólen (~5%) e outras substâncias como vitaminas, minerais, aminoácidos, fenólicos e flavonoides (GUIAR, 2002; PIETTA; GARDANA; PIETTA, 2002). Quanto a caracterização química de extratos de própolis, os estudos mostram que existem mais de 300 constituintes e novos componentes vem sendo identificados (CAUICH-KUMUL; CAMPOS, 2018; MARCUCCI, 1995).

Diversos métodos analíticos são utilizados para quantificar e qualificar os extratos de própolis, os métodos espectrofotométricos e os cromatográficos. Os métodos espectrofotométricos têm sido os mais utilizados por apresentarem baixo custo com reagentes, dispensa o uso de padrões analíticos individuais, as análises são rápidas, apresentam boa repetibilidade e reprodutibilidade, não requerem o uso de equipamentos sofisticados, e são aplicados em diferentes matrizes (GRANATO et al., 2016). Dentre os métodos para determinar os compostos fenólicos, o método de Folin-Ciocalteu, o qual é composto por sais de molibdato de sódio e tungstato de sódio e é usado juntamente com uma solução de carbonato de sódio gerando o ânion fenolato. Posteriormente, ocorre uma reação de óxido-redução entre ânion fenolato e o reagente Folin-Ciocalteu, ocorrendo uma alteração na coloração, da solução de amarelo para azul. A intensidade da cor azul está associada ao número de hidroxilas ou grupos oxidáveis dos compostos fenólicos. A reação ocorre em um período de 2 horas à temperatura

ambiente e na ausência de luz. E, finalmente, uma leitura espectrofotométrica é realizada no comprimento de onda de 765 nm (absorção máxima do complexo azul) (SINGLETON; ORTHOFER; LAMUELA-RAVENTÓS, 1999). E a cromatografia líquida de alta eficiência e cromatografia em fase gasosa têm sido utilizadas em diferentes estudos para identificar e quantificar a composição de extratos de própolis quanto a compostos fenólicos e flavonoides, entre outros (BITTENCOURT et al., 2015).

De acordo com Anjum et al. (2019), os principais compostos encontrados na própolis são flavonoides, ácidos aromáticos, ácidos graxos, fenóis, aminoácidos, polissacarídeos, enzimas (desidrogenase succínica, glicose-6-fosfatase, adenosina trifosfatase e fosfatase ácida) vitaminas B1, B2, B6, C e E, e minerais como Mn, Cu, Ca, Al, Si, V, Ni, Zn e Cr. A concentração desses compostos varia com o tipo da própolis, épocas de colheita, com as partes da planta (caules, folhas), origem geográfica, a sazonalidade, pela espécie produtora, e também pelo método de obtenção dos extratos (WAGH, 2013). Esses fatores são responsáveis pelos diferentes tipos de cor da própolis (amarelo-esverdeado ao marrom-escuro), sabor, aroma da própolis e textura (BROWN, 1989). Como consequência, os diferentes tipos de própolis são caracterizados por perfis químicos diferentes, de acordo com a sua origem vegetal, com a presença de compostos de tipos específicos como polifenóis, terpenóides, aldeídos, álcoois aromáticos, ácidos graxos, entre outros (WATANABE et al., 2011).

Os compostos fenólicos são a maior parcela de compostos orgânicos encontrados na própolis (SHEHATA et al., 2020). Eles possuem um caráter heterogêneo e possuem em suas estruturas um anel aromático com um ou mais substituintes hidroxílicos, apresentando-se como moléculas simples e também como moléculas com alto grau de polimerização (ACOSTA-ESTRADA; GUTIÉRREZ-URIBE; SERNA-SALDÍVAR, 2014; YEO; SHAHIDI, 2017). Dentre os compostos fenólicos presentes na própolis, os mais importantes são os flavonoides, ácidos fenólicos e seus ésteres (SHEHATA et al., 2020; WAGH, 2013).

Os ácidos fenólicos, quimicamente, têm pelo menos um anel aromático, em que pelo menos um hidrogênio está substituído por uma hidroxila (HELENO et al., 2015). Eles são divididos em dois grupos, ácidos hidroxibenzóicos e ácidos hidroxicinâmico, e são normalmente derivados de moléculas do ácido benzoico (ácido gálico) e derivados do ácido cinâmico (ácido p-cumárico, ácido caféico, ácido ferúlico) (Figura 2.1).

Fig. 2.1. Estrutura química comum dos ácidos fenólicos derivados (a) do ácido cinâmico e (b) do ácido benzóico.

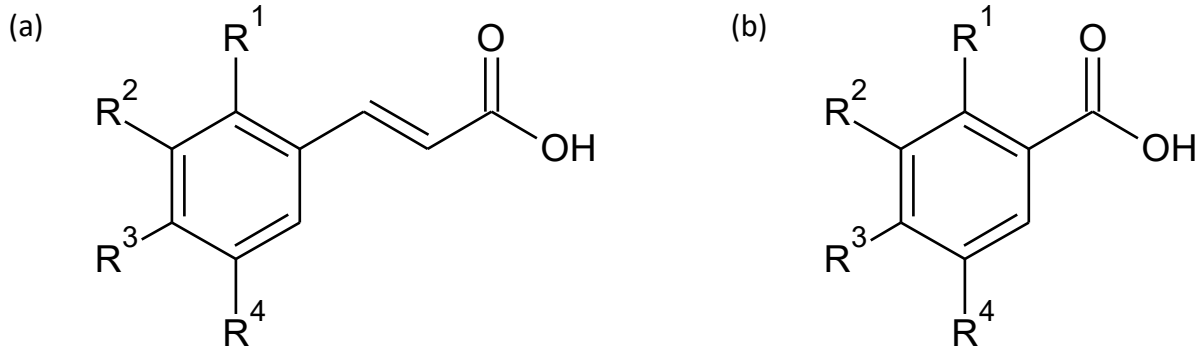

Fonte: adaptado de Heleno et al. (2015).

Os flavonoides possuem uma estrutura de carbono C6–C3–C6 são classificados nos grupos: flavonas, flavononas, flavonolóis, isoflavonas, flavanóis (catecinas), antocianinas, chalconas, flavononas, flavonas, isoflavonas, flavonóis, isoflavonoides, neoflavonoides, quercetina, entre outros (PANDEY et al., 2016; SELEEM; PARDI; MURATA, 2017), diferenciando de acordo com o grau de oxidação e nível de saturação no anel C e na presença de anéis adicionais (Figura 2.2) (PANDEY et al., 2016).

Fig. 2.2. Estrutura química comum dos flavonoides.

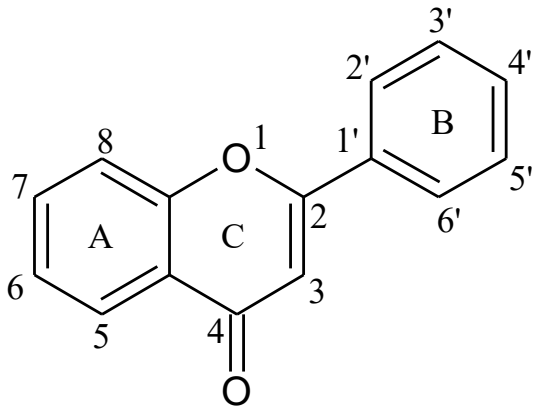

Fonte: adaptado de Wang, Li e Bi (2018).

Estudo comparando extratos de própolis de seis países diferentes, Egito, China, Bulgária, Brasil, Arabia Saudita e Omã, mostrou que todos os tipos de própolis apresentaram um teor significativo de compostos polifenólicos, sendo encontrados 33 diferentes desses compostos. A própolis do Brasil apresentou 12 diferentes compostos, sendo superiores aos demais (SHEHATA et al., 2020), provavelmente devido à grande diversidade de espécies de

plantas no Brasil, que podem contribuir para a diversidade de compostos polifenólicos em amostras de própolis. Os autores ressaltaram que houve diferenças significativas entre os teores fenólicos, flavonóides totais e capacidade antioxidante total dos diferentes tipos de amostras de própolis, indicando que essas diferenças são decorrentes das condições climáticas, da diversidade da flora ao redor da colmeia e da época de colheita.

Em outro estudo complementar, três tipos diferentes de própolis no Brasil (marrom, vermelha e verde) foram analisadas. Para à própolis marrom, os terpenos foram a principal classe química, quantitativamente e qualitativamente, além de apresentar uma variedade de ésteres, álcoois e aldeídos (OLEGÁRIO et al., 2019). Waller et al. (2017) estudando a própolis marrom brasileira observaram que os principais compostos fenólicos presentes nas amostras foram os ácidos p- cumárico, rutina, ácido clorogênico, ácido ferúlico e ácido caféico. Nesses estudos observou-se que a composição dos extratos de própolis apresenta variações em termos de composição quantitativa. Os compostos da própolis têm sido estudados quanto às suas atividades biológicas benéficas à saúde, incluindo atividades anti-inflamatória, antiviral (SFORCIN, 2016), antioxidante (ANDRADE et al., 2017), antipotozoário, anestésico, antitumoral (FROZZA et al., 2017) antimicrobiana (BITTENCOURT et al., 2015), antifúngico (PETER et al., 2019), anti-séptico, anti-mutagênico, anti-hepatotóxico além de ser usado para atividade citotóxica (TORETI et al., 2013), que estão associadas à sua rica composição de vários polifenóis (EL-GUENDOUZ et al., 2016; HUANG et al., 2014), vale ressaltar que além dessas propriedades, o extrato etanólico de própolis não mostrou efeito de citotoxicidade contra *Caenorhabditis elegans* após 24 h de exposição (ABDULLAH et al., 2019), indicando que é composto considerado seguro para ser aplicado em alimentos.

Dentre as atividades biológicas atribuídas à própolis, a atividade antioxidante é bem explorada e também a atividade anti-inflamatória (ANDRADE et al., 2017; FRANCHIN et al., 2018; PEIXOTO et al., 2021).

2.1.1.1 Atividade antioxidante e antimicrobiana

A demanda por alimentos e suplementos funcionais tem aumentado significativamente nas últimas décadas. Assim, esse apelo por ingestão de produtos mais saudáveis tem levado setores da indústria alimentícia e de suplementos alimentares a encontrar fontes naturais de antioxidantes e compostos funcionais.

Os compostos antioxidantes possuem capacidade de eliminação de radicais livres, que é a principal causa da oxidação de lipídios, ácidos nucléicos e proteínas, consequentemente inibindo a degradação da vitamina C, lipídios e outros compostos de oxidação (CHANDNA et al., 2014). Em outras palavras, os compostos fenólicos doam íons de hidrogênio aos radicais livres para proteger a célula das reações de oxidação, assim protegendo o produto da oxidação durante o armazenamento. É importante indicar que a atividade sequestradora de radicais livres dos extratos etanólicos de própolis é atribuída principalmente à presença de ácidos fenólicos, flavonoides e outros polifenóis (CAUICH-KUMUL; CAMPOS, 2018).

A capacidade antioxidante de alimentos auxilia na redução do risco de doenças, tais como: doença de Parkinson, doença de Alzheimer, artrite, cardiovascular, câncer e diabetes (KUROPATNICKI; SZLISZKA; KROL, 2013; WAGH, 2013). Portanto, é importante identificar compostos naturais e novas substâncias que podem neutralizar esses radicais livres para prevenir o estresse oxidativo. Os extratos de própolis têm sido aplicados em alimentos (suplementos alimentares) como fonte de compostos fenólicos (BRASIL, 2018).

A capacidade antioxidante pode ser determinada pelos métodos de captura do radical DPPH (1,1-difenil-2-picrilidrazina) e do radical ABTS+. A metodologia DPPH (1,1-difenil-2-picrilidrazina) apresenta alta sensibilidade e pode ser utilizada para quantificar antioxidantes de caráter hidrofóbico e hidrofílico. É um método simples e barato, o que justifica sua ampla utilização (BOROSKI et al., 2015). O radical DPPH apresenta dois anéis aromáticos de seis membros ligado a três grupos NO_2 e uma hidrazina, em que o átomo de nitrogênio está ligado diretamente ao anel, que apresenta um elétron desemparelhado, caracterizando a espécie como um radical livre, e sua capacidade de redução é na maioria das vezes avaliada por espectroscopia, a uma absorbância de 515 nm (BOROSKI et al., 2015). Mas essa avaliação de antioxidante não deve se basear em apenas uma única metodologia, sendo necessários outros métodos para caracterizar completamente um composto, como o método do radical 2,2-azinobis (3-etilbenzotiazolina-6-ácido sulfônico) (ABTS ponto radical^{+}). Similar ao método de redução do radical DPPH, o método ABTS é simples e barato, além disso fornece resultados rápidos. O radical ABTS é gerado por reações químicas ou enzimáticas, e é solúvel em água e também em solventes orgânicos (diferente do DPPH que é solúvel apenas em solventes orgânicos) permitindo a análise tanto de amostras hidrofílicas, como lipofílicas. O radical ABTS ($ABTS^{+}$) na presença de Trolox (ou de outro antioxidante doador de hidrogênio), o átomo de nitrogênio se liga o átomo de hidrogênio, resultando na descoloração da solução, e sua capacidade de antioxidade é na maioria das vezes avaliada a uma absorbância de 743 nm (MARC et al., 2004).

Também temos o método de FRAP (sigla do inglês para Ferric Reducing Ability Power), que se baseia na redução de um complexo férrico incolor (Fe^{3+} -tripiridiltriazina) a um complexo ferroso de cor azul (Fe^{2+}-tripiridiltriazina), com máxima absorção em 593 nm, através da ação de antioxidantes doadores de elétron em um meio acidificado. A redução é monitorada através de um espectrofotômetro UV (DUDONNÉ et al., 2009). Este método se destaca por ser de fácil execução, com resultados confiáveis e em um curto período de tempo, sendo muito utilizado na análise da capacidade antioxidante em plantas e alimentos, especialmente, em conjunto com o método DPPH (MOON; SHIBAMOTO, 2009).

Outra atividade importante dos extratos de própolis é a atividade antimicrobiana. A atividade antibacteriana da própolis é atribuída à presença de flavonoides, ácidos fenólicos, aldeídos, cetonas e terpenos (SANTOS et al., 2018; VASILAKI et al., 2019).

Há diversos estudos abordando a atividade antimicrobiana de extratos de própolis, e em sua maioria, eles mostram que o extrato de própolis tem melhores resultados de atividade antimicrobiana contra bactérias Gram-positivas quando comparado com a atividade contra bactérias Gram-negativas (ANJUM et al., 2019; JANSEN-ALVES et al., 2019; KIM; CHUNG, 2011).

Embora o mecanismo de ação para seu efeito antimicrobiano ainda não seja claramente compreendido, uma possível razão poderia ser a síntese de uma ampla variedade de enzimas hidrolíticas por microrganismos Gram-negativos (GRECKA et al., 2019; KATIYAR, 2023). Essas enzimas hidrolíticas podem interferir nos componentes ativos da própolis e resultar no desenvolvimento de resistência (BRYAN; REDDEN; TRABA, 2016). Outros autores sugerem que os constituintes da própolis interferem na inibição da divisão celular, síntese de ácidos nucleicos , síntese de proteínas, impedimento da função da membrana citoplasmática, alteração da permeabilidade da membrana, redução da capacidade de formar biofilmes, bacteriólise, inibição a via de geração de energia e reduzindo a resistência bacteriana a certos antibióticos convencionais (PRZYBYŁEK; KARPIŃSKI, 2019). Esses métodos podem ajudar a explicar por que a própolis tem um efeito antibacteriano, aumentando a permeabilidade da membrana e diminuindo o movimento bacteriano.

Azra et al. (2023) observaram valores de concentração mínima inibitória (CMI) variando de 10 a <40 (mg/mL) para *Escherichia coli, Salmonella typhimurium, Staphylococcus aureus e Listeria monocytogenes*. Observaram que a *E. coli* e a *Salmonella typhimurium* como bactérias Gram-negativas apresentaram maior resistência contra própolis pura quando comparadas com as bactérias Gram-positivas.

Pedonese et al. (2019) avaliaram a atividade antimicrobiana de uma própolis italiana contra bactérias Gram+ (*Listeria monocytogenes*, *Staphylococcus aureus*, *Bacillus cereus*) e bactérias Gram$^-$ (*Salmonella enterica* serovar Typhimurium, *Escherichia coli*, *Pseudomonas fluorescens*). O extrato de própolis apresentou valores de CMI de 0,89 - 1,78 mg/mL para bactérias Gram+, na faixa de 1,78 (*Pseudomonas fluorescens*) e 3,55 mg/mL para Gram-. E os valores para a concentração mínima bactericida (CMB) para Gram+ foram 3,55-7,11 mg/mL e 7,11-28,44 mg/mL para Gram-.

Mahdavi-Roshan (2022) relataram que o extrato aquoso de própolis pode controlar as contagens de bactérias totais, *Staphylococcus aureus*, *Escherichia coli*, leveduras e bolores em amostras de carne de frango embebidas com diferentes concentrações (0, 4, 8 e 12% v/p) durante 12 dias de armazenamento à 5 °C. O crescimento das bactérias foi mais lento com o aumento da concentração da própolis. Os resultados de análises sensorial mostraram que os escores de cor, odor das amostras diminuíram com o aumento do tempo de armazenamento, porém os menores escores foram observados na amostra contendo 12% de extrato aquoso de própolis, indicando que a concentração de 12% afetava a qualidade sensorial da carne de frango.

Vasilaki et al. (2019) avaliaram a substituição do sorbato de potássio por extrato de própolis (aquoso com solução de HP-β-ciclodextrina (11,1% m/m)) em refrigerantes de laranja. Eles encontraram inibição do crescimento de bactérias, leveduras e fungos durante o armazenamento nas bebidas com própolis. E, concluíram que estudos adicionais devem ser realizados para melhorar a estabilidade da cor e determinar a estabilidade a longo prazo durante o armazenamento. Nesse estudo não avaliaram a aceitação dos consumidores.

Pobiega et al. (2019) produziram cinco extratos de própolis polonês e detectaram que os compostos flavonóides majoritários foram pinocembrina, crisina, pinobancsina, apigenina e kaempferol e os ácidos fenólicos predominantes foram ácido *p*-cumárico, ácido ferúlico e ácido cafeico. Esses autores estudaram a concentração mínima inibitória (CMI), concentração mínima bactericida/fungicida (CMB/CMF) dos extratos desses extratos frente a 11 cepas, dentre essas quatro eram Gram+(*Staphylococcus aureus*, *Bacillus cereus*, *Listeria monocytogenes*, *Enterococcus faecalis*) e sete eram GRAM- (*Salmonella* Enteritidis, *Shigella sonnei*, *Klebsiella pneumoniae*, *Escherichia coli O157, Proteus mirabilis*, *Enterobacter aerogenes*, *Pseudomonas aeruginosa*). Os extratos apresentaram eficácia com valores de CMI e CMB variando de 1 a 8 mg/mL e ≥ 8 mg/mL, respectivamente, para as Gram+. Enquanto as Gram- apresentaram valores de CMI e CMB variando de 2 a 16 mg/mL e de 8 a 32 mg/mL, respectivamente, sendo a *E. coli* a bactéria mais resistente.

Diante do exposto, observou-se que a concentração de extrato de própolis é um fator importante na inibição do crescimento de patógenos de origem alimentar. E, é necessário escolher a concentração adequada, pois o aroma da própolis é forte e afeta os indicadores sensoriais. Portanto, a estabilização dos compostos bioativos da própolis poderia mascarar o forte odor da própolis, facilitando assim a aplicação da própolis na área alimentícia.

2.2 ENCAPSULAMENTO DE COMPOSTOS BIOATIVOS

O encapsulamento consiste no revestimento ou incorporação de compostos bioativos (encapsulado) em uma matriz ou sistema (encapsulante), que forma de partículas de diferentes tamanhos, variando de escala de nanométrica a micrométrica (ABDUL MUDALIP et al., 2021). O encapsulamento de compostos bioativos tem como objetivo proteger o encapsulado de oxidação e degradação térmica, controlar sua taxa de liberação sob determinadas condições, melhorar a qualidade sensorial ao mascarar o sabor desagradável (por exemplo, amargor de polifenóis) e proporcionar aumento da solubilidade e biodisponibilidade, devido às alterações causadas na superfície dos compostos (CORTÉS-MORALES; MENDEZ-MONTEALVO; VELAZQUEZ, 2021; MARTÍNEZ RIVAS et al., 2017).

Os compostos bioativos podem ser encapsulados por diferentes técnicas e a sua escolha depende da natureza do polímero, do composto a ser encapsulado, do uso pretendido, e das propriedades desejadas do produto final, entre outros fatores. Existem inúmeras técnicas de encapsulamento para a formação de cápsulas, como spray drying, coacervação, liofilização, nanoprecipitação e gelificação iônica, entre outras (ANDRADE et al., 2018; AZEVEDO et al., 2018; CORTÉS-MORALES; MENDEZ-MONTEALVO; VELAZQUEZ, 2021; JANSEN-ALVES et al., 2018; LIU et al., 2020; MARTÍNEZ RIVAS et al., 2017; SATO et al., 2020).

A escolha da técnica de encapsulação deve considerar um conjunto de elementos, como: custo, tamanho da partícula desejada, escala de produção, propriedades físicas e químicas do material de parede e do núcleo, mecanismo de liberação requerido. Uma vez escolhido o sistema de encapsulamento, ele deve apresentar facilidade na incorporação as matrizes, ser eficiente e não causar características indesejáveis na aplicação. A agregação entre o agente e o material pode ser de natureza química, física ou físico-química (JIA; DUMONT; ORSAT, 2016; SHISHIR et al., 2018).

Como mencionado anteriormente, existem diferentes tipos de metodologias utilizadas para produzir nanopartículas biopoliméricas. Destacando-se o método de nanoprecipitação anti-

solvente (ou deslocamento de solvente, ou deslocamento de solvente), para a preparação de nanopartículas.

2.2.1 Nanoprecipitação antissolvente

A nanoprecipitação descrita por Fessi et al. (1989), é uma técnica que tem como objetivo encapsular moléculas hidrofóbicas, e tem sido amplamente usada para produção de NPs (FESSI et al., 1989). A nanoprecipitação, também conhecida como precipitação antissolvente, provoca a formação de gotículas como resultado da turbulência interfacial entre duas fases imiscíveis (FESSI et al., 1989). Esta técnica é classificada como um método químico em que o polímero é gelatinizado em água sob altas temperaturas e após o resfriamento, precipitados pela adição da solução orgânica, gota a gota, à solução de polímero (fase aquosa), induzindo a supersaturação, que fornece uma força motriz para a precipitação do soluto (Figura 2.3a). A principal força motriz para a formação de partículas durante a precipitação do antissolvente é o desequilíbrio das interações moleculares entre aquosa e a solução orgânica (JOYE; MCCLEMENTS, 2013). Esta fase orgânica ao entrar em contato com uma fase aquosa que está sobre agitação magnética (após a formação das partículas, é importante que haja uma repulsão suficientemente forte entre elas para evitar que se agreguem), gera uma difusão para a fase aquosa devido ao excesso de água, com formação de gotículas de polímero, devido à sua hidrofobicidade, ocorrendo a precipitação, e gerando as nanoesferas ou nanocápsulas, contendo o composto ativo (Figura 2.3b e 2.3c) (CRUCHO; BARROS, 2017; FESSI et al., 1989). Nas nanoesferas, o composto encapsulado fica disperso em toda matriz polimérica, enquanto que, no segundo caso, o encapsulado fica no interior (MARTÍNEZ RIVAS et al., 2017).

Fig. 2.3. Representação das principais etapas da formação de partículas no processo de encapsulamento por Nanoprecipitação (a) e da formação de nanocápsulas (b) e nanoesferas (c).

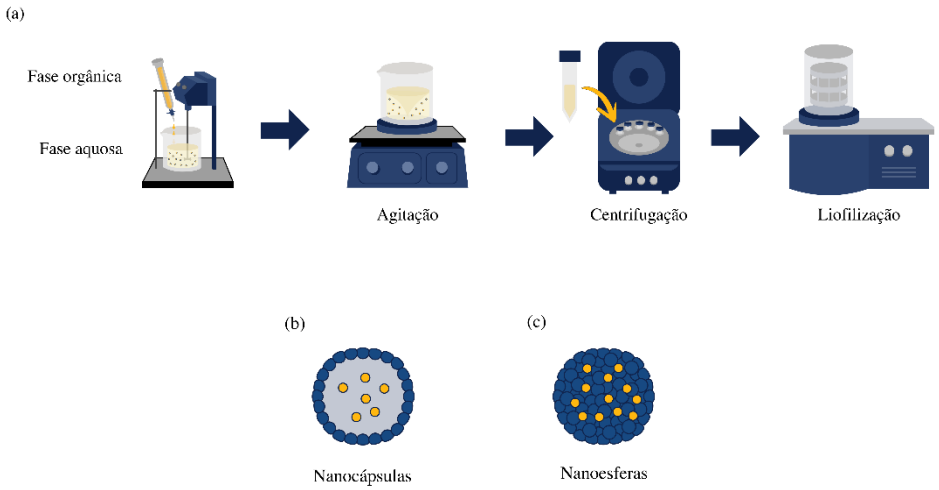

Fonte: A autora (2021).

Em seguida, os solventes são evaporados e um método de secagem é aplicado para remoção de água das NPs, sendo a liofilização o principal método de secagem empregado (CRUCHO; BARROS, 2017; FESSI et al., 1989). A nanoprecipitação é uma tecnologia promissora quando comparada a outros métodos de síntese, uma vez que é um técnica simples, de baixo custo, (dispensa o uso de fontes externas de energia), uso de baixas temperatura ou temperatura ambiente, menor risco de contaminação da amostra, não há necessidade de grandes quantidades de solventes tóxico (ASCHENBRENNER et al., 2013) e não necessita de um agente emulsificante, como em outros métodos (por exemplo, nanoemulsões) (CAICEDO CHACON et al., 2023b). Apesar de ser uma metodologia simples, é importante ressaltar que a principal limitação desse método é a floculação de partículas, e assim, ocorrendo a formação de grandes agregados (CAICEDO CHACON et al., 2023a).

Os solventes mais usados no método de nanoprecipitação são os orgânicos polares, como etanol, acetona, hexano, cloreto de metileno ou dioxano. E na fase não solvente (ou fase aquosa), geralmente se utiliza a água (MARTÍNEZ RIVAS et al., 2017), por ser miscível com o solvente polar em todas as proporções (CAICEDO CHACON et al., 2023b) .

2.2.2 Material de parede usado na nanoencapsulação

Os materiais formadores de partículas podem ser polímeros naturais, sintéticos ou semi-sintéticos. Na literatura, os biopolímeros mais comuns na produção de nanopartículas são a maltodextrina, quitosana, proteínas, amido, celulose e gomas (BARTHOLD et al., 2019; GARCÍA-CASAS et al., 2017; JAISON; CHANDRASEKARAN; MOTHILAL, 2020; LIU et al., 2022).

Esses biopolímeros são atualmente utilizados na indústria de alimentos devido às diversas aplicações e possíveis usos como aditivos alimentos. Os biopolímeros são "geralmente reconhecidos como seguros" e usados para aplicações em alimentos devido às suas fontes naturais, biocompatibilidade, não toxicidade, biodegradabilidade e propriedades mecânicas aceitáveis (VALENCIA et al., 2019).

Devido à sua alta aplicabilidade no setor alimentício, neste trabalho foram escolhidos dois biopolímeros obtidos da biomassa: o amido de mandioca (AM) e o amido de batata (AB). Eles foram utilizados como material de parede para a elaboração das NPs deste estudo.

2.2.2.1 Amido

O amido é a principal fonte de energia das plantas, sendo armazenado em tubérculos/raízes, frutos e grãos/sementes na forma de grânulos com diferentes formatos e tamanho de partícula variando entre 2 a 100 μm (DUFRESNE, 2014; DULARIA et al., 2019). Ele é constituído de amilose (20-35%), e amilopectina (80-65%) e essa razão de amilose/amilopectina depende da fonte botânica da qual o amido foi obtido (OBADI; XU, 2021). Tanto a amilose como a amilopectina são constituídas de alfa glucanos, conectados por ligações α 1-4 e α 1-6. A porcentagem de ligações α 1-6 na amilose e na amilopectina é de aproximadamente 1% e 5%, respectivamente. As ligações α 1-4 formam estruturas lineares, enquanto as ligações α 1-6, geram estruturas ramificadas. Portanto, a amilose se caracteriza por ser um biopolímero linear, enquanto que a amilopectina é ramificado (PÉREZ; BALDWIN; GALLANT, 2009).

A cristalinidade dos amidos nativos pode variar entre 15% e 45%, sendo classificada como tipo A, B e C, típico de cereal, tubérculo e mistura de amidos, respectivamente (DUFRESNE, 2014; ZOBEL, 1988). Os tipos A e B são as estruturas cristalinas mais comuns encontradas em amidos nativos. Além disso, o tipo C é considerado uma mistura de amidos tendo estruturas cristalinas do tipo A e B. Cada tipo de estrutura cristalina do amido fornece características físicas e químicas particulares aos grânulos, desejados ou não pelo setor

industrial (DULARIA et al., 2019; FROST et al., 2009; HE; WEI, 2017; PINTO et al., 2012). Os amidos apresentam birrefringência quando observados em microscópio óptico sob luz polarizada, devido ao modelo típico da cruz de mata (DUFRESNE, 2014).

O amido é amplamente utilizado no setor de alimentos. Entretanto, essa macromolécula não é solúvel em água à temperatura ambiente, e muitas das suas propriedades funcionais são exibidas somente após a desordem da estrutura do grânulo, que ocorre por aquecimento em meio aquoso, processo chamado de gelatinizacão (HASPERUÉ et al., 2016; PARKER; RING, 2001; STEENEKEN; WOORTMAN, 2009), cuja temperatura depende da fonte do amido (60 - 80 °C) (LIU et al., 2019).

Durante o processo de gelatinização, os cristalitos de amido derretem, provocando alteração na ordem molecular, estrutura e caráter birrefringente dos grânulos e, simultaneamente, ocorre a solubilização do amido. Nesse processo, a água entra primeiro nas regiões amorfas, que se expandem e transmitem forças disruptivas para as regiões cristalinas (BEMILLER, 2011).

Com a desordem da estrutura do grânulo ocorre a lixiviação de moléculas de amilose e amilopectina para fora do grânulo, atribuída devido a formação de pontes de hidrogênio, provocando mudanças irreversíveis nas suas propriedades, como na cristalinidade (STEENEKEN; WOORTMAN, 2009).

Na fécula de mandioca (amido da mandioca), os grânulos têm forma lenticular e/ou esférica, com tamanhos entre 2 - 45 μm, proporção de amilose/amilopectina de 17/83 e temperatura de gelatinizacão entre 65 - 70 ºC (BREUNINGER; PIYACHOMKWAN; SRIROTH, 2009). O amido de batata possui grânulos com tamanhos entre 5 - 100 μm, relação de amilose/amilopectina de 75/25 e temperatura de gelatinizacão entre 60 - 65 ºC (BREUNINGER; PIYACHOMKWAN; SRIROTH, 2009; CHEN et al., 2011; HAN et al., 2019; VALENCIA; DJABOUROV; DO AMARAL SOBRAL, 2016).

Nesse sentido, a indústria de alimentos vem tentando melhorar as propriedades físico-químicas dos amidos, uma vez que os amidos nativos não apresentam as características suficientes para garantir a qualidade dos produtos alimentares finais (BEMILLER, 2018). Uma alternativa recente para melhorar as propriedades físico-químicas ou adicionar novas funcionalidades aos amidos é sua modificação de tamanho, da microescala para a nanoescala, a qual traz como vantagens a redução do tamanho de partículas, consequentemente uma maior área de contato, bem como aumento solubilidade em água. Nesse sentido, as nanoestruturas de amido são definidas como materiais com pelo menos uma dimensão entre 1 e 1000 nm

(CAMPELO; SANT'ANA; PEDROSA SILVA CLERICI, 2020; SUN, 2018b). Os nanomateriais de amido (NMA) podem ser classificados como nanocristais (a) nanofibras (b), nanomicelas (c)), nanopartículas (d) e nanovesículas, conforme mostrado na Figura 2.4 (SUN, 2018b). Os nanocristais são plaquetas cristalinas resultantes da ruptura da estrutura semicristalina de grânulos de amido (GUTIÉRREZ; VALENCIA, 2021; LECORRE et al., 2012; LECORRE; BRAS; DUFRESNE, 2012), enquanto nanofibras e nanopartículas são definidas como estruturas cilíndricas e partículas sólidas amorfas, respectivamente (AHMAD et al., 2020; ASHRAF et al., 2019; LIU et al., 2017). Outros nanomateriais, como as nanomicelas são definidas como dispersões coloidais com um núcleo hidrofóbico e casca hidrofílica com base em nanomateriais de amido, (KOU et al., 2020), enquanto as nanovesículas chamadas nanolipossomas convencionais são vesículas lipídicas revestidas com nanomateriais de amido (SINTOV, 2020).

Fig. 2.4. Nanoestruturas à base de amidos.

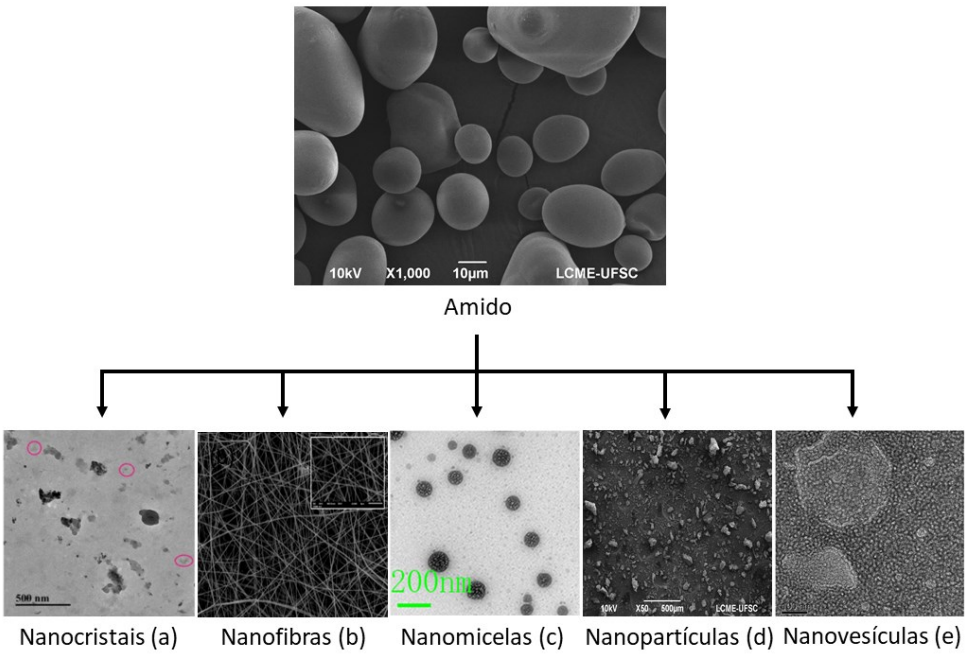

Fonte: Adaptado de Desai; Mondal; bera (2020); Fonseca et al. (2019); Kou et al. (2020); Sintov (2020)

2.2.2.2 Nanopartículas de amido

Uma série de ingredientes alimentares foram estabilizados com sucesso usando amido com boa eficiência de encapsulamento (AHMAD et al., 2019; AHMAD; GANI, 2021; LIU et al., 2020). Nos últimos anos, vários trabalhos (Tabela 1) têm usado NPs à base de amidos

produzidas pela técnica de precipitação antissolvente para estabilizar compostos bioativos, com o objetivo de aplicações farmacêuticas e alimentares devido à sua alta relação superfície/volume e compatibilidade, baixo custo, abundantes e de fácil síntese, além de ser uma fonte renovável (DONG et al., 2021).

Dessa forma, Acevedo-Guevara et al. (2018) concluíram que NPs obtidas a partir de amido nativo e acetilado oriundo de bananas verdes podem ser usadas para encapsular a curcumina (eficiência >80%). As NPA amido de banana acetilado mostraram a capacidade de encapsular mais moléculas de curcumina do que as NPA nativos, permitindo uma liberação mais controlada de curcumina sob condições gástricas.

Tabela 2.1. Aplicações de nanopartículas de amido (NPA), produzidas por precipitação antissolvente, como material de parede para estabilizar compostos bioativos.

Material de Parede (amidos)	Método de encapsulamento	Encapsulado	Principais resultados	Autores
Raiz de lótus	Precipitação antissolvente	Luteolina	O tamanho de partícula foi de 305 nm e eficiência de encapsulamento igual a 87,2%.	(CHEN et al., 2021)
Quinoa	Precipitação antissolvente combinado com ultrassom	Quercetina	Tamanhos de partícula menores que 166,25 nm e eficiência de encapsulamento superior a 26,62%.	(Jiang et al., 2022)
Milho normal	Precipitação antissolvente	β-caroteno	Tamanhos de partícula menores que 120 nm e eficiência de encapsulamento superior a 80%.	(Lee et al., 2022)
Batata e mandioca	Precipitação antissolvente	Antocianinas	Tamanhos de partículas menores que 900 nm e eficiência de encapsulamento entre 9,89 e 12,37%	Lima et al. (2021)
Castanha da Índia (HSC), castanha d'água (WSC) e caule de lótus (LSC)	Precipitação antissolvente combinado com ultrassom	Resveratrol	Tamanho de partículas entre 419 e 797 nm e eficiência de encapsulamento em torno de 72 ± 2%	Ahmad; Gani (2021)
Banana acetilado	Precipitação antissolvente	Curcumina	Tamanhos de partículas menores que 250 nm e eficiência de encapsulamento superior a 80%	Acevedo-Guevara et al. (2018)
Quinoa	Precipitação antissolvente	Piroxicam	Tamanhos de partículas entre 282 e 870 nm e eficiência de encapsulamento de 78%.	Bhatia; Rohilla (2020)
Milho anormal	Precipitação antissolvente	Antocianinas	Tamanhos de partículas entre 65 e390 nm e eficiência de estabilização acima de 45%	Escobar-Puentes et al. (2020)
Banana	Precipitação antissolvente	β-caroteno	Tamanhos de partículas menores que 250 nm e eficiência de encapsulamento de 95,32%	Santoyo-Aleman; Sanchez; Villa (2019)
Milho anormal	Precipitação antissolvente	Silibinina	Eficiência de encapsulamento de 89,93%	Wu; Wang; Wang (2020)

Mandioca acetilado	Precipitação antissolvente	Ácido gálico (AG) e hidroxitolueno butilado (HTB)	Tamanhos de partículas entre 500 e 900 nm	De Oliveira et al. (2018)

Fonte: A autora (2023).

Também foram produzidas NPs a partir de amido de castanha da Índia, castanha d'água e caule de lótus, e essas foram capazes de distribuir e liberar resveratrol de maneira eficiente nos locais específicos e exibem atividades antiobesidade e antidiabética mais altas do que o resveratrol livre após a digestão gastro-intestinal (AHMAD; GANI, 2021). Em outro trabalho, as NPA de quinoa carregadas com piroxicam intensificaram a atividade anti-inflamatória *in-vitro*, mostrando aproximadamente 78% da liberação do medicamento em HCl 0,1N após 2h (BHATIA; ROHILLA, 2020).

Lima et al. (2021) verificaram que NPA baseadas em amido de mandioca (AM) e amido de batata (AB) podem ser usadas para encapsulamento antocianinas (eficiência de encapsulamento ≈11%). Essas NPA carregadas com antocianinas de jambolão foram completamente dispersas em água e água acidificada em temperatura ambiente. Esses resultados sugerem que as NPA contendo antocianinas podem ser usadas como corante alimentar natural. Recentemente, Escobar-Puentes et al. (2020) produziram NPA a partir de amido de milho para estabilizar antocianinas, e obtiveram nanomateriais que poderiam ser utilizados para a liberação controlada de compostos bioativos visando aplicações como embalagens biodegradáveis de alimentos ou como aditivos antioxidantes na indústria alimentícia.

Na mesma linha, De Oliveira et al. (2018) usaram amido acetilado (mandioca e amido oxidado) para produzir NPs carregadas com ácido gálico (AG) e hidroxitolueno butilado (HTB). As NPs resultantes exibiram alta estabilidade térmica e eficiência de encapsulamento em torno de 90% para HTB e 10% para AG. Remanan e Zhu (2020) prepararam NPs a partir de quinoa e amido de milho para encapsular e aumentar a biodisponibilidade da rutina, bem como para melhorar a solubilidade em água visando aplicações em alimentos. Da mesma forma, Wu et al. (2020) concluíram que NPs a partir de amido de milho podem ser usadas para armazenar silibinina (SLB). As NPs de amido de milho carregadas com SLB tiveram melhores propriedades de dissolução e biodisponibilidade oral com liberação sustentada do que as NPs de SLB e SLB livres.

Sendo assim, é possível concluir que as NPA possuem grande potencial para melhorar a estabilidade, solubilidade, biodisponibilidade, bem como proteger de condições adversas de processamento e armazenamento de alimentos, e entre outras, de compostos bioativos, a fim de contribuir para o bem-estar e saúde humana.

2.2.3 Encapsulamento da própolis

A própolis apresenta um excelente perfil de compostos fenólicos, como já mencionado anteriormente, e tem despertado grande interesse no setor alimentício. Porém, os compostos têm caráter hidrofóbico, com baixa biodisponibilidade, instabilidade digestiva, rápido metabolismo e excreção, além de apresentar um aroma e sabor forte que limita a sua aplicação na indústria alimentícia. Portanto, o encapsulamento tem se mostrado uma alternativa, melhorando significativamente a solubilidade em água, suas características físico-químicas gerais, e a estabilidade térmica, bem como sua biodisponibilidade oral, que permite a liberação dos compostos bioativos, evitando a degradação dos compostos presentes.

Na literatura, várias pesquisas usaram diferentes matérias de paredes para preservar e estabilizar os compostos bioativos da própolis, e por meio de diferentes técnicas (Tabela 2). Os estudos em sua maioria trazem as características físico-químicas do material de parede empregado, das partículas, no que diz respeito ao tamanho de partículas, eficiência de encapsulamento, potencial zeta, e resultados de análises *in vitro*, em microrganismos.

Além de avaliar as propriedades físico-químicas dos encapsulados, os pesquisadores também têm procurado mostrar sua viabilidade e possibilidade de aplicação. Alguns autores realizaram a microencapsulação de própolis e, sequencialmente, adicionaram as micropartículas em alimentos. Bernardi et al. (2013) aplicaram microcápsulas de extrato de própolis em salame tipo italiano, e os resultados (cor, pH, perda de peso e a_w) foram semelhantes quando comparados com a amostra controle, evitando a oxidação do salame durante o armazenamento. Porém, a amostra com adição das micropartículas da própolis apresentou aceitação sensorial inferior. Em outro trabalho realizado por Spinelli et al. (2015), micropartículas foram produzidas utilizando a goma arábica e capsul (amido modificado), por spray drying. A capsul na proporção 1:20 (m/m) apresentou melhor carregamento do extrato da própolis durante atomização e também os melhores escores de análise sensorial, mascarando sabor e aroma quando adicionados em hambúrgueres de peixe, obtendo um produto com compostos fenólicos, o que proporciona um aumento da atividade antioxidante no produto.

Tabela 2.2. Principais técnicas e materiais de parede utilizados no encapsulamento de própolis nos últimos anos.

Técnica de encapsulamento/Própolis	Material de parede	Principais objetivos	Aplicação em matriz Alimentar	Resultados	Referência
Nanoprecipitação/ liofilização Própolis vermelha brasileira	Policaprolactona / plurônica	Desenvolver NPs poliméricas carregadas com extrato de própolis vermelha brasileira com atividade antioxidante e atividade citotóxica contra *Leishmania (V.) braziliensis*	N.i	As NPs carregadas com extrato de própolis vermelho apresentaram atividade citotóxica em *Leishmania (V.) braziliensis*	Do nascimento et al. (2016)
Nanoprecipitação/ Spray drying Própolis marrom (Egípcia e Brasileira)	Quitosana	Produzir nano em micropartículas (NMIs) carregada de própolis e avaliar sua liberação controlada (*in vitro*), bem como sua atividade anticâncer	N.i	As NMIs apresentaram eficiência de encapsulamento >73%. A nanoencapsulação e a nano-em-microencapsulação de extrato de própolis (EP) apresentaram uma liberação mais controlada e sustentada de EP em comparação com EP livre. Além disso, induziram mais efeito anticâncer do que o EP livre	Elbaz et al. (2016)
Nanoprecipitação Própolis vermelha – Alagoas Brasil	Matriz polimérica Eudragit E100®-plurônico e PCL-Plurônico	Desenvolver NPs poliméricas contendo extrato de própolis e caracterizar suas propriedades físico-químicas, antioxidantes compostos fenólicos, e avaliar o efeito em doenças crônicas e negligenciadas como a leishmaniose	N.i	Tamanho de partículas entre 140,4 a 280,2 nm e potencial zeta entre 54,6 a -12,7 Mv. As NPs de Eudragit E100®-plurônico apresentaram maior eficiência de encapsulamento de flavonoides (65,2-81,2%) enquanto as de PCL-Plurônico apresentaram resultados inferiores (28,0-55,3%), ambas com atividades contra leishmanicidas	Azevedo et al. (2018)
Spray drying Própolis de Tigre	Goma arábica (GO), goma de galactomanano (GG) (vinal) e	Desenvolver NPs de própolis utilizando diferentes matrizes de gomas com potenciais antioxidantes	N.i	A eficiência de encapsulamento foi > 81%. A adição de gomas influenciou de forma positiva na encapsulação dos compostos fenólicos. Sistema com GO	Busch et al. (2017)

	maltodextrina (MD)			apresentou menor conteúdo de fenólicos na superfície e maior na parte interna do material	
Spray drying Própolis verde brasileira	γ-Ciclodextrina (γCD)	Encapsular EP verde brasileira em γCD e avaliar o potencial anti-inflamatório no fígado de camundongo *in vivo*	N.i	O EP apresentou propriedades anti-inflamatórias e pode ser utilizado em processos inflamatórios crônicos	Rimbach et al. (2017)
Spray drying Própolis brasileira marrom, verde e vermelho	Goma arábica e MD	Caracterizar os extratos de diferente própolis, desenvolver pós desidratados utilizando goma arábica e MD como materiais de parede, bem como verificar a capacidade de reter compostos bioativos	N.i	A eficiência de encapsulamento foi entre 70-79% e apresentou boa retenção dos compostos bioativos. Micropartículas de própolis vermelha e verde apresentaram maiores teores de fenólicos totais e flavonoides quando comparados às micropartículas de própolis marrom, independentemente do material encapsulante	Andrade et al. (2018)
Spray drying Própolis marrom brasileira	Proteínas do arroz, ervilha, soja e ovoalbumina	Microencapsular o EP utilizando diferentes proteínas por spray drying e analisar a digestão *in vitro* em alimentos com alto teor de açúcar e gordura	queijo Minas frescal e pudim	A eficiência de encapsulamento foi > 70% e manteve-se a atividade antioxidante da própolis. A micropartículas de proteína de ervilha quando aplicadas no queijo tiveram o melhor perfil de liberação controlada dos compostos nas condições intestinais, atingindo 89,64% de liberação após 300 min de digestão *in vitro*, e para o pudim, a melhor liberação foi da proteína de arroz, liberando 100% dos compostos fenólicos na fase intestinal	Jansen-Alves et al. (2018)
Spray drying	Quitosana/ MD	Avaliar o efeito de revestimentos à base de quitosana comestível contendo extrato de própolis etanólico na preservação de filés	Filé de peixe cachama	O revestimento comestível com quitosana-extrato de própolis aumentou em até 8 dias a vida útil do filé de peixe	Márquez; Fuenmayor; Suarez

Própolis não especificada colombiana				As amostras revestidas com extrato de própolis etanólico previamente microencapsuladas em maltodextrina apresentaram percepção sensorial mais desejável e melhor textura, comparadas tanto aos filés não revestidos, e também quando comparado quanto aos filés revestidos com quitosana contendo as mesmas concentrações de extrato de própolis.	mahecha (2018)
Spray drying e liofilização Própolis da Nova Zelândia	Ciclodextrinas (CD) (α, β, γ)	Desenvolver NPs e avaliar a atividade anti-câncer gastro-intestinal e anti-inflamatórias das própolis encapsulada por CD (α, β, γ)	N.i	O γCD foi mais eficaz para encapsular a própolis da Nova Zelândia. As NPs apresentaram propriedades anti-proliferativo e anti-inflamatória indicando benefícios à saúde gastro-intestinal	Catchpole et al. (2018)
Spray drying Própolis não especificada da Turquia	MD, proteína de soro de leite isolada (PSI) e óleo de girassol	Investigar os efeitos da taxa de homogeneização (rpm), temperatura de entrada e saída nas propriedades físicas e químicas das micropartículas e aumentar a estabilidade dos compostos antioxidantes e fenólicos	N.i	Micropartículas obtidas em altas temperaturas de entrada e saída, e baixa taxa de homogeneização apresentaram maiores atividades antioxidantes e teores de fenólicos totais, com eficiência de encapsulamento variando entre 29,79 e 99,73%	Baysan; Elmas; Koç (2019)
Spray drying Própolis vermelha Brasileira	Caseí natos (CSPV10, CSPV18, CSPV28 e CSPV35)	Desenvolver partículas e avaliar as propriedades físico-químicas, propriedades antioxidantes, antibacterianas	N.i	Particulas em escala de micro a nanométrica entre 5263 e 41,32 nm, potencial zeta variando entre -32,1 a -42,4 mV. Os caseínatos CSPV50 e CSPV35 apresentaram os melhores valores de atividades antioxidante. Os extratos de própolis vermelha e	Do Nascimento et al. (2021)

				caseínatos apresentaram atividade antibacteriana	
Spray drying Própolis marrom brasileira	Proteína de ervilha (PDE)	Avaliar a influência de diferentes concentrações de extrato de própolis e também de PDE na atividade antioxidante e antimicrobiana de micropartículas	N.i	A eficiência de encapsulamento variou entre 49,40%-97,00%. As maiores eficiências foram observadas com o uso de 5% de extrato de própolis e 2% de PDE. Micropartículas preparadas com 2% de PDE e 2,5 e 5% de EP apresentaram atividade antimicrobiana contra *L. monocytogenes e S. aureus*	Jansen-Alves et al. (2019)
Spray drying/ spray-chilling A própolis vermelha, originária do Nordeste brasileiro	gordura vegetal e goma arábica	Produzir partículas obtidas por três técnicas: spray-drying, spray-chilling e spray-drying em combinação com spray-chilling e avaliar as propriedades físico-químicas e a cinética de liberação dos compostos bioativos foi avaliada em ensaios de digestão simulada *in vitro*	N.i	As partículas que apresentaram os melhores resultados na preservação dos compostos bioativos foram produzidas combinando as técnicas de spray-drying e spray-chilling. O estudo da liberação gastrointestinal apresentou liberações distintas em todas as fases (oral, gástrica e intestinal).	Sa et al. (2023)
Processo de secagem As próplis foram coletadas de Haryana, Punjab e Himachal Pradesh da Índia durante março a setembro de 2020	Mantodextrina (DE20)	Desenvolver pó de própolis seco a vácuo, sem álcool e rico em polifenóis		Os resultados mostraram maior TPC (20,98–30,91 mg GAE.g^{-1}), higroscopicidade entre 9,12–15,41%, valor de brancura de 66,13–74,85, e solubilidade entre 61.29 - 45,27%.	Pant et al. (2022)
Liofilização	Goma arábica	Investigar o efeito da digestão gastrointestinal dinâmica seguida de um	N.i	A bioacessibilidade foi maior para o EEPB encapsulado (21,4%-57,6%) do	Alencar et al. (2023)

A própolis vermelha crua foi coletada em Maceió, estado de Alagoas, Brasil (S 9° 38′ 53.3004" W 35° 43′ 2.0604") em novembro de 2019		modelo celular de permeabilidade intestinal na estabilidade dos compostos ativos e nas propriedades biológicas do extrato etanólico de própolis vermelha brasileira (EEPB), encapsulado ou não. Além disso, investigar a toxicidade aguda in vivo deste extrato após a digestão.		que para o não encapsulado (19,3%-30,2%). O encapsulamento afetou negativamente as atividades antioxidantes e anti-inflamatórias do EEPB após o transporte de células Caco-2. O EP pode ser considerado como tendo baixa toxicidade.	
Complexação A própolis foi coletada de colméias localizadas em Meydavoud, província de Khuzestan (a latitude é 31,4360 °N e a longitude é 49,0413 °E (coordenadas geográficas)), Irã no início de novembro.	Goma de amêndoa (AG) e caseinato de sódio (CAS)	Estudar a estabilidade térmica, a atividade antimicrobiana, a liberação gastrointestinal e a citotoxidade dos extratos e dos extratos encapsulados.	N.i	A estabilidade térmica e a atividade antibacteriana da própolis foram melhoradas após o encapsulamento. A própolis apresentou maior atividade antibacteriana contra bactérias Gram-positivas do que Gram-negativas. A própolis encapsulada mostrou uma liberação controlada em vários simuladores de alimentos e ambientes gastrointestinais. A avaliação da apoptose e o ensaio de MTT confirmaram que a própolis encapsulada induz menor citotoxicidade do que a própolis pura contra a linha celular de fibroblastos.	SALEHI et al. (2023)
Atomização assistida por fluidos supercríticos	Hidroxipropil-b-ciclodextrina(HPβCD)/ Polivinilpirrolidona(PVP)	Investigar a melhor relação própolis/material para encapsular o extrato de própolis	N.i	Partículas com alto conteúdo de polifenol são obtidas para ambos os transportadores, com eficiência de encapsulamento >90%. As formulações R= 1/5 para EEP-HPβCD e R= 1/3 para	Di Capua et al. (2018)

Própolis não especificada do Chile				EEP-PVP apresentaram os melhores resultados	
Difusão em emulsão Própolis egípcia marrom.	Emulsão: Álcool polivinílico (PVA), água destilada, álcool etílico	Avaliar o efeito de NPs de própolis no tratamento de fibrose hepática induzida por CCl_4 e nefropatia em modelo de rato albino	N.i	Os tamanhos de partícula obtidos variaram entre 5 e 10 nm. As NPs de própolis investigadas mostraram potencial no reparo do tecido renal, potencializam a regeneração dos hepatócitos; e também ajuda na recuperação na destruição hepatobilia	Izzularab; Megeed; Yehia (2020)
Método de difusão de solvente a quente própolis verde	Surfactantes: poloxâmero/lecitina de soja	Desenvolver NPs de própolis e avaliar sua atividade antimicrobiana *in vitro* contra *S. aureus* e isolados de leite mastítico, bem como a citotoxicidade para células epiteliais de mamária bovina.	N.i	Os tamanhos de partícula obtidos variaram entre 181 e 201 nm. A eficiência de encapsulamento variou entre 73 e 91%. As NPs apresentaram potencial antimicrobiano contra cepas de *S. aureus* dependendo da concentração e da formulação. As melhores formulações foram com 5% EP, 1% poloxâmero e 0,25 % lecitina; e 7% extrato de própolis, 4% poloxâmero e 1 % lecitina	Machado et al. (2019)
Emulsão óleo-em-água (O/A) Extrato etanólico de própolis (EEP) da Tailândia	Poli (ácido lático-co-glicólico) (PLGA)	Produzir NPs de PLGA carregadas EEP, e avaliar o perfil de liberação *in vitro*, a citotoxicidade e efeito inibitório contra a levedura patogênica *C. albicans*	N.i	As NPs de EEP apresentaram tamanho de partícula <500 nm e potencial zeta entre -1,2 ± 1,1 mV e -3,9 ± 0,5 mV, com eficiência de encapsulamento ~90%, com efeitos inibitórios sobre o crescimento de *C. albicans*	Iadnut et al. (2019)
Automontagem por interação eletrostática	quitosana (CS) e ácido hialurônico (HA)	Investigar as razões ideais de CS/HA e núcleo/parede para a formulação de nanopartículas carregadas com extrato de própolis (PE-NP), e os efeitos do PE-NP na solubilidade e estabilidade.	N.i	As proporções de CS para HA e núcleo para o material da parede ideal para a formulação de PE-NP foi 4:7 e 1:2, respectivamente. o PE-NP aumentou significativamente a solubilidade do PE	Kim et al. (2023)

				em 2,43 vezes em comparação com o PE livre.	
Automontagem eletrostática e hidrofóbica Própolis coletada na primavera em colônias de abelhas, A. *mellifera L.,* com choupo *(populus sp.)*	Zeína (Z)/carboximetil quitosana (CBMQ)	Otimizar as formulações com teor de própolis, relação de massa Z/CBMQ e relação massa CMCS/$Ca^{2+,}$ e avaliar a eficiência de encapsulamento, e além disso estudar o perfil de liberação *in vitro* e a atividade antioxidante das NPs	N.i	As NPs apresentaram formas esféricas, tamanho médio de partícula de ∼156 nm, potencial zeta de ∼-30 mV e eficiência de em encapsulamento superior a 83% foi observada na própolis-zeína/CBMQ reticulada de cálcio e com atividade alta de antioxidantes determinadas pelos métodos de ABTS e FRAP.	Zhang et al. (2018)
Emulsificação por inversão de fases Própolis verde de Minas Gerais	Nanoemulsões: óleo de milho, água destilada, monooleato de sorbitano e polissorbato 80	Estudar atividades antimicrobiana e antioxidante, e desenvolver uma nanoemulsão de EP para uso como conservante natural de alimentos	N.i	O EEP apresentou potencial antioxidante superior quando comparado a sua forma livre. As nanoemulsões com partículas entre 20 e 200 nm e valor médio de potencial zeta de $-11{,}61 \pm 0{,}90$ mV. A nanoemulsão foi estável a tratamento térmico e centrifugação, bem como reproduziu as propriedades biológicas avaliadas para o extrato livre, e apresentaram atividade contra bactérias gram-positivas. Os resultados da atividade antioxidante pelos métodos ABTS e DPPH apresentaram valores de IC_{50} variando de 0.023 a 41.47 e de 0.004 a 3.72, respectivamente.	Seibert et al. (2019)
Gelificação ionotrópica	Alginato	Desenvolver NPs a partir de extrato de própolis e extrato de jabuticaba encapsulada	N.i	A eficiência de encapsulamento atingiu 89,6% para composto fenólico total e	Dallabona et al. (2020)

Abelha sem ferrão Tubuna (Maringá, Sul do Brasil)		(jabuticaba: extrato de própolis, 2: 1 (V:V)) por gelificação ionotrópica usando o alginato, e com BERN		98,1% para concentração de antocianina monomérica total. Micropartículas resistentes ao pH gástrico (1,2) apresentando uma liberação lenta de cerca de 40% em 240 min	
Gelificação iônica Própolis da Malásia	quitosana	Desenvolver NPs de quitosana-própolis em diferentes formulações e estudar seu efeito em inibir a formação de biofilme por *E. faecalis*	N.i	O tamanho de partículas variou entre 247,1 nm e 512,3 nm com potencial zeta entre +35,5 mV e +74,1 mV, e eficiência de encapsulamento >77%. As NPs Inibiram o crescimento de bactérias, bem como a formação de biofilme por *Enterecoccus. faecalis*	Ong et al. (2017)
Gelificação ionotrópica com $CaCl_2$ Própolis não especificada do Egito	Alginato	Avaliar efeito antimicrobiano das NPs de alginato carregadas com própolis contra diferentes bactérias patogênicas	N.i	As NPs estáveis com potencial zeta de −72,26 ± 6,04, e com potencial contra *Salmonella enterica.*e *Staphylococcus aureus*, mas também *Escherichia coli , Proteus vulgaris, Citrobacter diversus*	Hegazi; El-Houssiny; Fouad (2019)
Sol-gel Própolis não especificada Bulgária	Prata/Ag-sílica	Produzir NPs de prata contendo sílica mesoporosa Ag-SBA-15 e Ag-MCM-41 carregados com própolis e estudar a liberação *in vitro* e atividade antimicrobiana em *Staphylococcus aureus*, *Escherichia coli* e *Candida albicans*	N.i	Eficiência de encapsulamento >71%. Os sistemas de sílica-prata carregados de própolis mostraram um efeito sinérgico da prata e da própolis contra cepas de bactérias e fungos	Popova et al. (2018)

N. i: Não informado. Fonte: A autora (2021).

Posteriormente, Reis et al. (2017) obtiveram microcápsulas de Capsul carregadas com extrato de própolis com eficiência de encapsulamento de 76 - 78% e as aplicaram em hambúrguer de peixe para reduzir a oxidação lipídica e, consequentemente, aumentar a vida útil desse produto. Os resultados mostraram uma inibição da deterioração oxidativa no produto, porém estudos seriam necessários para identificar uma concentração menor, para suavizar o sabor. Jansen-Alves et al. (2018) produziram microcápsulas de extrato de própolis pela técnica de spray drying utilizando diferentes materiais de parede (proteínas do arroz, ervilha, soja e ovoalbumina), e as adicionaram em duas matrizes alimentares, o queijo Minas frescal e pudim. Foi observado que a atividade antioxidante das micropartículas de própolis encapsuladas foi superior a 73%. E as amostras usando a proteína de ervilha como composto encapsulante foi mais eficaz no queijo Minas frescal.

Microcápsulas de quitosana/maltodextrina (MD) carregadas com extrato da própolis foram aplicadas em filés de peixe, e avaliou-se a qualidade delas durante 20 dias. Pode-se observar que a oxidação lipídica secundária dos músculos revestidos foi 12% a 15% menor em comparação com as amostras não revestidas após 12 dias, bem como melhora de sabor, odor e textura, e as amostras revestidas com quitosana/MD tiveram maior preferência pelos avaliadores (PIEDRAHÍTA MÁRQUEZ; FUENMAYOR; SUAREZ MAHECHA, 2019).

Zhang et al. (2018), sintetizaram NPs de grau alimentício como portadores de própolis a fim de expandir a biodisponibilidade oral. As NPs de própolis apresentaram atividade antioxidante e aumento na hidrossolubilidade, sugerindo que o complexo zeína/carboximetil quitosana foi eficiente e pode ser aplicado na indústria alimentícia, cosmética e farmacêutica. Nesse estudo não foi realizado estudo de análise sensorial.

Porém, ainda são poucos as referências que mostram a aplicação do extrato de própolis estabilizado na forma de nanopartícula ou micropartículas ou na forma de emulsões em sistemas alimentícios. Acredita-se que o maior desafio é estudar o sinergismo entre os compostos bioativos e o material encapsulante dentro de uma matriz alimentar, bem como avaliar sua influência no comportamento e nas propriedades dos alimentos, além da sensorial.

O desenvolvimento de novos produtos incorporados de compostos bioativos naturais destaca-se como uma estratégia de marketing interessante para a indústria, especialmente para produtos que requerem apelo de saudabilidade, como produtos de confeitaria (as balas), visto que é um produto consumido por um grupo de consumidores de crianças a idosos. Assim, sua fortificação com compostos fenólicos é uma forma de fornecer compostos benéficos para a saúde humana e atingir maior público (CAPPA; LAVELLI; MARIOTTI, 2015).

Nesse contexto, até o momento não existem relatos da produção de NPA de batata e de mandioca pela técnica de precipitação antissolvente estabilizando os compostos bioativos da própolis. Portanto, o objetivo foi obter nanopartículas de amido para estabilizar os compostos bioativos da própolis empregando a técnica de nanoprecipitação antissolvente e aplicar as nanopartículas como fonte de compostos fenólicos em balas de gelatinas.

CAPÍTULO 3

PRODUÇÃO E CARACTERIZAÇÃO DE NANOPARTÍCULAS DE AMIDO DE BATATA E DE MANDIOCA PELA TÉCNICA DE NANOPRECIPITAÇÃO ANTISSOLVENTE

Apresentado na forma de artigo

3 IMPACT OF THE ACIDIFIED HYDROETHANOLIC CONCENTRATION ON THE PHYSICOCHEMICAL PROPERTIES OF STARCH NANOPARTICLES PRODUCED BY ANTI-SOLVENT PRECIPITATION

Este capítulo relata a primeira fase experimental desta tese: produção e caracterização de nanopartículas de amido.

A partir desta etapa, foi escrito o primeiro trabalho de pesquisa, intitulado "Impact of the Acidified Hydroethanolic Solution on the Physicochemical Properties of Starch Nanoparticles Produced by Anti-Solvent Precipitation" publicado no Starch (fator de impacto (2021): 2.741; https://doi.org/10.1002/star.202100034). De acordo com as regras de assinatura da Wiley, os autores se reservam o direito de incluir o artigo em uma tese, desde que não seja publicado comercialmente.

Graphical abstract

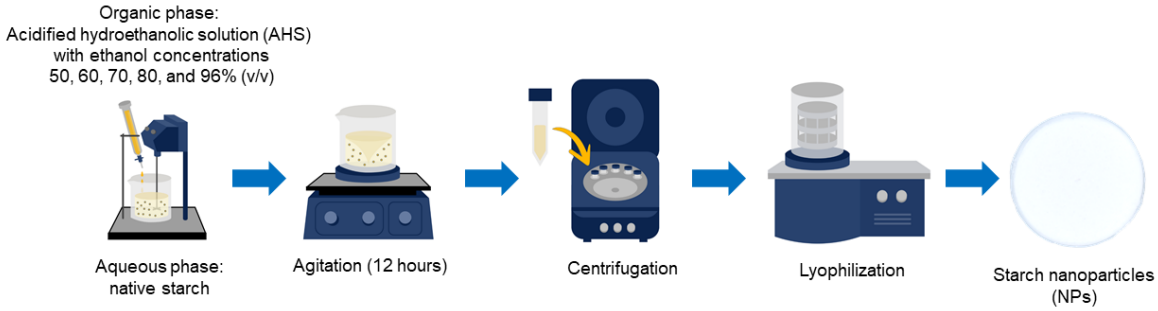

- Starch NPs were produced by antisolvent precipitation using different AHS.
- Particle size and surface charge of starch NPs were impacted with the ethanol concentration used in the AHS.
- Starch NPs have V-type crystalline structure and they were soluble in water at 30 ºC.

Abstract

This study aimed to understand the effect of the acidified hydroethanolic solution with different ethanol concentrations (50, 60, 70, 80, and 96%) on the physicochemical properties of potato and cassava starch nanoparticles (NPs) obtained by anti-solvent precipitation (AP). The recovery efficiency (RE) was investigated, and the starch NPs were characterized by particle size, surface charge, chemical bonds, crystalline structure, thermal properties, moisture content, water activity, solubility in water, and swelling factor. The starch NPs had particle size lower than 1000 nm and V-type crystalline structure. Furthermore, these nanomaterials showed high solubility values in water at 30 ºC and 90 ºC. In general, the ethanol concentration used in

the acidified hydroethanolic solution altered the RE, particle size and surface charge of nanoparticles.
Keywords: cassava starch; food gummies; nanoprecipitation; potato starch.

Abbreviations

AP: anti-solvent precipitation; a_w: water activity; CS: cassava starch; DLS: Dynamic light scattering; DSC: differential scanning calorimeter; DTGA: Differential thermal analysis; FTIR: Fourier-transform infrared; MC: moisture content; NPs: nanoparticles; CSNPs: starch nanoparticles based on cassava starch; PSNPs: starch nanoparticles based on potato starch; PS: potato starch; RC: Relative crystallinity; RC: Recovery efficiency; S: solubility in water; SF: swelling factor; TGA: thermogravimetric analysis; TPA: texture profile analysis; T_o: gelatinization onset temperature; T_p: gelatinization peak temperature; T_c: gelatinization conclusion temperature; ΔH: gelatinization enthalpy.

3.1 INTRODUCTION

Starch nanoparticles (NPs) are structures based on starch chains having at least one dimension between 1 and 1000 nm (CAMPELO; SANT'ANA; PEDROSA SILVA CLERICI, 2020; SUN, 2018a). These NPs have different thermal and solubility in water properties than those found in native starches, being promissory ingredients to be used in food applications (CHACON et al., 2020a; SUN, 2018a). Starch NPs are produced by "top-down" approaches through a breakdown of starch granules using physical, chemical, or enzymatic treatments (ANDRADE et al., 2020; CHACON et al., 2020a; SUN, 2018a).

Anti-solvent precipitation (AP) also known as nanoprecipitation is a chemical method used to produce starch NPs. In this approach, the starch granules are gelatinized, cooled, and then precipitated by the addition of an organic solvent (anti-solvent) dropwise to the starch solution (CHACON et al., 2019, 2020a; LIMA et al., 2021). According Joye and Mcclements (2013) the main driving force for the formation of NPs during AP is the imbalance of molecular interactions between anti-solvent, solvent, and solute. Particularly, at certain anti-solvent/solvent combinations, the solute-solute interactions are strong enough when compared with the solute-solvent or solute-antisolvent interactions. In this way, the solute precipitate forming nanomaterials. The main factors affecting the production of NPs by AP are the type of

solvent, anti-solvent, and temperature, as well as the mechanical stirring used to avoid NPs aggregation. AP is considered a simple and low cost technique used to produce food-grade NPs with controlled particle size (CHACON et al., 2019; CHIN; PANG; TAY, 2011).

Ethanol has been the most used organic solvent (anti-solvent) to precipitate starches previously gelatinized in water by AP (CHACON et al., 2019, 2020a; HEBEISH et al., 2014; QIN et al., 2016). Recently, Lima et al. (2021) observed that an acidified hydroethanolic solution (pH = 1) can be used as solvent to stabilize anthocyanins and as anti-solvent to precipitate cassava and potato starches by AP. After the precipitation, the authors observed cassava and potato NPs with particle sizes lower than 1000 nm, trapping anthocyanins in their structures. In this way, the acidified hydroethanolic solution could be used as an organic solvent to disperse bioactive compounds to be stabilized during the formation of starch NPs by AP. The main disadvantage of the AP method is the large volume of ethanol used to separate the starch from the water solution (CHACON et al., 2019, 2020a; HEBEISH et al., 2014; QIN et al., 2016). In the reviewed literature, no study has explored the effect of ethanol concentration used in the acidified hydroethanolic solutions and their impact on the physicochemical properties of starch NPs produced by AP.

Therefore, the objective of this present research was to study the effect of the ethanol concentration used in the acidified hydroethanolic solutions during the production of starch NPs by AP and its impact on the particle size, surface charge, chemical bonds, crystalline structure, phase transitions, moisture content, water activity, solubility in water, and swelling factor of these materials.

3.2 MATERIALS AND METHODS

3.2.1 Materials

Cassava starch (CS) and potato starch (PS) were purchased from Juréia and Shambala Naturais Food Industries (Santa Catarina, Brazil), respectively. Distilled water, ethanol (≥ 99.5%, Êxodo Científica, Brazil) and hydrochloric acid (37 wt%, Neon, Brazil) were used as solvents. Type A gelatin (Gelnex, Brazil) with 260 Bloom and 30 Mesh was used as a protein to manufacture the gummies.

3.2.2 Preparation of the starch nanoparticles

Starch NPs were prepared by the precipitation of CS and PS using the AP technique (CHACON et al., 2019, 2020a). Firstly, starch granules (2.5 g) were hydrated in 50 g of distilled water at 25 ºC for 30 min, under constant agitation (300 rpm). Thereafter, starch granules suspensions were gelatinized by heating at 90 ºC for 30 minutes. The starch suspensions were cooled to 30 ºC and then an acidified hydroethanolic solution was added drop wise for the gelatinized starch in a 1:1 (% v/v) ratio. The acidified hydroethanolic solution was prepared by diluting the absolute ethanol in water to obtain solutions with ethanol concentrations of 50, 60, 70, 80, and 96% v/v. Then, the hydroethanolic solutions were acidified by blending with hydrochloric acid (100:1 v/v, hydroethanolic solution:HCl 37 wt%, pH = 1).

The resulting slurry obtained after the mixture of the gelatinized starch suspension with the acidified hydroethanolic solution was kept in magnetic agitation with constant stirring for 12 hours. Then, the slurry was centrifuged at 25 ºC, using a centrifuge (Kasvi, Brazil) with 1700xg force at 4000 rpm for 15 minutes to separate the starch NPs from the solvents. Starch NPs were centrifuged three times with an ethanol solution in water (80% v/v), and finally washed with absolute ethanol (99.6%). The starch NPs were removed by centrifugation using the same centrifuge and then the ethanol in the samples was evaporated using a forced-air convection oven (Solidsteel, Brazil) at 60 ºC for 10 min. In sequence, the starch NPs were frozen at -24 ºC for 48 h, and finally lyophilized (Liotop L 101). The resulting starch NPs based on CS and PS were finely macerated and stored in desiccators with controlled relative humidity (RH) of 10% at 25 °C for 14 days before analysis. PS and CS also were conditioned at 10% RH for 14 days.

3.3 CHARACTERIZATION OF THE STARCH NANOPARTICLES

3.3.1 Recovery efficiency (RE)

The RE was calculated according to Eq. (3.1):

$$\text{RE}\ (\%) = \frac{\text{DW}_{\text{NPs}}}{\text{DW}_{\text{native starch}}} * 100 \qquad (3.1)$$

where DW_{NPs} is the dry weight of starch NPs obtained after lyophilization (g) and $DW_{native\ starch}$ is the dry weight of each native starch used to produce starch NPs (g).

3.3.2 Particle size distribution and surface charge

Dynamic light scattering (DLS) measurements were performed using a LUMiSizer (LUM GmbH, Germany) and a Zetasizer Nano ZS (Malvern, England) to analyze the native starches (CS and PS) and starch NPs. Before analyses, the suspensions based on native starches (0.5% w/v) and starch NPs (0.03% w/v) in ultrapure Mili-Q water were sonicated for 30 min at 40 KHz, using a sonicator bath (Ultracleaner 1650, Unique, Brazil) (AHMAD et al., 2019).

Zetasizer Nano ZS (Malvern, England) was used to study the surface charge of native starches and starch NPs. Before analyses, the samples were diluted in deionized water (0.03%, w/v), controlling pH (pH = 6), and sonicated at 40 KHz for 30 min in the same sonicator bath.(AHMAD et al., 2019).

3.3.3 Chemical bonds

Fourier-transform infrared spectrometer (FTIR, Cary 600, Agilent, US) was used to evaluate the chemical bonds of native starches and starch NPs. The spectra were obtained in the infrared region between 4000 and 400 cm^{-1} and using 4 cm^{-1} resolution. In each analysis were performed 32 scans. Samples were blended with KBr before analyses (CAPELLO et al., 2019).

3.3.4 Crystalline structure

Native starches and starch NPs were analyzed using an X-ray diffractometer (Rigaku MiniFlex 600 DRX, Japan) equipped with Cu-Kα radiation (λ = 0.154056 nm) in the diffraction ranges (2θ) between 3 and 60° and using a rate of 10 °/min (CHACON et al., 2019). The Eq. (3.2) (Bragg's law) was used to calculate the interplanar spacing d (nm) from the diffraction angle at the maximum intensity of the peaks/halos found in the X-ray diffractograms.

$$n\lambda = 2d\sin\theta \tag{3.2}$$

where n is the reflection order (n = 1), λ is the wavelength of CuKα radiation, and θ is the reflection angle.

Relative crystallinity (RC, %) in each sample was calculated using Eq. (3.3) proposed by Komiya.Nara and Komiya (1983) .

$$RC\ (\%) = \left(\frac{A_c}{A_c + A_a}\right) * 100 \quad (3.3)$$

where A_c and A_a are the areas related to the crystalline and amorphous regions in the X-ray diffractograms for each sample, respectively.

The starch crystallinity also was studied using a polarized light microscopy.(YU et al., 2015) Firstly, suspensions based of native starches and starch NPs in distilled water were prepared and then placed on a slide and finally covered with glycerin and a coverslip. Native starches and starch NPs were photographed using a polarizing light microscope (ML-9400, Meiji, Japan) with 10× and 20× magnification, equipped with a camera with a trinocular tube attached to a USB camera (1.2 megapixel). Photos were taken at random sample spots using the free software AMCAP (AMCAP Direct Show Video Capture Sample v.8.12, ©Microsoft Corp.).

3.3.5 Thermal properties

Thermal transitions of suspensions based on native starches and starch NPs in distilled water were analyzed in a differential scanning calorimeter (DSC, PerkinElmer Jade®, USA), using hermetically sealed aluminum pans. Native starches and starch NPs were weighed in aluminum pans and mixed with distilled water in a 1:2 w/w starch:water ratio. An empty aluminum pan was used as reference. The pans were sealed hermetically and allowed to equilibrate for 1 h at room temperature and then heated from 20 to 90 °C, with a heating rate of 10 °C/min, under a N_2 flow rate of 45 mL/min (QIN et al., 2016). Thermal transitions related to the starch gelatinization such as onset (T_o), peak (T_p), and conclusion (T_c) temperatures, as well as enthalpy (ΔH, expressed in Joules per gram of dry starch) were obtained from the DSC thermograms using Pyris Data Analysis software®.

Thermal stability of native starches and starch NPs was studied using a thermogravimetric balance (TGA/DTA STA 449 F3 Jupiter, Netzsch, Germany). Native starches and starch NPs (10 mg) were heated from 30 to 700 ºC, using a heating rate of 10

ºC/min and a platinum pan as reference. Thermogravimetric analysis were carried out using a flow of 100 mL/min of dry N_2 (CAPELLO et al., 2019).

3.3.6 Moisture content and water activity

The moisture content (MC) of native starches and starch NPs was determined gravimetrically using a forced-air convection oven (Odontobras, Brazil) at the temperature of 105 °C. The samples were weighted periodically until there was no further mass variation (≈ 24 h).(MERZ et al., 2020) MC values were expressed as gram of water per gram of dry material.

The water activity (a_w) of native starches and starch NPs was carried out at 25 ºC using a water activity meter (Aqualab Model Series 3 instrument, Decagon Devices Inc., Pullman, WA, USA).(CHACON et al., 2020a)

3.3.7 Solubility in water and swelling factor

Solubility in water (S) and swelling factor (SF) tests were carried out according to the methodology proposed by Andrade-Mahecha et al.(ANDRADE-MAHECHA; TAPIA-BLÁCIDO; MENEGALLI, 2012) Firstly, each sample (W ≅ 0,150 g) was mixed with 15 mL of distilled water and heated at 30 or 90 ºC for 30 min, being that each 10 min the samples were shaken for 10 s in a vortex. In sequence, the tubes containing the samples were cooled until room temperature and then centrifuged at 4000 rpm (Kasvi, Brazil) for 15 minutes. The supernatant liquid was placed in crucibles previously weighed and then dried at 105 ºC for 48 hours. In sequence, the remaining weight in the crucible (W_r) was used to calculate S value by Eq. (3.4). The mass of the gelatinous material adhered to the wall of the tube was considered as sediment and it was weighed (W_t) and then used to calculate the SF values using Eq. (3.5).

$$S\ (\%) = \frac{W_r}{W} * 100 \tag{3.4}$$

$$SF = \frac{W_t}{W - W_r} \tag{3.5}$$

3.3.8 Statistical analyses

All the tests were performed at least two times for each sample with exception of TPA analyses which were determined at least three times in each sample. The results were expressed as means ± standard deviation. The experimental data were analyzed using Analysis of variance (ANOVA) and Tukey test with multiple comparisons was performed with a 5% significance level using the software Statistica 10.0 (StatSoft®, USA).

3.4 RESULTS AND DISCUSSIONS

3.4.1 Recovery efficiency

RE increased with the ethanol concentration used in the acidified hydroethanolic solution (Table 3.1), indicating that more ethanol in the solution lead to the starch supersaturation, providing a driving force for starch NPs precipitation.(JOYE; MCCLEMENTS, 2013) In the reviewed literature, no study has investigated the effect of ethanol concentration on the RE of starch NPs obtained by AP.

Table 3.1. Recovery efficiency (RE, %) of starch nanoparticles based on PS (PSNPs) and CS (CSNPs) obtained with different acidified hydroethanolic solutions (50, 60, 70, 80, and 96%).

Sample	RE (%)
PS	-
PSNPs-50%	70.56±3.36[a]
PSNPs-60%	79.73±2.51[ab]
PSNPs-70%	84.26±3.38[b]
PSNPs-80%	78.87±4.24[ab]
PSNPs-96%	83.96±3.81[b]
CS	-
CSNPs-50%	74.52±4.64[ab]
CSNPs-60%	78.96±3.58[ab]

CSNPs-70%	73.12±5.24[a]
CSNPs-80%	87.36±1.24[bc]
CSNPs-96%	90.35±3.93[c]

*All values were expressed as mean ± standard error (n ≥ 3). Means in the same column for the same starch source and followed by different superscripts are significantly different ($p < 0.05$).

3.4.2 Particle size distribution and surface charge

Native starches displayed a monomodal particle size distribution with particle size diameter oscillating between 6 and 50 µm and between 2 and 30 µm in PS and CS, respectively (Fig 3.1). Both particle size distributions are in accordance with those results informed by Chacon et al., (2020a) and Lima et al., (2021) in PS (10 e 100 µm) and CS (2 e 30 µm), respectively.

Fig. 3.1. Particle size distribution of potato starch and cassava starch.

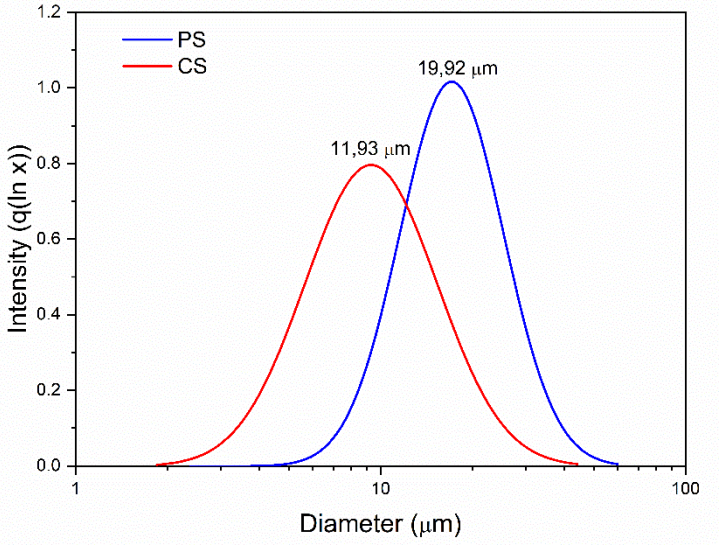

Source: Alves et al. (2021).

NPs presented a bimodal particle size distribution. In this sense, starch NPs based on PS (Fig. 3.2a) and CS (Fig. 3.2b) exhibited a first particle size distribution between 15.3 and 98.8 nm, and a second population with particle size ranged between 157.6 and 588.6 nm. In general, starch NPs based on PS were smaller when compared with those produced using CS (Fig. 3.2). The ethanol concentration used in the acidified hydroethanolic solutions impacted the population of starch NPs with particle size between 157.6 and 588.6 nm. Hence, a reduction

in the particle size of this population was observed when the ethanol concentration was ≥ 80% (Fig. 3.2), confirming that the ethanol concentration has an important role to separate the starch chains from water and then precipitate the starch NPs. According to Campelo; Sant'ana,Clerici (2020) starch NPs could be defined as particles that have at least one dimension smaller than 1000 nm, therefore, in the current research all modified starches by AP can be classified as starch nanomaterials. The particle size distributions obtained in this study are lower than those reported by Ahmad and Gani (2021) studying starch-based nanoparticles (horse chestnut, water chestnut and lotus) stem to encapsulate resveratrol with values between 419 and 797 nm, and Lima et al., (2021) studying starch nanoparticles from PS and CS obtained particle size values between 30 and 100 nm for a first population, and between 200 and 900 for a second population, both authors used the antisolvent precipitation technique and the solvent was pure ethanol.

Fig. 3.2. Particle size distribution of: (a) potato starch nanoparticles (PSNPs); (b) cassava starch nanoparticles (CSNPs), both prepared with different acidified hydroethanolic solutions (ethanol concentration: 50, 60, 70, 80, and 96%).

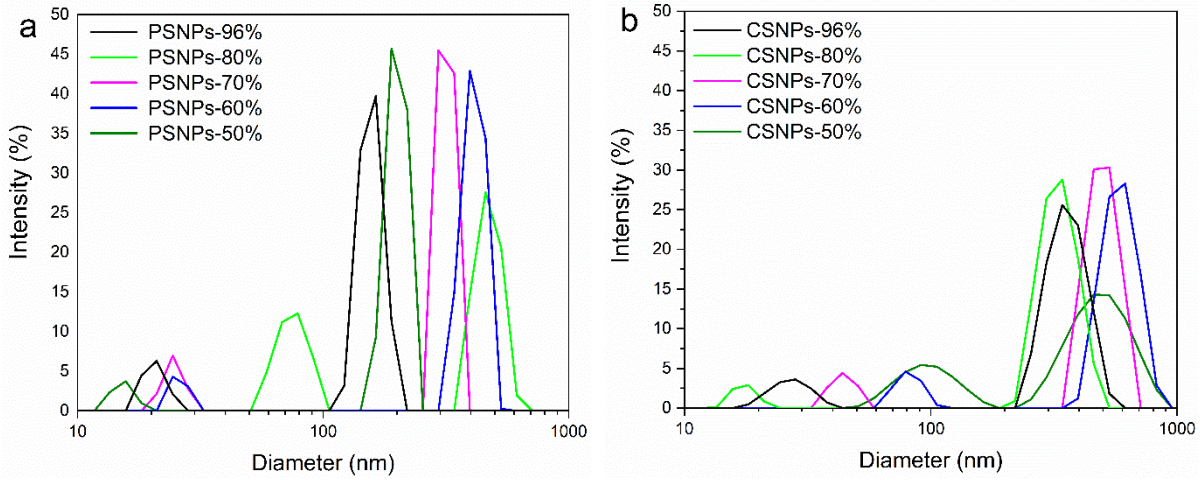

Source: Alves et al. (2021), with permission.

The surface charge (zeta potential) of native starches oscillated between −12.5 mV and −44.0 mV in PS and CS, respectively (Table 3.2).

Table 3.2. Zeta potential (ZP) of potato starch (PS), cassava starch (CS), and starch nanoparticles based on PS (PSNPs) and CS (CSNPs) obtained with different acidified hydroethanolic solutions (50, 60, 70, 80, and 96%).

Sample	ZP (mV)
PS	-12.5±3.04[a]
PSNPs-50%	-22.50±1.22[b]
PSNPs-60%	-21.53±0.93[b]
PSNPs-70%	-26.40±2.76[b]
PSNPs-80%	-23.17±0.21[b]
PSNPs-96%	-24.57±1.25[b]
CS	-43.97±3.87[a]
CSNPs-50%	-20.40±0.44[b]
CSNPs-60%	-18.77±0.97[b]
CSNPs-70%	-17.33±0.74[b]
CSNPs-80%	-20.27±4.52[b]
CSNPs-96%	-16.03±2.06[b]

All values were expressed as mean ± standard error ($n \geq 3$). Means in the same column for the same starch source and followed by different superscripts are significantly different ($p < 0.05$).

A low surface charge in PS could be due to the presence of potassium (phosphate ester groups), as well as by the higher particle size in this raw material when compared with CS(NODA, 2021). Regarding the nanomaterials, all starch NPs had negative surface charge values varying between −21.5 to −26.4 mV for starch PSNPs, and between −16.0 to −20.4 mV for CSNPs (Table 3.2). Starch NPs prepared with PS showed more negative surface charge values due to the smaller particle size in these nanomaterials when compared with those produced using CS. Similar surface charge values were observed by Agi et al. (2019) in starch NPs produced from CS by AP at high temperature (60 ºC), assisted with ultrasonication and using absolute alcohol (palm wine) as an organic solvent, and by Ahmad et al., (2019) in starch NPs produced by AP from horse chestnut, water chestnut, and lotus stem starches, using absolute ethanol as an organic solvent.

3.4.3 Chemical bonds

Regarding the Fourier transform infrared spectra (Fig. 3.3) obtained with native starches, stretching of hydroxyl groups were detected between 3700–3000 cm^{-1} followed by stretching vibrations of C-H groups at 2921 cm^{-1} (AGI et al., 2019; QIN et al., 2016). The band at 1649 cm^{-1} was attributed to bending vibrations of O-H, indicating the presence of water molecules hydrating the starch structure (AGI et al., 2019). The peaks centered at 1168 and 1158 cm^{-1} corresponds to the CO bonds stretching of carbohydrates (VALENCIA et al., 2015b). Stretching of C=O groups were observed at 1082 cm^{-1} (LIMA et al., 2021). The band centered at 1000 cm^{-1} was associated with intramolecular hydrogen bonding of the hydroxyl groups at C-6 and it is typical of materials with partial crystallinity. Finally, the band with peak at 928 cm^{-1} was correlated with the symmetric elongation of C–O–C groups, respectively (Fig. 3.3) (VALENCIA et al., 2015b).

Fig. 3.3. FTIR spectra of: (a) potato starch (PS) and potato starch nanoparticles (PSNPs); (b) cassava starch (CS) and cassava starch nanoparticles (CSNPs). Starch NPs were prepared using different acidified hydroethanolic solutions (ethanol concentration: 50, 60, 70, 80, and 96%).

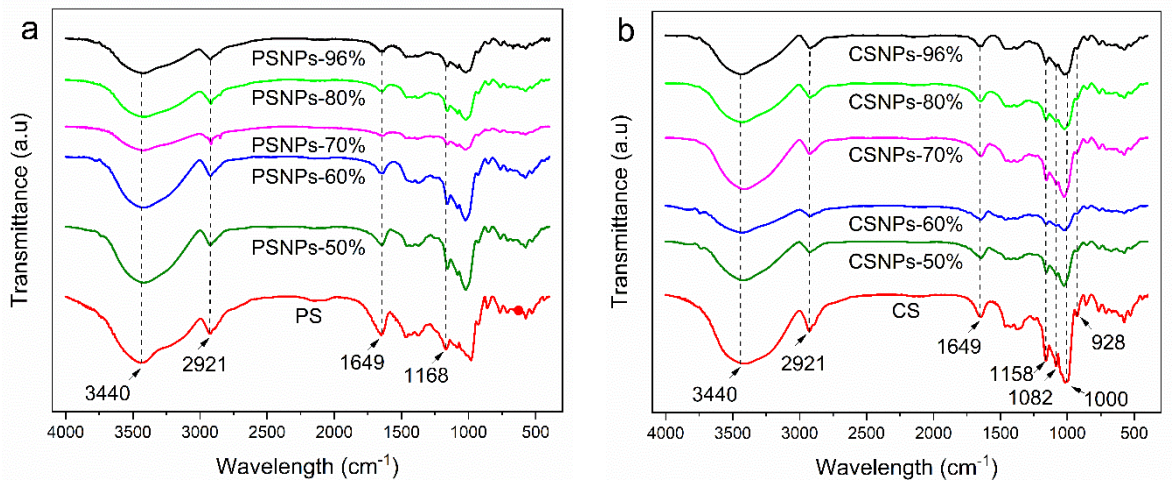

Source: Alves et al. (2021), with permission.

The starch NPs exhibited the same bands observed previously in PS and CS, however the band intensity in starch NPs at 1649 cm^{-1} deceased, suggesting that starch NPs have less water molecules hydrating their structure (Fig. 3.3). Furthermore, a decreasing in the bands centered at 1000 and 928 cm^{-1} indicated that starch NPs have less crystalline regions as a consequence of polymer chain fragmentation during AP (Fig. 3.3) (LIMA et al., 2021).

3.4.4 Crystalline structure

The X-ray diffractograms of native starches were typical of partial crystalline materials. In this way, PS exhibited a diffraction pattern of B-type crystal structure, with diffraction peaks at angles of 2θ ≈ 5° (d = 1.77 nm), 17° (d = 0.52 nm), 19.5° (d = 0.45 nm), 22° (d = 0.40 nm), and 24° (d = 0.39 nm) (Fig. 3.4a). In contrast, CS showed a diffraction pattern of A-type crystal structure, with diffraction peaks at angles of 2θ ≈ 15° (d = 0.59 nm), 17° (d = 0.52 nm), 18° (d = 0.49 nm), and 23° (d = 0.39 nm) (Fig. 3.4b). In the current research, the X-ray diffractograms of PS and CS are in accordance with the literature (CHACON et al., 2019; LIMA et al., 2021; VALENCIA; HENAO; ZAPATA, 2012).

Fig. 3.4. X-ray diffractograms of: (a) potato starch (PS) and potato starch nanoparticles (NPs-PS); (b) cassava starch (CS) and cassava starch nanoparticles (CSNPs). Starch NPs were prepared using different acidified hydroethanolic solutions (ethanol concentration: 50, 60, 70, 80, and 96%). Polarized light micrographs of: (c) PS; (d) CS; PSNPs prepared with an acidified hydroethanolic solution with ethanol concentration of (e) 50% and (f) 96%; and CSNPs prepared with an acidified hydroethanolic solution with ethanol concentration of (g) 50% and (h) 96%.

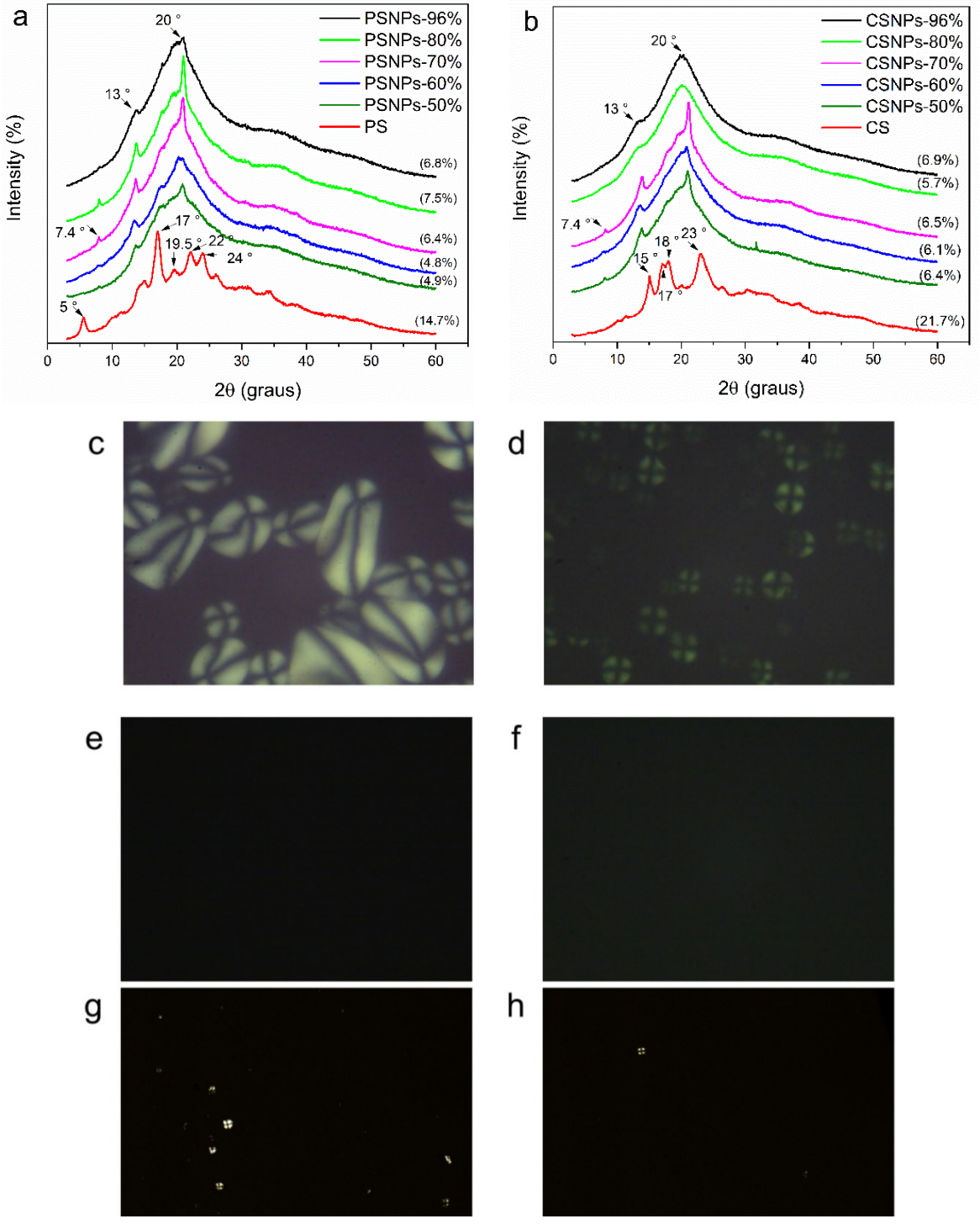

Source: Alves et al. (2021), with permission.

The starch NPs had X-ray diffractograms typical of materials with V-type structure with diffraction peaks at 2θ ≈ 7.4° (d = 1.23 nm), 13° (d = 0.68 nm), and 20° (d = 0.44 nm) (Fig. 3.4a and 3.4b). Similar results were also reported in the literature for starch nanomaterials produced by AP (LIMA et al., 2021; YAN et al., 2018).

In the current research, X-ray diffractograms of starch NPs are in concordance with the reduction in the crystalline regions observed in the FTIR spectra at 1000 cm^{-1} (Fig. 3.3). In the same way, RC values confirmed the crystalline phase reduction in starch NPs, hence, PS and CS had RC values between 14.7 and 21.7%, whereas the RC values in starch NPs oscillated between 4.8 and 7.5% (Fig. 3.4a and 3.4b). The crystallinity decreasing in starch NPs was due to the destruction of crystalline regions in starch granules during gelatinization and precipitation by contact with ethanol (YAN et al., 2018). The Maltese cross typical of native starch granules was observed by polarized light microscopy analyses in PS and CS, confirming the presence of crystalline regions in the studied starch granules (Fig. 3.4c and 3.4d). In contrast, less starch NPs having the Maltese cross were observed by polarized light microscopy analyses, confirming which these materials have a low crystallinity (Fig. 3.4e-h).

3.4.5 Thermal Properties

Regarding the DSC thermograms, PS and CS suspensions in water had an endothermic peak during the heating cycle from 0 to 90 ºC, associated with the starch gelatinization. The endothermic peak was centered between 53 and 58 ºC in PS and between 52 and 59 ºC in CS. Furthermore, ΔH values in PS and CS were 22.33 ± 0.87 and 5.07 ± 0.19 J/g of dry starch, respectively (Fig. 3.5). Differences in ΔH values could be associated with differences in particle size in each starch as discussed in Section 3.5.2 (SINGH; LARA; TLALI, 2017). The ΔH values in PS and CS were comparable with those informed in the literature for the same starches,(KARLSSON; ELIASSON, 2003; VALENCIA; DJABOUROV; DO AMARAL SOBRAL, 2016) as well as when compared with other natives starches (LUCIANO et al., 2017; VALENCIA et al., 2015a, 2015b). In contrast, starch NPs did not have endothermic peak during the heating cycle, confirming the presence of less crystalline structures in these materials, not being detected by DSC. DSC results in starch NPs are in concordance with those previously discussed in FTIR and X-ray results (Fig. 3.5). Lima et al. (2021) also observed the same behavior in starch NPs based on PS and CS prepared by AP.

Fig. 3.5. DSC thermograms of: (a) potato starch (PS) and potato starch nanoparticles (PSNPs); (b) cassava starch (CS) and cassava starch nanoparticles (CSNPs). Starch NPs were prepared using different acidified hydroethanolic solutions (ethanol concentration: 50, 60, 70, 80, and 96%).

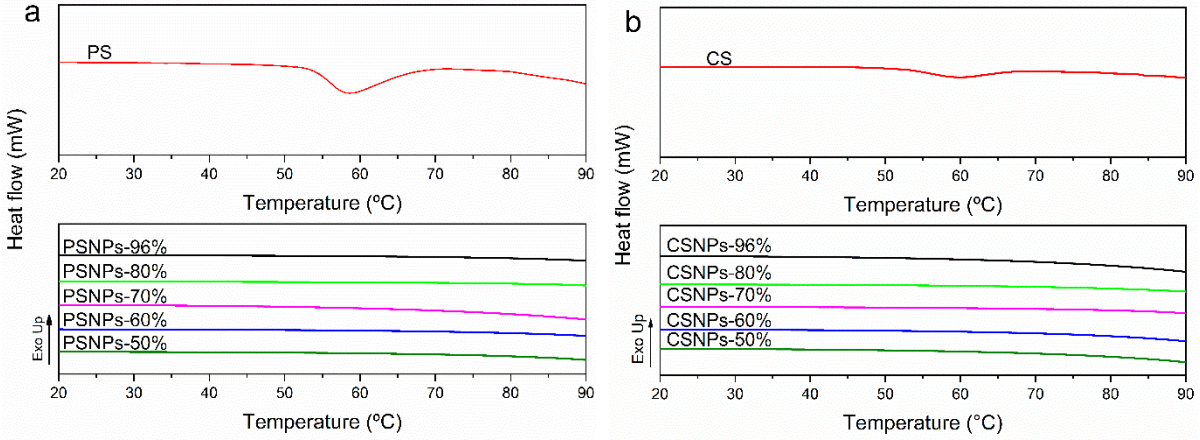

Source: Alves et al. (2021), with permission.

About the thermal stability in native starches and starch NPs, it was observed that PS and CS have three main decomposition stages in the thermogravimetric (TGA) curves (Fig. 3.6a and 3.6b) (CHACON et al., 2019). The first region occurred between 25 and 120 ºC, associated with water evaporation. In sequence, the second stage was observed between 121 and 303 ºC in PS and between 121 and 318 ºC in CS. This second stage was correlated with the devolatilization of starch granules. Finally, the third region at temperatures higher than 303 ºC in PS or 318 ºC in CS were associated to the biochar or unburnt carbon formation (CHACON et al., 2019, 2020b). Differential thermal analysis (DTGA) curves from native starches revealed a peak that was correlated with the end of the second stage in the native starches (Fig. 3.6c and 3.6d). In the present research, the TGA and DTGA curves were typical of native starches (CHACON et al., 2019; LIMA et al., 2021).

Fig. 3.6. Thermogravimetry curves of: (a) potato starch (PS) and potato starch nanoparticles (PS NPs) and (b) cassava starch (CS) and cassava starch nanoparticles (CSNPs). Derivative of the thermogravimetric curves of: (c) PS and PSNPs and (d) CS and CSNPs. Starch NPs were prepared using different acidified hydroethanolic solutions (ethanol concentration: 50, 60, 70, 80, and 96%).

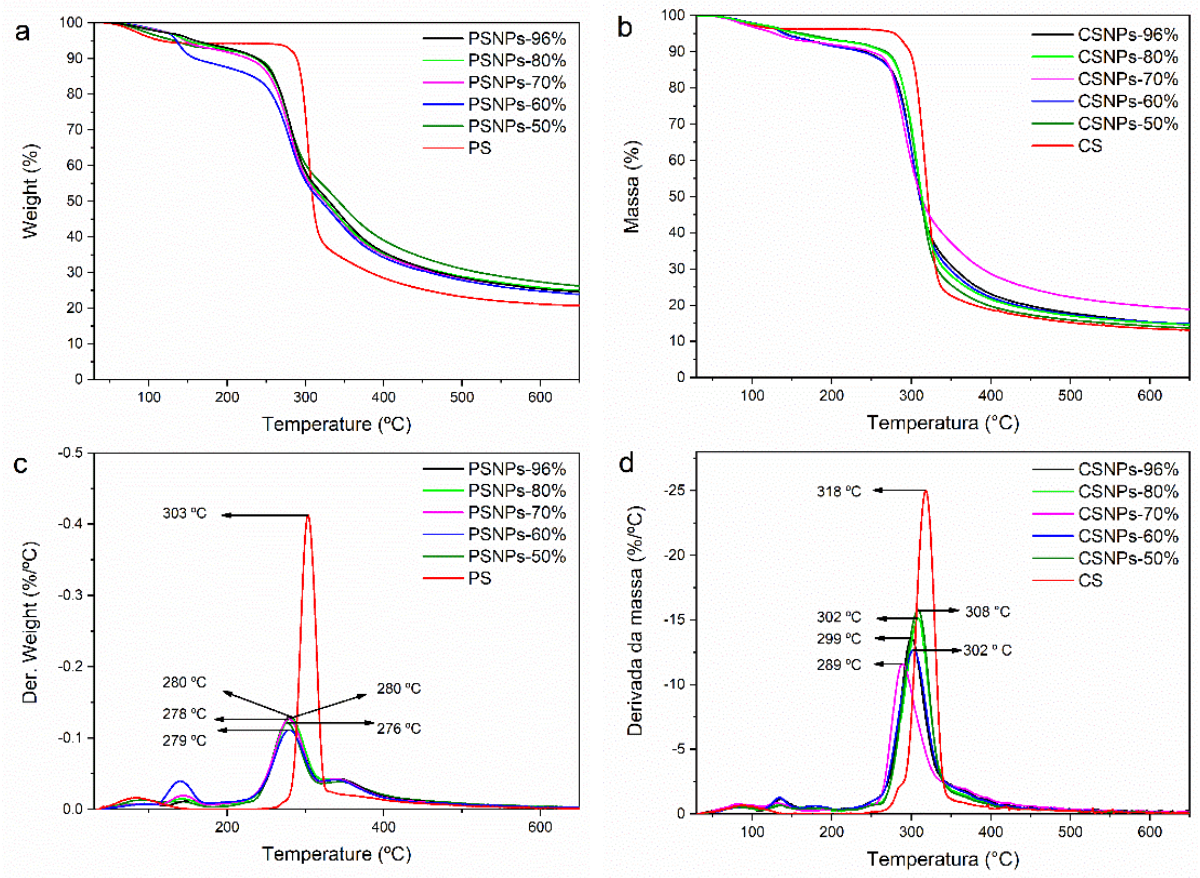

Source: Alves et al. (2021), with permission.

Starch NPs showed the same three decomposition stages observed in the native starches (Fig. 3.6a and 3.6b), however, in the DTA curves (Fig. 3.6c and 3.6d) two peaks were observed. The first peak could be due to the moisture desorption from the surface and the second one was correlated with the decomposition of the studied materials due to the thermal degradation (CHACON et al., 2020b). Interestingly, the second peak in the DTA curves of starch NPs was displaced to lower temperatures when compared with PS and CS (Fig. 3.6c and 3.6d), suggesting that thermal degradation of starch NPs started earlier as a consequence of the particle size reduction in these materials (CHACON et al., 2019).

DSC, TGA, and DTGA results demonstrated that the ethanol concentration used in the acidified hydroethanolic solutions during the production of the starch NPs did not show a considerable effect on the thermal properties of these nanostructures.

3.4.6 Moisture content and water activity

CS and PS moisture content (MC) and water activity (a_w) values oscillated between 10.9 and 14.3% and 0.60 and 0.65, respectively (Table 3.3. MC and a_w values in the native starches are in concordance with the literature and they are typical of foods with moderate chemical and microbiological stability (LIMA et al., 2021).

Table 3.3. Moisture content (MC), water activity (a_w), of potato starch (PS), cassava starch (CS), and starch nanoparticles based on PS (PSNPs) and CS (CSNPs) obtained with different acidified hydroethanolic solutions (50, 60, 70, 80, and 96%).

Sample	MC (%)	a_w
PS	14.34±0.62^{a}	0.65±0.01^{a}
PSNPs-50%	7.56±0.59^{bc}	0.31±0.01^{bc}
PSNPs-60%	6.93±0.62^{c}	0.27±0.03^{c}
PSNPs-70%	8.84±0.49^{b}	0.31±0.04^{bc}
PSNPs-80%	7.88±0.34b^{c}	0.28±0.02^{c}
PSNPs-96%	7.21±0.75^{c}	0.34±0.02^{b}
CS	10.90±0.12^{a}	0.60±0.00^{a}
CSNPs-50%	5.84±0.10^{b}	0.30±0.01^{b}
CSNPs-60%	6.10±0.56^{b}	0.31±0.04^{b}
CSNPs-70%	7.31±0.15^{cd}	0.32±0.02^{b}
CSNPs-80%	6.50±0.29^{bc}	0.30±0.03^{b}
CSNPs-96%	7.53±0.21^{d}	0.31±0.05^{b}

All values were expressed as mean ± standard error ($n \geq 3$). Means in the same column for the same starch source and followed by different superscripts are significantly different ($p < 0.05$).

As previously observed in FTIR results (see Section 3.5.3), starch NPs have fewer water molecules hydrating their structure, hence, MC and a_w values in these materials were lower when compared with those obtained in the native starches (Table 3.3). Considering that all samples were conditioned under the same RH (10%), higher MC and a_w values in the native starches when compared with the starch NPs can be explained due to the necessity of water molecules to hydrate the crystalline structure of the starches (LOURDIN et al., 2015). In contrast, starch NPs have less crystalline structure, not being necessary the presence of

moderate amounts of water molecules. According to Chirife and Buera (1994) a_w values between 0.2 and 0.4 are typical of food with high chemical and microbiological stability. In the current research, most starch NPs had a_w values lower than 0.4, indicating which these systems are low moisture products which are not susceptible to chemical reactions and microorganism growth when stored at 10% RH (AL-MUHTASEB; MCMINN; MAGEE, 2002). However, these nanomaterials could absorb high amounts of water molecules when exposed at high relative humidities (CHACON et al., 2020a).

3.4.7 Solubility in water and swelling factor

The solubility in water (S) at 30 ºC of the native starches was low and oscillated between 0 and 5.27% (Table 3.4). The S values at 30 ºC confirm that the native starches are not water-soluble at this temperature. However, S values increased from 0 % to 18.31 % and from 5.27 % to 44.49% for PS and CS, respectively, when the water was heated to 90 ºC (Table 3.4). Furthermore, swelling factor (SF) at 90 ºC were higher than 50 g/g, being typical of native starches (Table 3.4) (CHACON et al., 2020a; VALENCIA et al., 2015a). Solubility in water and swelling factor depend on the type of starch and its botanical source, amylose-amylopectin ratio, molecular weight distribution, and particle size.(SINGH et al., 2003) The amylopectin content is directly associated with solubility in water and swelling factor of starch granules (SINGH et al., 2003; VAMADEVAN; BERTOFT, 2020). According to Vamadevan and Bertoft (2020) CS has a higher amylopectin content than PS. Therefore, in the current research, CS had higher S and SF values when compared with PS (Table 3.4). In the current research, the S and SF values in CS and PS are in concordance with those informed in the literature for the same starches (SINGH et al., 2003; VAMADEVAN; BERTOFT, 2020).

Starch NPs had S values at 30 °C oscillating between 40.76 and 89.34%, being altered by the type of native starch. Furthermore, the S values were higher than 80% when the starch NPs were dispersed in hot water (90 ºC) (Table 3.4). The S values indicate that starch NPs are more soluble in water at 30 ºC or 90 ºC when compared with PS and CS.

Table 3.4. Solubility in water (S), and swelling factor (SF) of potato starch (PS), cassava starch (CS), and starch nanoparticles based on PS (PSNPs) and CS (CSNPs) obtained with different acidified hydroethanolic solutions (50, 60, 70, 80, and 96%).

Sample	30 ºC		90 ºC	
	S (%)	SF (g/g)	S (%)	SF (g/g)
PS	0.00±0.00^{a}	2.22±0.17^{a}	18.31±4.24^{a}	55.75±5.24^{a}
PSNPs-50%	72.84±7.93^{b}	6.68±0.41^{b}	94.49±3.18^{b}	17.10±2.53^{bc}
PSNPs-60%	62.29±6.86^{c}	8.04±0.81^{c}	93.43±2.24^{b}	22.38±2.74^{b}
PSNPs-70%	56.43±7.12^{c}	5.92±0.71^{bd}	89.91±2.05^{b}	10.08±2.23^{c}
PSNPs-80%	52.70±3.24^{c}	6.84±0.96^{b}	91.92±2.94^{b}	8.57±1.38^{c}
PSNPs-96%	40.76±5.61^{d}	4.96±0.73^{d}	90.64±1.87^{b}	10.03±0.74^{c}
CS	5.27±1.15^{a}	2.05±0.02^{a}	44.49±8.07^{a}	69.33±11.82^{a}
CSNPs-50%	80.59±7.88^{bc}	8.40±0.99^{b}	85.74±1.01^{b}	5.71±0.97^{b}
CSNPs-60%	77.99±4.14^{b}	10.10±0.65^{c}	81.79±4.50^{b}	7.87±1.06^{b}
CSNPs-70%	89.34±6.67^{c}	8.12±7.06^{b}	84.15±4.29^{b}	10.76±1.63^{b}
CSNPs-80%	86.53±4.43^{bc}	13.00±0.39^{d}	88.85±2.83^{b}	10.93±4.01^{b}
CSNPs-96%	83.08±9.59^{bc}	8.27±0.53^{b}	88.40±5.57^{b}	10.14±3.95^{b}

All values were expressed as mean ± standard error ($n \geq 3$). Means in the same column for the same starch source and followed by different superscripts are significantly different ($p < 0.05$).

The AP precipitation impacted the swelling behavior of starch NPs when compared with the native starches. Hence, starch NPs showed lower swelling factor (SF) values than PS and CS at 90 ºC ($p < 0.05$) (Table 3.4). The SF in starch NPs oscillated between 4.96 and 13.00 g/g, at 30 °C, and between 5.71 and 22.38 g/g, at 90 °C, suggesting that starch NPs did not swell because these samples have high S values at the same temperatures. Furthermore, these nanoparticles did not swell due to the starch chain modification during AP. These results are in concordance with those informed by Chacon et al. (2020a) for PS and starch NPs produced by AP.

Solubility in water and swelling factor are important properties of starches since that water is the universal solvent in food products. Based on S and SF values, it is possible to suggest that starch NPs can be used as a raw material in food products where the starch must be solubilized at 30 ºC.

3.5 CONCLUSIONS OF CHAPTER 3

In the current research, potato and cassava starch nanoparticles (NPs) were obtained by anti-solvent precipitation (AP) using acidified hydroethanolic solutions with different ethanol concentrations (50, 60, 70, 80, and 96%). The obtained starch NPs showed bimodal distribution with particle size lower than 1000 nm. Also, these nanomaterials displayed V-type crystalline structure and high solubility in water at 30 ºC and 90 ºC. The ethanol concentration used in the acidified hydroethanolic solution impacted the recovery efficiency and some physicochemical properties of starch NPs such as particle size and surface charge.

CAPÍTULO 4

PRODUÇÃO E CARACTERIZAÇÃO DE NANOPARTÍCULAS DE AMIDO CARREGADAS COM OS COMPOSTOS FENÓLICOS DO PE MARROM ACIDIFICADO

Apresentado na forma de artigo

4 ANTIOXIDANT NANOPARTICLES BASED ON STARCH AND THE PHENOLIC COMPOUNDS FROM PROPOLIS EXTRACT: PRODUCTION AND PHYSICOCHEMICAL PROPERTIES.

Este capítulo relata a segunda fase experimental desta tese: a produção e caracterização de nanopartículas de amido carregadas com os compostos fenólicos do PE acidificado.

A partir desta etapa, foi escrito o segundo artigo experimental intitulado “Antioxidant Nanoparticles Based on Starch and the Phenolic Compounds from Propolis Extract: Production and Physicochemical Properties” publicado na revista Starch (fator de impacto (2021): 2.741; https://doi.org/10.1002/star.202100289). De acordo com as regras de assinatura da Wiley, os autores se reservam o direito de incluir o artigo em uma tese, desde que não seja publicado comercialmente.

Graphical abstract

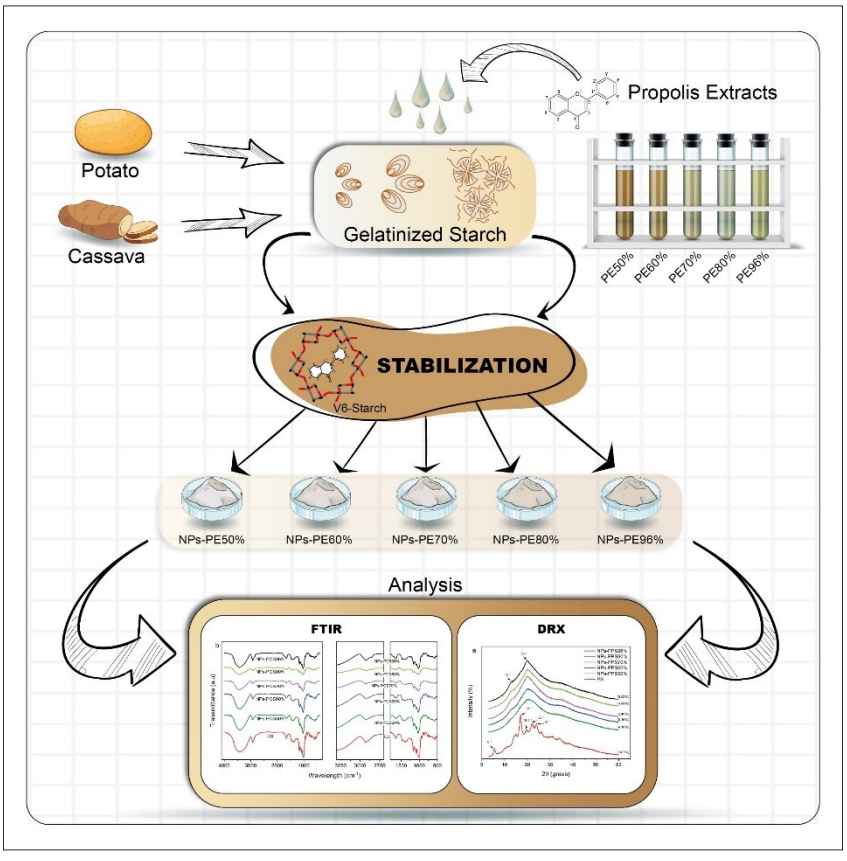

Highlights

- Starch nanoparticles (NPs) could stabilize the phenolic compounds of propolis.
- Starch NPs have antioxidant activity, and they are soluble in hot water.

- Starch NPs containing phenolic compounds have V6h-type crystalline structure.

Abstract

Propolis has health beneficial properties attributed to their phenol composition. Although, it has low water solubility, strong taste, and aroma, limiting its application in the food industry. This study explores the stabilization of phenolic compounds from propolis extract (PE) during the production of potato and cassava starch nanoparticles (NPs) by anti-solvent precipitation. Phenolic content and antioxidant capacity (ABTS and DPPH) of acidified PE obtained with different ethanol concentrations were determined. Starch NPs based on cassava and potato starch were characterized in terms of physicochemical properties, including loading efficiency, particle size distribution and surface charge, moisture content, water activity, chemical bonds, crystalline structure, thermal stability, color, and solubility in water. Fourier-transform infrared spectra and X-ray diffractograms revealed that the phenolic compounds of PE were stabilized with the starch NPs, in this way, at least 54.91% of phenolic compounds from PE were stabilized by the starch NPs. Starch NPs stabilizing the phenolic compounds displayed brown color and high solubility in hot water (90 ºC). This research reports for the first-time information regarding the stabilization of phenolic compounds from PE using starch NPs. These starch NPs have a great potential to be used in food formulations or to manufacture active food packaging.

Keywords: bioactive compounds; cassava starch; nanomaterials; potato starch.

Abbreviations

AP: anti-solvent precipitation; a_w: water activity; CS: cassava starch; DLS: Dynamic light scattering; DSC: differential scanning calorimeter; DTGA: Differential thermal analysis; FTIR: Fourier-transform infrared; GAE: gallic acid equivalent; Loading Efficiency (LE); LTPC: loaded total phenolic compounds; MC: moisture content; NPs: nanoparticles; potato starch nanoparticles (PSNPs-PE) and cassava starch nanoparticles (CSNPs-PE) loading the phenolic compounds from acidified propolis extracts (PE); CSNPs: starch nanoparticles based on cassava starch; starch nanoparticles (NPs), GRAS: Generally Recognized as Safe, PSNPs: starch nanoparticles based on potato starch; PE: propolis extract; PS: potato starch; RC: Relative crystallinity; RC: Recovery efficiency; S: solubility in water; TGA: thermogravimetric analysis; phenolic content TPC: total phenolic content; T_o: gelatinization onset temperature; T_p:

gelatinization peak temperature; T_c: gelatinization conclusion temperature; XRD: X-ray diffraction; zeta potential (ZP).

4.1 INTRODUCTION

Nanomaterials are defined as structures having at least one dimension between 1 and 1000 nm, these structures can be used as reinforcing or antimicrobial materials in food packaging, or as delivery systems and stabilizing agents in foods (ALVES et al., 2021; CAMPELO; SANT'ANA; PEDROSA SILVA CLERICI, 2020). Starch nanomaterials are a kind of nanostructures and they can be classified as nanocrystals, nanofibers, nanomicelles, nanoparticles, and nanovesicles, being produced by means of "top-down" and "bottom-up" approaches such as acid and enzymatic hydrolysis, anti-solvent precipitation, high-pressure homogenization, ultrasonication, electrospinning, self-assembly, and emulsification (ALVES et al., 2021; CAMPELO; SANT'ANA; PEDROSA SILVA CLERICI, 2020).

Particularly, starch nanoparticles (NPs) can be produced by anti-solvent precipitation (AP), a "top-down" approach where GRAS (Generally Recognized as Safe) reagents are used aiming food applications (CHACON et al., 2019, 2020a; HEBEISH et al., 2014). In the AP method, gelatinized starch granules in water are precipitated by the addition of ethanol or acidified ethanol (anti-solvent), resulting in starch NPs with particle size lower than 1000 nm (ALVES et al., 2021; CAMPELO; SANT'ANA; PEDROSA SILVA CLERICI, 2020; CHACON et al., 2019, 2020a; ALVES et al., 2021; HEBEISH et al., 2014).

AP method using starch NPs has been applied to develop starch nanomaterials with functional properties. In this way, Ahmad et al. (2019) stabilized catechin in starch NPs produced from three starch sources (horse chestnut, water chestnut, and lotus stem). The authors concluded that these nanomaterials protected the catechin against the gastric environment and retained the bioactivity of catechins during the *in-vitro* digestion process. In another research, García-gurrola et al. (2021) stabilized the phenolic compounds from arugula (*Eruca sativa*) leaves using starch NPs produced from waxy corn and concluded that the developed nanomaterials displayed high antioxidant properties. The same authors speculated that the functional nanoparticles could be used as a colloidal system in food and pharmaceutical formulations. In the same line, Lima et al. (2021) stabilized anthocyanins using starch NPs produced from cassava and potato starches and observed that the bioactivity of anthocyanins loaded on starch NPs was preserved. The same authors suggested the application of these functional starch NPs as natural colorants in food formulations. Finally, Remanan and Zhu,

(2020) used starch NPs based on quinoa and maize starch to stabilize rutin, a phenolic compound with therapeutic properties. The authors concluded that the starch NPs had a high potential for stabilize polyphenols (rutin) and preserve its bioactivity during simulated *in-vitro* digestion test.

Propolis is a resinous and heterogeneous material collected by bees (*Apis mellifera* L.) from different parts of plants. This natural compound has high amounts of flavonoids and phenolic acids, being used worldwide in traditional medicine, as well as in pharmaceutical, cosmetic, and food applications due to its antibacterial, antifungal, anti-inflammatory, antiseptic, antiproliferative, anticarcinogenic, and antioxidant properties (IRIGOITI et al., 2021; KOWACZ; POLLACK, 2020; ONG et al., 2017; OROIAN; URSACHI; DRANCA, 2020; REYES; LANDGRAF; SOBRAL, 2021; TAVARES et al., 2021; ZULHENDRI et al., 2021).

The use of propolis as a food ingredient is still limited due to its low solubility in water, strong flavor, and aroma which change the organoleptic properties of foods (BODINI et al., 2013; IRIGOITI et al., 2021). Thus, some researchers have reported the encapsulation of propolis as an alternative to mask flavors/aromas, maintaining the organoleptic properties in Italian-style salami (BERNARDI et al., 2013b), fish burger (SPINELLI et al., 2015), hamburger meat (REIS et al., 2017), pudding and Minas Frescal cheese (JANSEN-ALVES et al., 2018) and fish fillets (PIEDRAHÍTA MÁRQUEZ; FUENMAYOR; SUAREZ MAHECHA, 2019). The stabilization of phenolic compounds from propolis in starch NPs appears as an alternative to develop new starch nanomaterials with functional properties, adding value to the propolis in the food sector. Previously, our research group produced starch NPs based on potato and cassava starch by AP, using different ethanol concentrations (ALVES et al., 2021). However, be noted that for our current knowledge, no research has explored the stabilization of phenolic compounds from propolis using starch NPs. Hence, this study was carried out to develop and characterize starch NPs loaded with the phenolic compounds from acidified PE. Cassava and potato starches were selected as sources to produce the NPs due to their availability, low cost, and recent use to produce these nanomaterials by AP (CHACON et al., 2020a; ALVES et al., 2021; LIMA et al., 2021).

4.2 MATERIALS AND METHODS

4.2.1 Materials

Native starches isolated from cassava and potato were purchased from Juréia and Shambala Naturais Food Industries (Santa Catarina, Brazil), respectively. Brown propolis was kindly donated by Breyer & Cia Ltda (União Vitória, PR, Brazil). In the current research, brown propolis was used due to its high availability in Brazil and antioxidant activity (OLEGÁRIO et al., 2019). Distilled water, ethanol (≥ 99.6%, Êxodo Científica, Brazil) and hydrochloric acid (37 wt%, Neon, Brazil) were used as solvents. Potassium chloride and sodium carbonate were purchased from Dinâmica (Brazil). Folin-Ciocalteu, 2,2-diphenyl-1-picrylhydrazyl (DPPH), and 2,2'-azino-bis (3-ethylbenzothiazoline-6-sulfonic acid) (ABTS) were acquired directly from Sigma-Aldrich (Brazil). All reagents used were of analytical grade and they were used as received.

4.2.2 Production of brown propolis extracts

Propolis extracts were performed in a batch mode according to the method of Cavalaro et al. (2019), with slight modifications. Ground brown propolis was added to hydroethanolic solutions in a 1:35 ratio (% w/v). The hydroethanolic solutions were prepared by diluting the absolute ethanol in water to obtain solutions with ethanol concentrations of 50, 60, 70, 80, and 96% v/v (ALVES et al., 2021). The extraction was carried out using an ultrasonic bath at 40 kHz (Ultracleaner 1650, Unique, Brazil) for 20 minutes, with a total extract volume of 100mL, ensuring that all samples had the same contact surface. After the extraction, the propolis extracts were centrifuged at 25 ºC using a centrifuge (Kasvi, Brazil) with 1700 × g force at 4000 rpm for 15 minutes. In sequence, the extracts were filtered using filter paper and stored into amber flasks at -24 ºC under absence of light until analysis.

4.2.3 Characterization of brown propolis extracts

The total phenolic content (TPC) in each brown propolis extract (PE) was determined by the Folin-Ciocalteu spectrophotometric method (SINGLETON; ORTHOFER; LAMUELA-RAVENTÓS, 1999). The PE was diluted in ethanol (≥ 99.6%) in a 1:2 (% v/v) ratio. Thereafter, 100 µL of the ethanolic extract was transferred to test tubes and mixing with 7.9 mL of distilled water and 0.5 mL of Folin-Ciocalteu reagent (2N), followed by homogenization in vortex. In

sequence, 1.5 mL of sodium carbonate solution 20% (w/v) was added and then homogenized in vortex. The test tubes were kept in dark at room temperature for 2 h. The absorbance of solutions was measured at a wavelength of 760 nm, using a spectrophotometer (QUIMIS, Q898U2M5, Diadema, SP, Brazil) and a blank solution with ethanol concentration of 95.6%. TPC results were expressed as milligrams of gallic acid equivalent (GAE) per g of fresh brown propolis according to a calibration curve with concentrations varying between 0 and 750 µg of GAE/mL of extract ($y = 0.0011x + 0.0548$, $R^2 = 0.9993$).

The antioxidant capacity was determined by the DPPH radical (2,2-diphenyl-1-picrylhydrazyl) scavenging method informed by Brand-Williams, Cuvelier and Berset (1995), with slight modifications. Firstly, 100 µL of each PE was mixed with 2.9 mL of DPPH, followed by homogenization in vortex. The samples were kept in dark at room temperature for 30 min, then, the absorbance was read at a wavelength of 517 nm using the same spectrophotometer. The Trolox results were expressed as µmol of Trolox per g of fresh brown propolis, according to a calibration curve with concentrations varying between 0 and 750 µmol Trolox/L ($y = -0.0006x + 0.7766$, $R^2 = 0.9753$)

Free radical ABTS+ was captured according to the methodology proposed by Re et al. (1999). An aliquot of 30 µL of extract was transferred to test tubes with 3.0 mL of the ABTS+ radical and homogenized in vortex. The samples were kept in dark at room temperature for 6 min and the absorbance value was read in the same spectrophotometer at a wavelength of 734 nm. Results were expressed as µmol of Trolox per g of propolis, according to a calibration curve with concentrations varying between 0 and 1500 µmol /mL ($y = -0.0003x + 0.6931$, $R^2 = 0.9978$).

4.2.4 Production of starch nanoparticles loaded with the phenolic compounds from propolis extract

Starch NPs were produced through the AP technique by Alves et al. (2021). Dispersions (5% w/w) of CS and PS were prepared in distilled water at 25 ºC and then they were heated at 90 ºC for 30 minutes to guarantee the starch gelatinization. In sequence, the gelatinized starch solutions were cooled to 30 ºC and then an acidified PE was added drop wise for the gelatinized starch in a 1:1 (% v/v) ratio. The PE extracts were acidified to separate the starch nanoparticles, hence, acidified PE was prepared by blending each PE (see Section 4.2.2.)

with hydrochloric acid (100:1 v/v, hydroethanolic solution: HCl 37 wt%, pH = 1) (ALVES et al., 2021)

The resulting slurry obtained after the mixture of the gelatinized starch solution with the acidified PE was kept in magnetic agitation with constant stirring for 12 hours. Then, the slurry was centrifuged at 25 ºC using a centrifuge (Kasvi, Brazil) with 1700 × g force at 4000 rpm for 15 minutes to separate the starch NPs from the solvents. Starch NPs were centrifuged three times with an hydroethanolic solution (80% v/v), and finally washed with absolute ethanol (99.6%). Starch NPs were removed by centrifugation using the same centrifuge and the ethanol in the starch NPs was evaporated using a forced-air convection oven (Solidsteel, Brazil) at 60 ºC for 10 min. In sequence, starch NPs were frozen at -24 ºC for 48 h, and finally lyophilized (Liotop L 101). The resulting starch NPs loading the phenolic compounds from PE were finely macerated and stored in desiccators with silica gel at 25 °C for further analysis.

4.2.5 Characterization of the starch nanoparticles loaded with the phenolic compounds from propolis extract

4.2.5.1 Loading Efficiency (LE) and loaded total phenolic compounds (LTPC) on starch nanoparticles

The LE of the phenolic compounds from acidified PE stabilized with starch NPs was calculated as proposed by Quiroz et al. (2020) (Eq. 4.1):

$$\text{LE}\ (\%) = \left(\frac{\text{TPC}_\text{i} - \text{TPC}_\text{s}}{\text{TPC}_\text{i}}\right) * 100 \tag{4.1}$$

where TPC_i is the initial TPC of the PE before stabilization with starch NPs and TPC_s is the TPC of supernatant collected after the first centrifugation at 4000 rpm for 15 min (see Section 4.2.4.). The quantification of TPC was carried out using the same method informed in Section 4.2.3.

LTPC on starch NPs was calculated as the product between TPC of each PE (see Section 4.2.3.) and the LE previously obtained in each starch NPs.

4.2.5.2 Particle size distribution and surface charge

Particle size and surface charge of starch NPs loading the phenolic compounds from acidified PE were determined using a LUMiSizer (LUM GmbH, Germany) and a Zetasizer Nano ZS (Malvern, England), respectively. Before analyses, starch NPs were dispersed in ultrapure Mili-Q water (0.03% w/v, pH = 6) and sonicated for 30 min at 40 KHz, using a sonicator bath (Ultracleaner 1650, Unique, Brazil) (AHMAD et al., 2019).

4.2.5.3 Moisture content (MC) and water activity (a_w)

The MC of starch NPs loading the phenolic compounds from acidified PE was determined gravimetrically (drying at 105 ºC) and the a_w of the same nanoparticles was carried out at 25 ºC using a water activity meter (Aqualab Model Series 3 instrument, Decagon Devices Inc., Pullman, WA, USA), both following the methodologies informed by Alves et al. (2021), MC values were expressed as gram of water per gram of dry starch nanoparticle.

4.2.5.4 Chemical bonds

Infrared spectroscopy (FTIR) studies were performed to qualitatively determine the chemical groups of starch NPs loading the phenolic compounds from PE. Samples blended with KBr were analyzed using a Fourier-transform infrared spectrometer (FTIR, Cary 600, Agilent, US) in the infrared region between 4000 and 400 cm^{-1}, with resolution of 4 cm^{-1}. In each analysis were performed 32 scans (CAPELLO et al., 2019).

4.2.5.5 Crystalline structure

X-ray diffraction (XRD) patterns were recorded using X-ray diffractometer (Rigaku MiniFlex 600 DRX, Japan) equipped with Cu-Kα radiation (λ = 0.154056 nm). The diffractograms were obtained in the diffraction ranges (2θ) between 3 and 60°, using a rate of 10 °/min (ALVES et al., 2021). The Bragg's law (Eq. 4.2) was used to calculate the interplanar spacing d (nm) from the diffraction angle at the maximum intensity of the peaks/halos found in the XRD patterns.

$$n\lambda = 2d\sin\theta \tag{4.2}$$

where n is the reflection order (n = 1), λ is the wavelength of CuKα radiation, and θ is the reflection angle.

Relative crystallinity (RC, %) of starch NPs loading the phenolic compounds from PE was calculated using Eq. (4.3) proposed by Nara and Komiya (NARA; KOMIYA, 1983).

$$\mathrm{RC}\ (\%) = \left(\frac{A_c}{A_c + A_a}\right) * 100 \quad (4.3)$$

where A_c and A_a are the areas related to the crystalline and amorphous regions in the X-ray diffractograms for each sample, respectively.

4.2.5.6 Thermal stability

Thermal stability of starch NPs loading the phenolic compounds from acidified PE was investigated using a thermogravimetric balance (TGA/DTA STA 449 F3 Jupiter, Netzsch, Germany). Samples of approximately 10 mg were heated from 30 to 700 ºC, with heating rate of 10 ºC/min. A platinum pan was used as reference and the TGA curves were carried out using a flow of 100 mL/min of dry N_2 (CAPELLO et al., 2019).

4.2.5.7 Color

The color of starch NPs loading the phenolic compounds from acidified PE was evaluated using a high-resolution digital camera (Nikon AF-SDX Nikkor 18-55mm1:3.5–5.6G VR II, 0.28m/0.92 ft. ø 52) configured in automatic mode, without flash and zoom (55×). A chamber with homogeneous illumination using a diffused fluorescent lamp source and a standard white plate as the background were used for photos acquisition. Samples were positioned inside the chamber and photos were taken and then analyzed using ImageJ v 1.52a software® altogether with the Color Space Converter plugin (DALLABONA et al., 2020).

CIELab coordinates were used for color characterization, being used the L^* (lightness, 0–100), a^* (redness (+) to greenness (-)), and b^* ((yellowness (+) to blueness (−)) coordinates (CÁRDENAS-PÉREZ et al., 2017).

4.2.5.8 Solubility in water (S)

The S test was carried out according to the methodology proposed by Alves et al. (2021) Approximately 0.150 g (W) of each sample was mixed with 15 mL of distilled water and then heated at 90 ºC for 30 min. The samples were shaken each 10 min for 10 s in a vortex. After that, the samples were cooled until room temperature and then centrifuged at 4000 rpm (Kasvi, Brazil) for 15 minutes. The supernatant liquid was placed in crucibles previously weighed and then dried at 105 ºC for 48 hours. In sequence, the remaining weight in the crucible (W_r) was used to calculate S value by Eq. (4.4).

$$S\ (\%) = \frac{W_r}{W} * 100 \quad (4.4)$$

4.2.6 Statistical analyses

All results were expressed as means ± standard deviation (n ≥ 3). The experimental data were analyzed using Analysis of variance (ANOVA) and Tukey test with multiple comparisons, was performed with a 5% significance level using the software Statistica 10.0 (StatSoft®, USA). Pearson's correlation was performed using Excel® software.

4.3 RESULTS AND DISCUSSIONS

4.3.1 Characterization of brown propolis extracts

The total phenolic compounds (TPC) in propolis extracts increased with the ethanol concentration, suggesting that ethanol successfully extracted these compounds from brown propolis. Hence, TPC values increased from 10.85 to 27.63 mg of GAE/g of propolis in PE with an ethanol concentration varying between 50 % and 96%, respectively (Table 4.1). Similar behavior was observed by Cavalaro et al. (2019) who studied different process conditions to extract the phenolic compounds from green propolis by ultrasound, and by Dallabona et al. (2020) in PE (hydroethanolic solution of 70% (v/v) and propolis/solvent ratio of 1:25 (w/v)) produced by maceration method (48 h) followed by an ultrasonic bath. These authors found a mean TPC value of 18.6 mg GAE/g of propolis, which was lower than the TPC value found in current research for the same ethanol concentration (Table 4.1). In another study, brown

propolis extracts from four Brazilian states and obtained in a thermostatic bath at 75 ± 2 °C for 30 min had TPC values oscillating between 6.12 and 45.84 mg of GAE/g of propolis. Differences in TPC values were correlated with the geographical origin of each propolis (OLEGÁRIO et al., 2019). Other factors such as bee species, propolis color, time of collection, and extraction also could impact the TPC values (PICCINELLI et al., 2011).

Table 4.1. Total phenolic compounds (TPC) and antioxidant capacity by DPPH and ABTS of the propolis extract (PE) obtained with different ethanol concentrations (50, 60, 70, 80, and 96%).

PE	TPC (mg of GAE /g of propolis)	DPPH (µmol TROLOX/g of propolis)	ABTS (µmol TROLOX/g of propolis)
PE50%	10.85 ± 1.06^{a}	39.24 ± 0.27^{a}	33.13 ± 1.66^{a}
PE60%	16.35 ± 0.90^{b}	37.82 ± 0.80^{a}	50.65 ± 1.25^{b}
PE70%	21.20 ± 0.59^{c}	46.26 ± 1.38^{b}	72.78 ± 3.80^{c}
PE80%	24.82 ± 0.51^{d}	51.53 ± 2.06^{c}	91.54 ± 2.79^{d}
PE96%	27.63 ± 1.17^{e}	52.46 ± 0.67^{c}	95.17 ± 3.15^{d}

GAE: gallic acid equivalent. All values were expressed as mean ± standard error using the replicates of three experiments. Mean values with different letters within the same column were significantly different ($p < 0.05$).

The antioxidant capacity of the propolis extracts showed a significant increase as the ethanol concentration increased in the PE ($p < 0.05$) (Table 4.1). The high antioxidant capacity was obtained for EP96% with values of 52.46 and 95.17 µmol TROLOX/g of propolis for the radical DPPH and ABTS, respectively. It is possible to observe that, although the extracts exhibited good antioxidant activities by the DPPH and ABTS methods, the ABTS radical scavenging values were higher than the DPPH (Table 4.1). This behavior could be attributed to the presence of hydrophilic and lipophilic antioxidants that are better reflected by the ABTS assay (FLOEGEL et al., 2011) when compared with DPPH assay which detects mainly hydrophobic compounds (KIM et al., (2002). Dallabona et al. (2020) reported lower concentrations of DPPH (25.7 µmol/g of propolis) and ABTS (17.1 µmol/g of propolis) for Brazilian propolis extracts when compared with the DPPH and ABTS values found in the current research. However, in another research, Jansen-Alves et al. (2019) obtained higher DPPH values (51.12 µmol TROLOX/g of propolis) in PE of Brazilian brown propolis from Rio

Grande-RS, using an ethanol concentration of 80% and obtained by stirring at room temperature for 24 h.

The correlation between the TPC and the antioxidant activity (DPPH and ABTS) was evaluated by Pearson's correlation coefficient (r). A strong correlation was observed between the phenolic compounds and the DPPH and ABTS methods (r = 0.92 and r = 0.98, respectively), confirming that the antioxidant activity of brown propolis is related to the TPC. Andrade et al. (2017) also evaluated the correlation coefficients in brown, green and red propolis extracts, and found a good correlation between the phenolic compounds and the ABTS and DPPH methods (r = 0.76 and r = 0.89, respectively).

4.3.2 Characterization of starch nanoparticles loaded with the phenolic compounds from propolis extract

4.3.2.1 Loading Efficiency (LE) and loaded total phenolic compounds (LTPC) on starch nanoparticles (NPs)

LE values were not altered with the ethanol concentration in acidified PE and starch type, hence, LE oscillated between 55 and 70% without a statistical difference (Table 4.2). In contrast, LTPC values increased with the ethanol concentration used in each acidified PE, indicating that more phenolic compounds were stabilized in starch NPs (Table 4.2). LE and LTPC results suggest that the phenolic compounds from acidified PE were successfully loaded in the starch NPs. In the current research, LE values were higher to those informed by Garcia-Gurrola et al. (2021) in starch NPs loaded with the phenolic compounds from Arugula (*Eruca sativa*) leaves extract and obtained by AP.

Table 4.2. Loading efficiency (LE), loaded total phenolic compounds (LTPC) of potato starch nanoparticles (PSNPs-PE) and cassava starch nanoparticles (CSNPs-PE) loading the phenolic compounds from acidified propolis extracts (PE) with different ethanol concentration (50, 60, 70, and 96%).

Sample	LE (%)	LTPC (mg of GAE /g of propolis)
PSNPs-PE50%	70.63 ± 2.92[a]	6.88±0.28[a]
PSNPs-PE60%	64.41 ± 6.27[a]	10.53±1.03[ab]
PSNPs-PE70%	62.77 ± 4.03[a]	13.31±0.85[b]
PSNPs-PE80%	55.94 ± 7.11[a]	13.89±1.77[b]
PSNPs-PE96%	54.91 ± 7.71[a]	15.41±2.16[b]
CSNPs-PE50%	64.12 ± 5.11[a]	6.25±0.50[a]
CSNPs-PE60%	66.55 ± 1.78[a]	10.88±0.29[b]
CSNPs-PE70%	60.85 ± 0.96[a]	12.90±0.20[bc]
CSNPs-PE80%	59.89 ± 0.43[a]	14.87±0.11[c]
CSNPs-PE96%	64.23 ± 4.83[a]	18.02±1.35[d]

All values were expressed as mean ± standard error using the replicates of three experiments. Mean values with different letters within the same column were significantly different ($p < 0.05$).

4.3.2.2 Particle size distribution and surface charge

NPs based on potato (PSNPs-PE) and cassava (CSNPs-PE) starch loaded with the phenolic compounds from acidified PE displayed bimodal distribution with particle size from 58.26 to 618 nm (Fig. 4.1a), and from 24.27 to 614.43 nm (Fig. 4.1 b), respectively. In general, an increase in the particle size was observed in all starch NPs as the LTPC increased in the starch NPs. Previously, it was observed a reduction in the particle size on starch NPs with the increase in the ethanol concentration (ALVES et al., 2021). However, in the current research, the acidified PE at high ethanol concentration showed more total phenolic compounds concentrations (Table 4.1). In this way, the presence of phenolic compounds could modify the molecular arrangement and increase the particle size of starch NPs (Fig. 4.1). Similar results were found in the literature regarding the stabilization of hydrophobic active compound with starch NPs (AHMAD; GANI, 2021; GARCÍA-GURROLA et al., 2021).

Fig. 4.1. Particle size distribution of: (a) potato starch nanoparticles (PSNPs-PE); (b) cassava starch nanoparticles (CSNPs-PE) loading the phenolic compounds from propolis extracts (PE) with different ethanol concentration (50, 60, 70, and 96%).

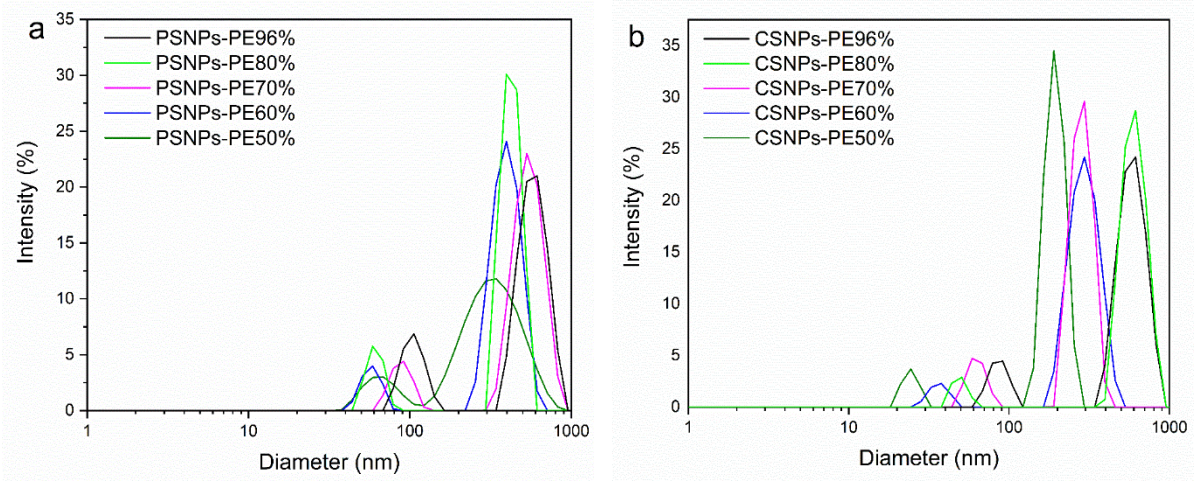

Source: Alves et al. (2022), with permission.

The zeta potential (ZP) is used to determine the surface charge and stability of colloidal suspensions and it is indicative of good colloidal stability. According to DLVO theory, ZP values in modules between 0 - 10 mV, 10 - 20 mV, and 20 - 30 mV are typical in highly unstable, relatively stable, and moderately stable particles, respectively. Furthermore, ZP values higher than 30 mV are associated with high stable particles (BANERJEE et al., 2016; PARK et al., 2017). All starch NPs loading the phenolic compounds from acidified PE had negative ZP values typical of moderately stable particle systems (Table 4.3).

Table 4.3. Zeta potential (ZP) of potato starch nanoparticles (PSNPs-PE) and cassava starch nanoparticles (CSNPs-PE) loading the phenolic compounds from acidified propolis extracts (PE) with different ethanol concentration (50, 60, 70, and 96%).

Sample	ZP (mV)
PSNPs-PE50%	-31.70 ± 1.84[a]
PSNPs-PE60%	-26.10 ± 1.13[a]
PSNPs-PE70%	-28.93 ± 0.21[a]
PSNPs-PE80%	-27.07 ± 0.47[a]
PSNPs-PE96%	-25.85 ± 0.49[a]
CSNPs-PE50%	-25.40 ± 1.11[a]
CSNPs-PE60%	-25.95 ± 0.78[a]
CSNPs-PE70%	-26.10 ± 0.30[a]
CSNPs-PE80%	-25.03 ± 0.35[a]
CSNPs-PE96%	-17.27 ± 0.29[b]

All values were expressed as mean ± standard error using the replicates of three experiments. Mean values with different letters within the same column were significantly different ($p < 0.05$).

It is desirable to promote electrostatic repulsion between particles, preventing agglomeration and keeping stable the NPs in suspension (MÜLLER; JACOBS, 2002). Comparing with a previous study of our research group, the ZP values of starch NPs loading the phenolic compounds from acidified PE (PSNPs-PE and CSNPs-PE) were more negative when compared with the same nanoparticles produced with similar ethanol concentration in the hydroethanolic solutions, but without the phenolic compounds from propolis (ALVES et al., 2021). This result suggests that the phenolic compounds modified the surface charge of starch NPs, reducing their ZP values.

4.3.2.3 Moisture content (MC) and water activity (a_w)

Low MC is necessary to ensure the physicochemical and microbiological stability of starch nanoparticles, avoiding their agglomeration and increasing their shelf life. Starch NPs loaded with the phenolic compounds from PE had low MC and a_w values, oscillating between 7.18 – 10.38 % and between 0.23 – 0.42, respectively (Table 4.4).

Table 4.4. Moisture content (MC) and water activity (aw) of potato starch nanoparticles (PSNPs-PE) and cassava starch nanoparticles (CSNPs-PE) loading the phenolic compounds from acidified propolis extracts (PE) with different ethanol concentration (50, 60, 70, and 96%).

Sample	MC (%)	a_w
PSNPs-PE50%	9.53 ± 1.76[a]	0.38 ± 0.00[a]
PSNPs-PE60%	9.42 ± 1.77[a]	0.37 ± 0.03[a]
PSNPs-PE70%	8.76 ± 0.65[a]	0.34 ± 0.02[a]
PSNPs-PE80%	8.84 ± 0.80[a]	0.37 ± 0.04[a]
PSNPs-PE96%	8.86 ± 0.89[a]	0.36 ± 0.02[a]
CSNPs-PE50%	7.18 ± 0.54[a]	0.42 ± 0.03[ab]
CSNPs-PE60%	10.09 ± 0.73[a]	0.39 ± 0.00[b]
CSNPs-PE70%	9.41 ± 0.42[a]	0.23 ± 0.00[b]
CSNPs-PE80%	7.27 ± 1.51[a]	0.26 ± 0.00[b]
CSNPs-PE96%	10.38 ±0.20[a]	0.26 ± 0.03[b]

All values were expressed as mean ± standard error using the replicates of three experiments. Mean values with different letters within the same column were significantly different ($p < 0.05$).

MC and a_w values of starch NPs loaded with the phenolic compounds from acidified PE are typical of dried materials having high microbiological stability (AL-MUHTASEB; MCMINN; MAGEE, 2002). MC and a_w values were similar to those obtained by Da Silva et al. (2013) (MC = 4.9 - 12.6 %, a_w = 0.25 - 0.39) in microparticles based on gum arabic/starch stabilizing PE and dried by spray-drying.

4.3.2.4 Chemical bonds

Fourier transform infrared (FTIR) spectra of starch NPs loaded with the phenolic compounds from PE exhibited similar bands due to the presence of the same functional groups in each sample (Fig. 4.2). All the starch NPs exhibited the vibration of hydroxyl groups typical of starch chains at 3400 cm^{-1}. The short bands between 3000 and 2900 cm^{-1} were attributed with asymmetric and symmetric vibrations in C=H groups and with the stretching of aliphatic compounds (BERGO; SOBRAL; PRISON, 2010). These bands are typical of lipids from amylose–lipid complex (VALENCIA et al., 2015b). However, the same bands (3000 and 2900 cm^{-1}) are typical in propolis containing fatty acids (PÉREZ-VERGARA et al., 2020). In

this way, the increase of band intensity at 3000 and 2900 cm^{-1} in starch NPs could be correlated with the increase in the amounts of fatty acids loaded in each sample (Fig. 4.2).

Fig. 4.2. FTIR spectra of: (a) potato starch nanoparticles (PSNPs-PE); (b) cassava starch nanoparticles (CSNPs-PE) loading the phenolic compounds from propolis extracts (PE) with different ethanol concentration (50, 60, 70, and 96%).

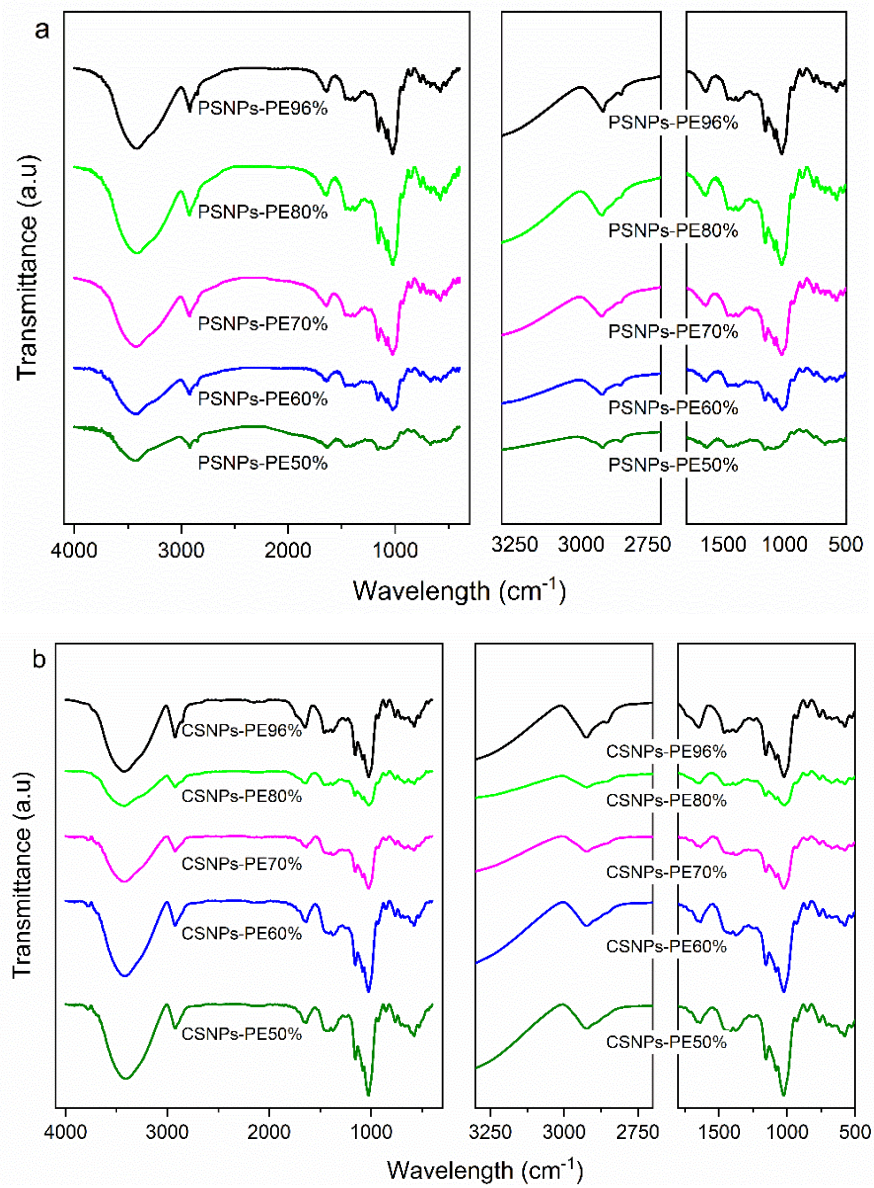

Source: Alves et al. (2022), with permission.

All starch NPs loaded with the phenolic compounds from acidified PE exhibited bands associated with the absorbance of hydroxyl groups (3310 cm^{-1}) and C=O elongation (1657 cm^{-1}) typical of starch chains. The band at 1645 cm^{-1} was associated with the presence of water molecules hydrating the starch NPs (ALVES et al., 2021). The same band (1645 cm^{-1}) also was

also correlated with stretching vibrations of C=C and C=O groups from flavonoids and asymmetric bending vibration of N–H groups from amino acids, typical compounds in propolis (IRIGOITI; YAMUL; NAVARRO, 2021). The increase in the band intensity at 1645 cm^{-1} also could be correlated with the presence of flavonoids and amino acids from PE in starch NPs (Fig. 4.2).

4.3.2.5 Crystalline structure

Starch NPs loaded with the phenolic compounds from PE showed V_{6h}-type crystalline structure, exhibiting diffraction peaks at 2θ = 13.0° (d = 0.68 nm) and 20.0° (d = 0.44 nm) (Fig. 4.3) (SHI et al., 2019).

Fig. 4.3. X-ray diffractograms of: (a) potato starch nanoparticles (PSNPs-PE); (b) cassava starch nanoparticles (CSNPs-PE) loading the phenolic compounds from propolis extracts (PE) with different ethanol concentration (50, 60, 70, 80 and 96%).

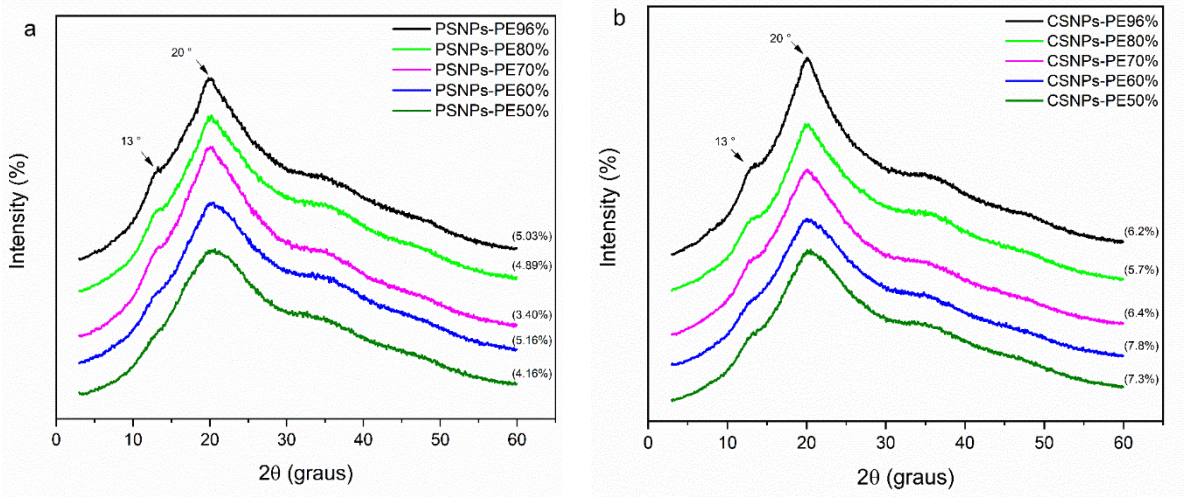

Source: Alves et al. (2022), with permission.

The V_{6h}-type crystalline structure is composed of 6 glucose units per helical turn and it is considered the most effective V-type structure to stabilize bioactive compounds (PÉREZ-VERGARA et al., 2020; SHI et al., 2019). Recently, our research group observed the formation of V_{6a}-type (2θ = 7.4°, 13.5°, and 20.8°) crystalline structure in starch NPs produced by AP and using hydroethanolic solutions with ethanol concentrations between 50 and 96% (ALVES et al., 2021). However, in the current study, the presence of phenolic compounds in the acidified PE (having the same ethanol concentrations) modified the helical turn of amylose from V_{6a} to V_{6h}-type. According to the literature, the V_{6h}-type has more water molecules hydrating its

structure when compared with the V_{6a}-type crystalline structure (PÉREZ-VERGARA et al., 2020; SHI et al., 2019). MC values confirmed this structural modification since that the starch NPs loaded with the phenolic compounds from PE had higher MC when compared with the same starch NPs produced without PE (ALVES et al., 2021). In this research, the modification of V_{6a} to V_{6h}-type crystalline structure could be associated with the stabilization of hydrophilic and lipophilic antioxidants from acidified PE (see Section 4.3.1).

Relative crystallinity (RC) in all starch NPs loaded with the phenolic compounds from PE oscillated between 3.40 and 7.80% (Fig. 4.3). These RC values were similar to those informed previously in starch NPs produced by anti-solvent precipitation using different ethanol concentrations (ALVES et al., 2021). According to XRD results, anti-solvent precipitation strongly affected the crystal structure of starches, resulting in NPs with low crystallinity (Fig. 4.3) when compared with their native starches (potato and cassava) (ALVES et al., 2021). The low RC in these materials could be important for their application as carriers of phenolic compounds in foods and drugs (TEODORO et al., 2015).

4.3.2.6 Thermal stability

Starch NPs loading the phenolic compounds from PE showed thermogravimetric (TGA) curves typical of starch nanomaterials (CHACON et al., 2019; ALVES et al., 2021). Hence, TGA curves displayed three main decomposition stages in each sample, firstly, the water evaporation was observed between 25 and 120 ºC, followed by the devolatilization of starch NPs and phenolic compounds from acidified PE (between 121 and 303 ºC) and finally the unburnt or biochar carbon formation at temperatures higher than 303 ºC (Fig. 4.4). Similar behavior was observed in potato and starch NPs produced with different ethanol concentrations, but without PE, (ALVES et al., 2021) suggesting that the incorporation of phenolic compounds in starch NPs did not alter the thermal stability and biochar formation of the resulting nanomaterials.

Fig. 4.4. Thermogravimetry curves of: (a) potato starch nanoparticles (PSNPs-PE); (b) cassava starch nanoparticles (CSNPs-PE). Derivative of the thermogravimetric curves of: (c) potato starch nanoparticles (PSNPs-PE); (d) cassava starch nanoparticles (CSNPs-PE) loading the phenolic compounds from propolis extracts (PE) with different ethanol concentration (50, 60, 70, 80 and 96%).

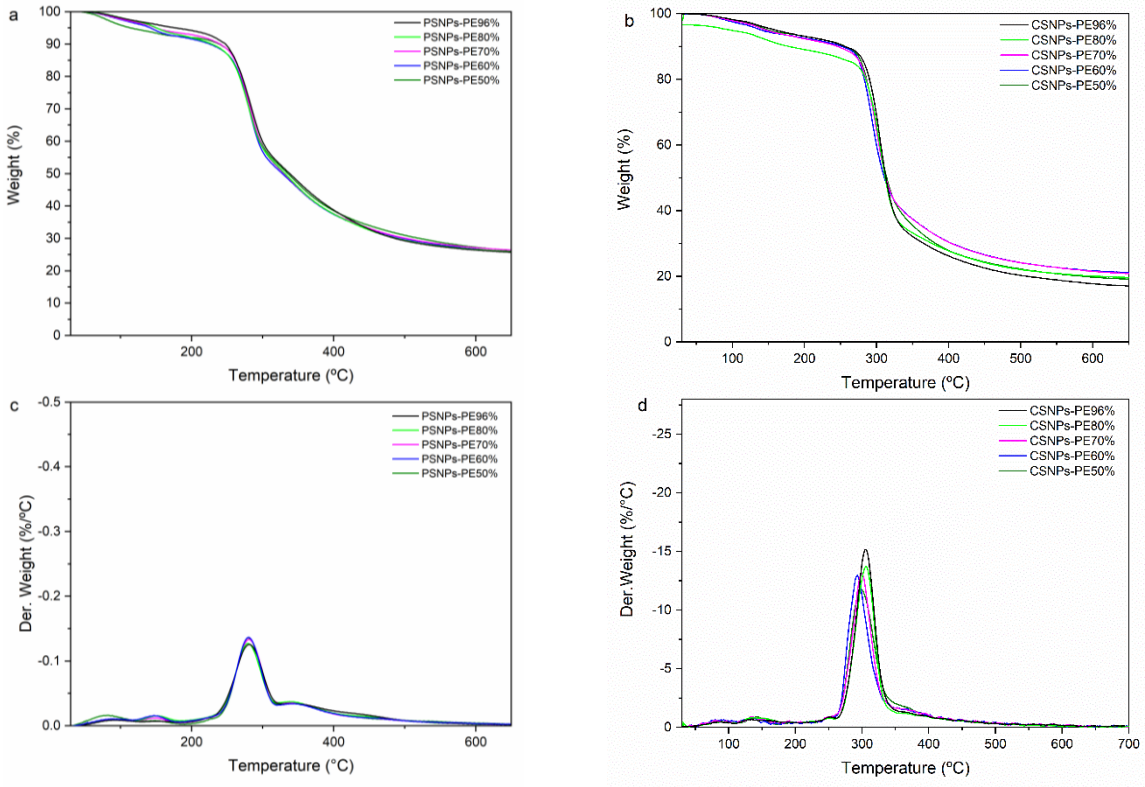

Source: Alves et al. (2022), with permission.

4.3.2.7 Color

Color is of the important factor for quality and visual description of food product. The increase in LTPC significantly decreased ($p < 0.05$) the L^* values in starch NPs (Table 4.3), confirming the stabilization of phenolic compounds in starch NPs. Similar results were observed for starch-based films containing beeswax and ethanolic propolis extract (87.69 and 91.03%) (PÉREZ-VERGARA et al., 2020).

Regarding the a^* coordinate, these values were low, but slight increased with the increase in LTPC in starch NPs, indicating that there was a reduction in gray intensity and a tendency to brown. The b^* coordinate values were between -2.71 and 9.00 for PSNPs-PE and between -3.28 and 4.75 for CSNPs-PE (Table 4.5). Interestingly, PSNPs-PE96% and CSNPs-PE96% showed a more intense brown color than those produced using lower ethanol concentrations (Table 4.5). This result is due to the higher LTPC in PSNPs-PE and CSNPs-PE

as discussed previously in Section 4.3.2.1**.** Irigoiti, Yamul and Navarro (2021) also found a decreasing in lightness and a color enhancement in co-crystallized powders when increased the load of different contents of propolis by co-crystallization in sucrose.

Table 4.5. Color parameters (L*, a* and b*) of potato starch nanoparticles (PSNPs-PE) and cassava starch nanoparticles (CSNPs-PE) loading the phenolic compounds from propolis extracts (PE) with different ethanol concentration (50, 60, 70, 80 and 96%).

Sample	Color parameter		
	L^*	a^*	b^*
PSNPs-PE50%	91.86 ± 0.05^{a}	1.81 ± 0.01^{a}	-2.71 ± 0.01^{a}
PSNPs-PE60%	88.8 2 ±0.03^{b}	1.97 ± 0.00^{ab}	0.91 ± 0.10^{b}
PSNPs-PE70%	89.69 ± 0.23^{c}	2.03 ± 0.08^{b}	0.21 ± 0.18^{c}
PSNPs-PE80%	85.17 ± 0.36^{d}	2.55 ± 0.08^{c}	6.78 ± 0.37^{d}
PSNPs-PE96%	82.36 ±0.33^{e}	2.41 ± 0.07^{c}	9.00 ± 0.05^{e}
CSNPs-PE50%	91.63 ± 0.03^{a}	2.35 ± 0.01^{a}	-3.28 ± 0.01^{a}
CSNPs-PE60%	91.41 ± 0.02^{ab}	2.39 ± 0.01^{a}	-2.91 ± 0.00^{b}
CSNPs-PE70%	90.10 ± 0.00^{c}	2.66 ± 0.00^{b}	-1.09 ± 0.02^{c}
CSNPs-PE80%	90.53 ± 0.05^{bc}	1.99 ± 0.06^{c}	-0.38 ± 0.13^{d}
CSNPs-PE96%	86.66 ± 0.82^{d}	2.23 ± 0.22^{ac}	4.75 ± 0.17^{e}

All values were expressed as mean ± standard error using the replicates of three experiments. Mean values with different letters within the same column were significantly different ($p < 0.05$).

4.3.2.8 Solubility in water (S)

Starch NPs loading the phenolic compounds of acidified PE had S values between 74.74 to 89.11% (Table 4.6), being superior when compared with native potato (S = 18.31%) and cassava (S = 44.49%) starches , but lower than the S values informed in starch NPs produced with different ethanol concentrations (81.79% ≤ S ≤ 94.49%), but without PE (ALVES et al., 2021). The reduction in S values could be correlated with the presence of phenolic compounds in the starch NPs, however, S values confirm the high-water solubility of the starch NPs produced in the current research. Based on S results, the starch NPs loading the phenolic compounds of acidified PE could be used as additives in food formulations or to manufacture active food packaging. Further studies could investigate the effect of temperature on the thermal degradation of phenolic compounds loaded in starch NPs.

Table 4.6. Solubility in water (S) of potato starch nanoparticles (PSNPs-PE) and cassava starch nanoparticles (CSNPs-PE) loading the phenolic compounds from acidified propolis extracts (PE) with different ethanol concentration (50, 60, 70, 80 and 96%).

Sample	S (%)
PSNPs-PE50%	88.25 ± 1.81[a]
PSNPs-PE60%	89.04 ± 4.68[a]
PSNPs-PE70%	86.43 ± 5.05[a]
PSNPs-PE80%	89.11 ± 3.16[a]
PSNPs-PE96%	83.30 ± 1.69[a]
CSNPs-PE50%	84.19 ± 4.02[a]
CSNPs-PE60%	84.63 ± 2.05[a]
CSNPs-PE70%	82.24 ± 5.97[a]
CSNPs-PE80%	82.80 ± 3.66[a]
CSNPs-PE96%	74.74 ± 3.43[b]

All values were expressed as mean ± standard error using the replicates of three experiments. Mean values with different letters within the same column were significantly different ($p < 0.05$).

4.4 CONCLUSIONS OF CHAPTER 4

In this study, the different ethanol concentrations used in the propolis extract impacted the retention of phenolic compounds in starch nanoparticles. The obtained starch nanoparticles had particle size lower than 1000 nm, as well as high concentrations of phenolic compounds and antioxidant activity. Furthermore, these starch nanoparticles displayed V-type crystalline structure, low moisture content and water activity, suggesting that these powders are not susceptible to microbial growth during storage. Finally, starch nanoparticles containing the phenolic compounds showed brown color typical of propolis extract and high solubility in hot water, indicating that these nanomaterials could be used as additives in food formulations or to manufacture food packaging with antioxidant properties.

CAPÍTULO 5

PRODUÇÃO E CARACTERIZAÇÃO DE NANOPARTÍCULAS DE AMIDO CARREGADAS COM OS COMPOSTOS BIOATIVOS DO EP VERDE ACIDIFICADO

Apresentado na forma de artigo

5 STARCH NANOPARTICLES CONTAINING PHENOLIC COMPOUNDS FROM GREEN PROPOLIS: CHARACTERIZATION AND EVALUATION OF ANTIOXIDANT, ANTIMICROBIAL AND DIGESTIBILITY PROPERTIES

É importante ressaltar que neste capítulo foi utilizada a própolis verde para obtenção dos extratos de própolis, pois em testes preliminares foi observado que os extratos de própolis marrom (estudados no capítulo 3) não apresentaram atividade antimicrobiana. Além disso, o ultrassom para obtenção de extratos de própolis do Capítulo 3 foi quebrado e passamos a obter extratos com ultrassom de ponta combinado com shaker. Com base nos resultados obtidos no Capítulo 3, foi possível continuar apenas com o extrato obtido na concentração de 96% de etanol acidificado.

Este capítulo relata a terceira fase experimental desta tese, que envolve o estudo das propriedades antimicrobianas e de digestibilidade de nanopartículas de amido carregadas com compostos fenólicos de PE.

A partir desta etapa, foi escrito o terceiro artigo experimental intitulado "Nanopartículas de amido contendo compostos fenólicos da própolis verde: Caracterização e avaliação de propriedades antioxidantes, antimicrobianas e digestibilidade" que está submetido (ainda não publicado) ao International Journal of Biological Macromolecules.

Graphical abstract

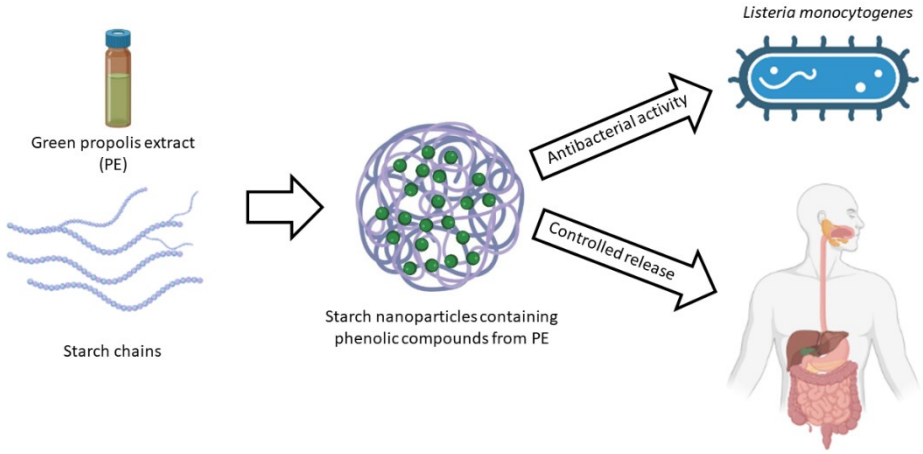

Highlights

- Starch nanoparticles (NPs) stabilizing phenolic compounds were produced.

- NPs stabilizing phenolic compounds displayed antioxidant activity.
- Active NPs had antibacterial activity against *L. monocytogenes*.
- Phenolic compounds can be released from NPs.

Abstract

In this study was investigated the production of nanoparticles through nanoprecipitation using cassava and potato starches as carriers to stabilize bioactive compounds from green propolis extract (PE). Additionally, the antioxidant and antimicrobial activities of phenolic compounds stabilized with starch nanoparticles (SNPs), as well as their release under gastrointestinal conditions were investigated. PE exhibited antioxidant and antibacterial properties, specially PE3 (PE produced using sonication by 20 min and stirring at 30 °C for 24h) had the highest concentrations of *p*-coumaric acid, rutin, kaempferol and quercetin. Contact angle results showed that potato and cassava starch nanoparticles were more hydrophobic due to the presence of phenolic compounds on their surfaces. The active SNPs from PE showed antibacterial activity against *L. monocytogenes*, at 750 mg of propolis/mL. Controlled release of phenolic compounds was observed from the nanoparticles when exposed under simulated gastrointestinal conditions, indicating the potential use of these nanomaterials as ingredients to manufacture functional foods.

Keywords: active nanomaterials, biopolymer nanoparticles, carbohydrates, natural antimicrobials.

Abbreviations

AP: anti-solvent precipitation; CS: cassava starch; GAE: gallic acid equivalent; Loading Efficiency (LE); MIC: minimum inhibitory concentration; MBC: minimum bactericidal concentration; PSNPs-PE: potato starch nanoparticles loading the phenolic compounds from acidified propolis extracts; CSNPs-PE: cassava starch nanoparticles loading the phenolic compounds from acidified propolis extracts PE; CSNPs: starch nanoparticles based on cassava starch; GRAS: Generally Recognized as Safe; PSNPs: starch nanoparticles based on potato starch; PE: propolis extract; PS: potato starch; SNPs: starch nanoparticles; SH: starch hydrolysis; TPC: total phenolic content;; WCA: water contact angle.

5.1 INTRODUCTION

Propolis is a natural resinous mixture produced by bees that exhibits a variety of biological activities due to its main bioactive chemical constituents, essential and aromatic oils, phenolic acids, and polyphenols such as flavonoids. More than 300 constituents have been identified in propolis, depending on their origin. The chemical composition of crude propolis was found to contain 50% resins and balsams, 30% waxes, 10% essential oils, 5% pollen, and 5% assorted organic and mineral compounds as constituents (ŠTURM et al., 2019). The ratio of various constituents to their chemical composition depends on the time and place of collection. Propolis has great potential to be used as a food additive due to its various biological properties, such as antioxidant, antimicrobial, antitumor, anti-inflammatory, immunomodulatory and antiproliferative. In the literature, several studies reveal that the effectiveness of propolis in numerous applications is based on the synergistic effect of its various components (PASUPULETI et al., 2017; SFORCIN, 2016; TORETI et al., 2013; XAVIER et al., 2017).

Therefore, the development of foods enriched with bioactive compounds isolated from propolis has attracted attention in recent years. However, the main limitation of propolis is its low bioavailability, low permeability, and deficiency during human digestion, which restricts it to obtain better health benefits. In addition, there are fundamental challenges for its large-scale application, including solubility, poor biodistribution with lower absorption and photosensitivity, and strong taste. In the literature, many of the reported methods for the stabilization of the phenolic compound from propolis require synthetic chemicals with several steps that can lead to dissolution of the bioactive compounds during the stabilization process. In addition, a few number of studies have investigated the stability, bioaccessibility and bioavailability, as well as the release under gastrointestinal conditions of phenolic compounds isolated from propolis extract (BODINI et al., 2013; NORI et al., 2011).

Nanomaterials obtained using starches can be used in various food applications due to their small size, large surface area, excellent biocompatibility, low toxicity and attractive physical and chemical properties. (ALVES et al., 2021; CAICEDO CHACON et al., 2023a; QIU et al., 2018). In addition, biopolymer-based nanoparticle matrices have “generally recognized as safe” (GRAS) status, are non-toxic and environmentally friendly (CAICEDO CHACON et al., 2023a; QIU et al., 2018). In particular, SNPs have shown the capacity to

stabilize bioactive compounds with hydrophobic properties and allow a controlled release (ACEVEDO-GUEVARA et al., 2018).

One of the techniques to stabilize the phenolic compounds from propolis is through the antisolvent precipitation (AP) method. In this method, two phases are used, an aqueous phase containing a water-soluble macromolecule (i.e., starch) and an organic phase containing the active compound. Then, the macromolecule is precipitated by dripping the organic phase, and the macromolecule/active compound is stabilized during its precipitation (MARTÍNEZ RIVAS et al., 2017; QIN et al., 2016). The AP method is known for its simplicity and low cost, as well as the fact that toxic or environmentally harmful reagents are not required (QIU et al., 2019).

In the literature, there is little research available about the stabilization of phenolic compounds using SNPs, as well as the study of these materials with respect to antimicrobial activity, starch hydrolysis, and release under gastrointestinal conditions. Therefore, this study aims to produce starch nanoparticles loaded with the phenolic compounds from propolis and produced by AP method, as well as to investigate the potential use of these nanomaterials as natural antimicrobials, understanding the behavior of these active nanomaterials when exposed to simulated gastrointestinal conditions.

5.2 MATERIALS AND METHODS

5.2.1 Materials

In this research, native starches isolated from cassava (Juréia Food Industry, Santa Catarina, Brazil) and potato (Shambala Naturals Food Industry, Santa Catarina, Brazil) were used as macromolecules. The source of bioactive compounds was green propolis (Breyer®, Formigas – Minas Gerais, Brazil). Distilled water was used as the universal solvent, whereas ethanol (≥ 99.6%, Êxodo Científica, Brazil) and hydrochloric acid (37 wt%, Neon, Brazil) were used in the production of propolis extracts. For total phenolic compounds, DPPH radical scavenging, free radical ABTS+, ferric reducing antioxidant power were used potassium chloride and sodium carbonate were purchased from Dinâmica (Brazil). Folin-Ciocalteu, 2,2-diphenyl-1-picrylhydrazyl (DPPH), 2,2'-azino-bis (3-ethylbenzothiazoline-6-sulfonic acid) (ABTS) and ferric reducing antioxidant power (FRAP). All reagents were acquired directly from Sigma-Aldrich (Brazil) and they were of analytical grade.

5.2.2 Production of green propolis extracts

The extraction of phenolic compounds from green propolis was carried out using sonication and mechanical stirring. Propolis extract (PE) was prepared by dispersing 2.85 g of green propolis in 100 mL of a hydroethanolic solution (96% v/v) and then sonicated using an ultrasonic probe device (4 mm diameter) (Eco-Sonics, model QR500, Indaiatuba, SP-BR) with a digital timer, operating with a power of 500 W (100% amplitude), a frequency of 20 kHz at 30 °C by Alves, Monteiro and Valencia (2022) with some modifications. The resulting propolis extracts were named PE1 (sonicated for 20 min) and PE2 (sonicated for 40 min), PE3 (sonicated for 20 min with mechanical stirring at 30 °C for 24h at 120 rpm) and PE4 (sonicated for 20 min with mechanical stirring at 30 °C for 48 h at 120 rpm). Next, each PE was centrifuged at 25 ºC in a centrifuge (Kasvi, Brazil) with a force of 1700 × g at 4000 rpm for 15 minutes, and finally filtered through qualitative filter paper and stored in amber bottles at -24 ºC in the absence of light until analysis.

5.2.2.1 Characterization of green propolis extracts

Total phenolic compounds (TPC) of PE was measured using the method described by Alves, Monteiro and Valencia (2022). PE was diluted in ethanol (≥ 99.6%) in a 1:40 (% v/v) ratio. An aliquot of 100 µL of the ethanolic extract was mixed with 7.9 mL of distilled water and 0.5 mL of Folin-Ciocalteu reagent (2N), followed by homogenization in vortex. In sequence, 1.5 mL of sodium carbonate solution 7.5% (w/v) was added and then homogenized in vortex. The test tubes were kept in dark at room temperature for 2 h. The absorbance of solutions was measured at a wavelength of 760 nm, using an UV-Vis spectrophotometer (QUIMIS, Q898U2M5, Diadema, SP, Brazil) and a blank solution with ethanol concentration of 95.6%. TPC results were expressed as milligrams of gallic acid equivalent (GAE) per g of green propolis. A calibration curve made with concentrations oscillating between 0 - 750 µg of GAE/mL of extract ($y = 0.0011x + 0.0548$, $R^2 = 0.9993$) was used in this quantification.

DPPH radical scavenging was quantified according the previous study of Alves et al. (2022). In summary, 100 µL of PE was mixed with 2.9 mL of a DPPH solution (0.1 mM) at room temperature. The mixture was kept in a dark place for 30 min. Then, the same UV–Vis spectrophotometer was used to measure the absorbance of samples at 515 nm. Trolox results

were expressed as μmol of Trolox per g of green propolis. A calibration curve made with concentrations oscillating between 0 - 750 μmol Trolox/L ($y = -0.0006x + 0.7766$, $R^2 = 0.9753$) was used in this quantification.

Free radical ABTS+ was determined according to the methodology proposed by Re et al. (1999). An aliquot of 30 μL of PE was transferred to test tubes with 3.0 mL of the ABTS+ radical and homogenized in vortex. The samples were kept in dark at room temperature for 6 min and the absorbance value was read in the same UV-Vis spectrophotometer at a wavelength of 734 nm. Free radical ABTS+ results were expressed as μmol of Trolox per g of propolis. The quantification was done using a calibration curve made with concentrations varying between 0 - 1500 μmol /mL ($y = -0.0003x + 0.6931$, $R^2 = 0.9978$).

The ferric reducing antioxidant power (FRAP) of PE was performed according to Ebner et al. (1996). Briefly, 10 μL of PE and 290 μL of FRAP reagent were added onto a microplate. This solution was kept in the dark at room temperature for 30 min and absorbance was measured at 593 nm in a microplate reader (Tecan Infinite M200). The analyses were performed in triplicate with a blank for each sample (10 μL of solvent + 290 μL of FRAP). Trolox was used as a reference and values were calculated using a calibration curve with concentrations varying between 50 and 500 μM. FRAP results were expressed as μmol of Trolox equivalent per g of dry extract (μmol TE/g extract).

The chromatographic profile of the PE was obtained using high-performance liquid chromatography coupled to a diode array detector (DAD). Sample preparation involved a cleanup step through solid phase extraction (SPE) using a previously activated C18 column (Chromabond, C18 EC) with 2.0 mL of methanol. An aliquot of PE was solubilized in HPLC grade methanol and 2.0 mL of this sample was eluted into the cartridge, using methanol (100%) as eluent. The resulting fraction from the SPE, had the solvent removed in a rotoevaporator and was then resolubilized to a concentration of 20.0 mg/mL. Finally, the solution was filtered through a PTFE membrane (Cobetter, Unichro®) with a pore size of 0.45 μm, directly in an HPLC vial for injection into a chromatographic system (DA SILVA et al., 2022).

To obtain the chromatograms, a Restek Ultra C18 column (250 x 4.6mm (di); 4.8μm) was used with an eluent system consisting of water:acetic acid (1%) (phase A) and acetonitrile (phase B). The run was performed in gradient mode with a ramp from 5 to 100% B in 35 minutes and maintained at 100% for five minutes at the end of the run. The mobile phase flow was 0.9mL/min, the oven temperature was kept constant at 40 ºC, and the sample injection volume was 10μL. Data were acquired through a DAD-type detector, with selected wavelengths of 280,

300 and 320nm, and processed in Shimadzu's LabSolutions software (DA SILVA et al., 2022). The phenolic compounds were identified by comparing the DAD spectra and retention times of injected standards with those of the samples injected (DA SILVA et al., 2022). The quantification of the phenolic compounds was performed using the external standard method. The equations obtained through linear regression were used to quantify each identified compound by applying the values of the sample's peak areas. To obtain the means and standard deviation, samples were injected in duplicate.

5.2.3 Production of starch nanoparticles loaded with the phenolic compounds from propolis extract

SNPs were produced by AP method Alves, Monteiro and Valencia (2022). Dispersions (5% w/w) of cassava (CS) and potato (PS) starch were prepared in distilled water at 25 ºC and then they were heated at 90 °C for 30 minutes. In sequence, gelatinized starches were cooled to 30 ºC and PE (previously acidified with HCl, pH 1) was added with the aid of a peristaltic pump (flow of 0.7 mL/min) drop wise for the gelatinized starch in a 1:1 (% v/v) ratio.

After mixing the gelatinized starch solution with the PE, the resulting slurry was kept in magnetic agitation with constant stirring for 12 hours. Then, the slurry was centrifuged at 25 ºC using a centrifuge (Kasvi, Brazil) with 1700 × g force at 4000 rpm for 15 minutes to separate SNPs from the solvents. SNPs were centrifuged three times with a hydroethanolic solution (80% v/v), and finally washed with absolute ethanol (99.6%). SNPs were removed by centrifugation using the same centrifuge and the ethanol in the SNPs was evaporated using a forced-air convection oven (Solidsteel, Brazil) at 60 ºC for 10 min. In sequence, SNPs were frozen at -18 ºC for 48 h, and finally lyophilized (Liotop L 101). The resulting SNPs loading the phenolic compounds from PE were finely macerated and stored in desiccators with silica gel at 25 °C for further analysis.

5.2.4 Characterization of the starch nanoparticles loaded with the phenolic compounds from propolis extract

5.2.4.1 Loading efficiency (LE)

The LE of the phenolic compounds from acidified PE stabilized with SNPs was calculated as proposed by Quiroz et al. (2020) (Eq. 5.1):

$$\text{LE}\ (\%) = \left(\frac{\text{TPC}_\text{i} - \text{TPC}_\text{s}}{\text{TPC}_\text{i}}\right) * 100 \quad (5.1)$$

where TPC_i and TPC_s are the initial total phenolic compounds (TPC) of the PE before stabilization with SNPs and TPC of supernatant collected after the first centrifugation at 4000 rpm for 15 min (see Section 5.2.3), respectively. The quantification of TPC was carried out using the same method informed in Section 5.2.2.1.

5.2.4.2 Particle size distribution, surface charge and water contact angle

Particle size and surface charge of SNPs were determined using a LUMiSizer (LUM GmbH, Germany) and a Zetasizer Nano ZS (Malvern, England), respectively. For the particle size measurements, SNPs were dispersed in ultrapure Mili-Q water (0.03% w/v, pH 4.0 to 7.0) and sonicated for 30 min at 40 KHz, using a sonicator bath (Ultracleaner 1650, Unique, Brazil) (AHMAD et al., 2019).

To water contact angle, the samples were compressed into tablets using a thermopress and a cylindrical mold. About 0.2 g of sample was deposited in the mold and 1 ton of force was applied. The pellets were approximately 1.5 mm thick and 1 cm in diameter. The compressed samples then had their contact angles analyzed in a goniometer, dropping 5 µL of water over them. The final result is the average of 10 measurements taken over a 5 s interval (AMIRABADI; MILANI; SOHBATZADEH, 2020; GRZEGORZEWSKI et al., 2010).

5.2.4.3 Release behavior under simulated gastrointestinal conditions

The *in vitro* digestibility tests of nanoparticles with and without the addition of propolis were carried out according to the gastrointestinal digestion simulation protocol defined by INFOGEST and described by Minekus et al. (2014) and Brodkorb et al. (2019), with some modifications. The simulation was performed sequentially for the oral (matrix release fraction in the mouth), gastric (matrix release fraction in the stomach) and intestinal (matrix release fraction through the small intestine) phases. The fluids of each stage had the following composition:

- Salivary simulation fluid (SSF): 15.1 mM KCl, 3.7 mM KH2PO4, 13.6 mM $NaHCO_3$, 0.15 mM $MgCl_2$(H2O), 0.06 mM (NH4)2CO3, 1.1 mM HCl and 1.5 mM $CaCl_2(H_2O)_2$;

- Gastric simulation fluid (SGF): 6.9 mM KCl, 0.9 mM KH_2PO_4, 25 mM $NaHCO_3$, 47.2 mM NaCl, 0.12 mM $MgCl_2(H_2O)$, 0.5 mM $(NH4)_2CO_3$, 15 .6 mM HCl and 0.15 mM $CaCl_2(H_2O)_2$;

- Intestinal simulation fluid (SIF): 6.8 mM KCl, 0.8 mM KH_2PO4, 85 mM $NaHCO_3$, 38.4 mM NaCl, 0.33 mM $MgCl_2(H_2O)$, 8.4 mM HCl and 0.6 mM $CaCl_2(H_2O)_2$;

Initially, all solutions used in the experiment were heated to 37 °C, and the simulation was performed at the same temperature. Samples (0.250 g) were transferred to a falcon tube (10 mL) and the oral phase simulation was started by adding SSF 1:1 (m/v) and human salivary α-amylase solution (75 U/mL, Sigma-Aldrich A1031). The mixture was then adjusted to pH 7 and incubated at 37 °C in a water bath under agitation at 180 rpm for 2 min. Then, the oral bolus was mixed with SGF 1:1 (v/v), adjusted to pH 3 with 1M HCl and added with swine pepsin solution (2,000 U/mL, Sigma-Aldrich P7012). The mixture was then incubated at 37 °C in a water bath under agitation at 100 rpm for 2 h. For the small bowel phase, gastric chyme was mixed with SIF 1:1 (v/v), containing pancreatin (200 U/mL based on α-amylase activity, Sigma-Aldrich P7545) and bile salts (10 mM, Sigma-Aldrich B3883). The pH was adjusted to 7 using 1M NaOH and the samples were again incubated at 37 ˚C in a water bath under agitation at 100 rpm for 2 h. During the intestinal phase, samples of 100 µL of the mixture were taken at different time intervals (80, 120 and 180 min). Absolute ethanol was added to the collected samples in a 4:1 ratio to stop all enzymatic reactions and kept at room temperature for 30 minutes. The ethanolic mixtures were then centrifuged (4000 × g, 15 min) and the supernatants were collected for glucose measurement. Then all samples were centrifuged at 4677 g for 15 min (Kasvi, Brazil) and stored at -20 °C until further analysis. The *in vitro* digestion experiments were performed in duplicate.

5.2.4.3.1 Glucose measurement and starch hydrolysis

To determine the amount of glucose in the *in vitro* digested samples, the D-glucose assay procedure (GOPOD, Labtest) was used to quantify the amount of glucose present at each time point. The supernatants collected in the previous step were incubated with amyloglucosidase (from *Aspergillus niger)* to convert α-amylase products into glucose

(ROVALINO-CÓRDOVA; FOGLIANO; CAPUANO, 2018). Supernatants (0.1 mL) were mixed with amyloglucosidase solution (27 U/mL) in sodium acetate buffer (pH 4.8). Then, the aliquots were combined with 1 mL of GOPOD reagent and incubated for 10 min at 37 °C and the absorbance of the samples was read at 510 nm against the blank reagent. The percentage of starch hydrolysis in each sample was expressed as follows:

$$SH\ (\%) = \frac{Sh}{Si} = \frac{Gp}{Si} * 0.9 \qquad (5.2)$$

where SH is the percentage of starch hydrolysis, Sh is the amount of starch hydrolyzed at different times in the intestinal phase, Si is the initial amount of starch in the sample and Gp is the amount of glucose produced due to starch hydrolysis. A conversion factor of 0.9 was applied based on the molecular weight of a starch monomer divided by the molecular weight of glucose to convert the glucose content into the corresponding amount of starch (GOÑI; GARCIA-ALONSO; SAURA-CALIXTO, 1997).

5.2.4.4 Microbial analysis

To prepare the *L. monocytogenes* inoculum (TCC 7474), 100 µL of the suspensions were thawed and transferred to a tube containing 10 mL of BHI broth, incubated at 37 °C for 24 h and then seeded in *Listeria Agar by Ottaviani & Agosti* (ALOA) to verify their characteristics (greenish cultures). A colony was harvested from the ALOA plates, inoculated into tubes containing 10 mL of BHI broth, then incubated under agitation at 210 rpm at a temperature of 37 °C and cultivated for 8 h until the stationary phase of culture (10^9 CFU/mL) (Fig 5.1).

Fig. 5.1. Preparation of *L. monocytogenes* inoculum in BHI broth.

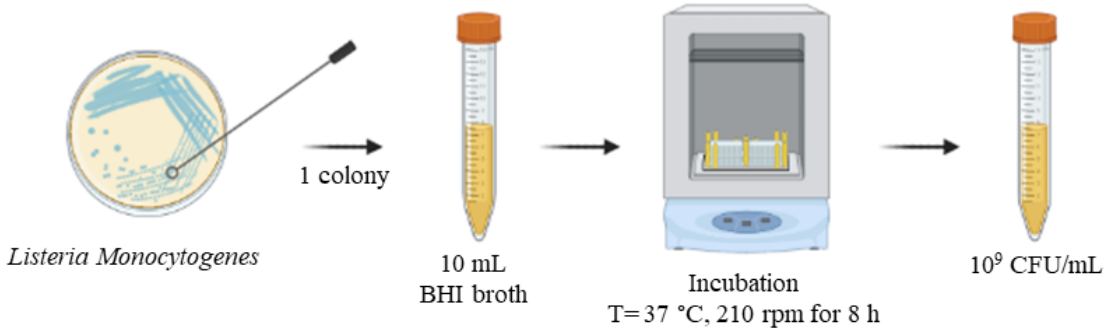

Source: Author.

After that, the dilution and inoculation methodology in culture medium was performed according to Cano et al. (2016), with modifications. After preparing, the bacterial culture, the inoculum was diluted in an Eppendorf tube with 0.9 mL of peptone water (0.1%) to obtain 10^8 CFU/mL inoculum concentration.

Tubes containing 10 mL of BHI agar, extract and nanoparticle masses were added. Subsequently, were vortexed for 2 min for complete homogenization. Then, this volume was poured into petri dishes (60 mm) until complete solidification of the medium. Then, 50 µL of the inoculum (10^8 CFU/mL) was spread on the surface of the plate containing BHI agar + extract or BHI agar + NPs. The plates were incubated for 24 h at 37 °C (Fig 5.2).

Fig. 5.2. Dilution and inoculation of *L. monocytogenes* in culture medium.

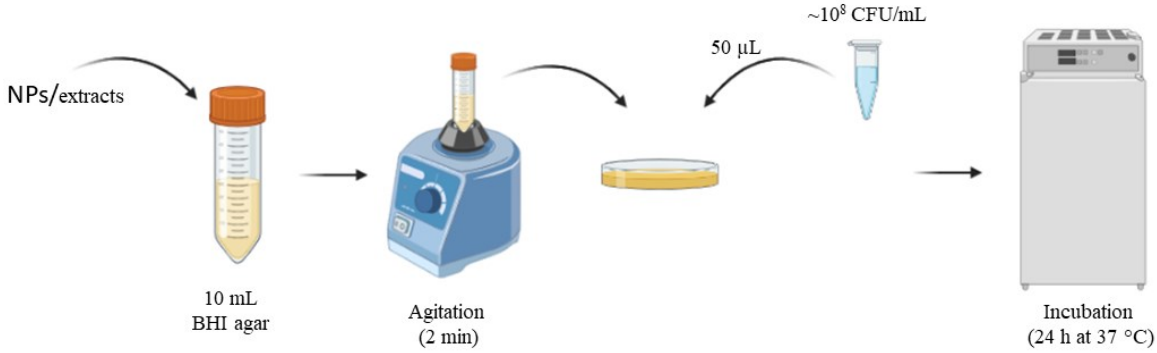

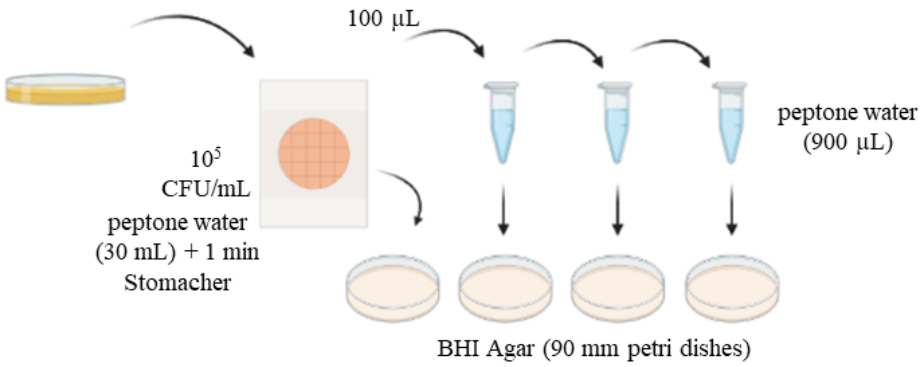

source: author.

Due to the coloring of the extract and nanoparticles, cell recovery was performed as follows: BHI agar from plate was transferred to a sterile plastic bag and diluted in peptone water (1:1) while stirring in a stomacher bag mix (Servilab) for 1 min. Then plating was performed. Serial dilutions in peptone water were prepared and 100 µL aliquots of the dilutions were seeded on the surface of BHI Agar (in 90 mm petri dishes) for quantification of *L. monocytogenes* and then incubated in BOD at 37 °C for 48 h and 24 h, respectively. The mean CFU/mL count (and standard deviation) of two independent samples from each sampling.

The minimum inhibitory concentration (MIC) of the PE and NPs was defined as the lowest concentration capable of inhibiting bacterial growth and the minimum bactericidal concentration (MBC) as the lowest concentration that leads to bacterial death.

5.2.5 Statistical analyses

All results were expressed as means ± standard deviation ($n \geq 3$). The experimental data were analyzed using Analysis of variance (ANOVA) and Tukey test with multiple comparisons, was performed with a 5% significance level using the software Statistica 10.0 (StatSoft®, USA). Pearson's correlation was performed using Excel® software.

5.3 RESULTS AND DISCUSSIONS

5.3.1 Green propolis extracts composition

In the propolis extracts, a total of 8 compounds were detected, showing the peaks with the identified substances, being: Protocatechuic ac. (1); chlorogenic ac (2); ac. caffeic (3); rutin

(4); p-coumaric ac (5); quercetin (6); ac. cinnamic (7); kaempferol (8). For some of the remaining peaks in the chromatogram (Fig. 5.3), it was not possible to identify the corresponding compounds due to a lack of reference compounds.

Fig. 5.3. Chromatogram of the propolis extract produced using sonication by 20 min and stirring at 30 °C for 24h (PE3).

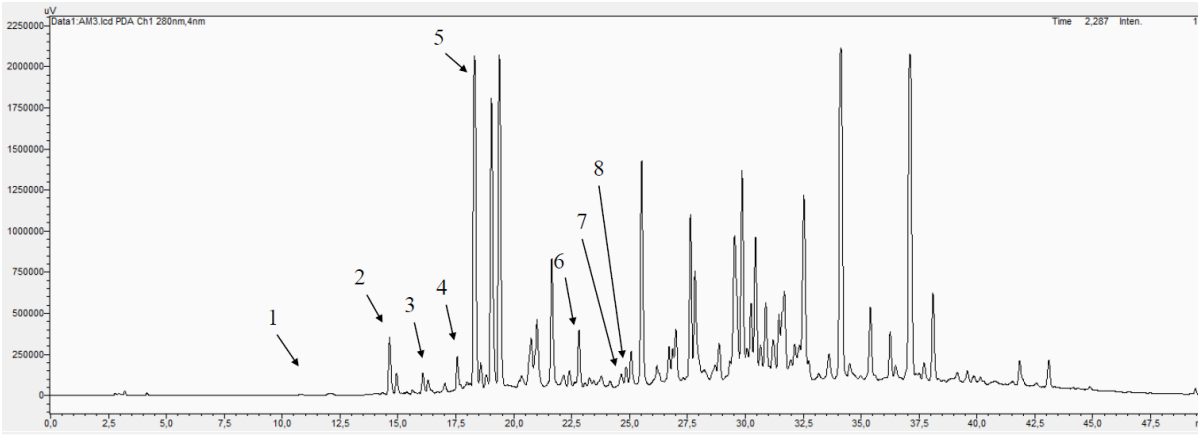

1 = Protocatechuic ac, 2 = Chlorogenic ac, 3 = ac. Caffeic , 4 = rutin, 5 = p-coumaric ac, 6 = quercetin, 7 = ac. cinnamic, 8 = kaempferol

PE3 showed the higher concentration compounds, among them: *p*-coumaric acid (15.96 mg/g extract), rutin (5.176 mg/g extract), kaempferol (0.781 mg/g extract), cinnamic acid (0.863 mg/g extract) and quercetin (5,376 mg/g of extract) were higher when compared to the other extracts (Table 5.1). Thus, PE3 was considered the best PE sample. These results agree with assessed the total phenol content of propolis samples from different regions of Brazil (TIVERON et al., 2016).

Table 5.1. Concentration of individual phenolic components for propolis extract (PE) obtained by HPLC. Total phenolic compounds (TPC) and antioxidant capacity by DPPH, FRAP, and ABTS of the PE3.

Compounds	Phenolic compounds (mg/g PE)			
	PE1	**PE2**	**PE3**	**PE4**
chlorogenic acid	4.67 ± 0.03^{d}	6.79 ± 0.21^{a}	5.64 ± 0.08^{c}	6.20 ± 0.08^{b}
caffeic acid	1.38 ± 0.08^{b}	1.68 ± 0.07^{a}	1.67 ± 0.01^{a}	1.86 ± 0.05^{a}
***p*-coumaric acid**	11.30 ± 0.18^{c}	12.80 ± 0.10^{b}	15.96 ± 0.04^{a}	15.76 ± 0.09^{a}
cinnamic acid	0.52 ± 0.04^{c}	0.67 ± 0.01^{b}	0.86 ± 0.01^{a}	0.75 ± 0.01^{b}
rutin	4.53 ± 0.06^{b}	4.75 ± 0.01^{b}	5.18 ± 0.01^{a}	5.51 ± 0.14^{a}
kaempferol	0.60 ± 0.05^{a}	0.65 ± 0.08^{a}	0.78 ± 0.03^{a}	0.66 ± 0.02^{a}
quercetin	3.67 ± 0.01^{c}	4.40 ± 0.05^{b}	5.38 ± 0.18^{a}	4.29 ± 0.12^{b}

Sample	TPC (mg of GAE/g of extract)	DPPH (µmol TROLOX/g of extract)	FRAP (µmol TROLOX/g of extract)	ABTS (µmol TROLOX/g of extract)
PE3	763.36 ± 30.73	727.60 ± 10.05	202.61 ± 3.51	2516.33 ± 189.77

PE1: 20 min Ultrasound at 30°C; PE 2: 40 min Ultrasound at 30°C; PE3: 20 min Ultrasound + 24 h Shaker (120 rpm) at 30°C; PE4: 20 min Ultrasound + 48 h Shaker (120 rpm) at 30°C. Mean values with different letters within the same column were significantly different ($p < 0.05$).

GAE: gallic acid equivalent. All values were expressed as mean ± standard error using the replicates of three experiments.

Based on the previous literature, these values are comparable or superior to many plant extracts that are rich in phenolic compounds. Polyphenolic compounds, such as caffeic acid and ferulic acid, extracted from propolis have antimicrobial activity. Several studies reported the excellent antioxidant activity of green propolis extract (PE) attributed to its rich phenolic composition, which includes chlorogenic acid, *p*-coumaric acid and artepilin C. Among all compounds already identified in propolis, *p*-coumaric acid is the chemical compound that attracts the attention of researchers, due to its numerous biological properties. *p*-coumaric acid has also potential to treat different injuries by acting as antiulcerogenic (BARROS et al., 2008), antimicrobial, anticancer and antimutagenic (PEI et al., 2016).

Furthermore, it was analyzed the total phenolic content and antioxidant capacity of PE3 (Table 5.1). The green propolis extract had a total phenol content of 763.36 mg GAE/g, DPPH of 727.60 (µmol TROLOX/g of extract), ABTS of 2516,33 (µmol TROLOX/g of extract), FRAP of 202.61 (µmol TROLOX/g of extract) (Table 5.1). These results are higher

with those reported by Cruz et al. (2021) that assessed the total phenol and flavonoid content of propolis extracts from different regions of Brazil where the total phenol content ranged between 17.59 mg GAE/g and 79.84 mg GAE/g. Previously, Calavaro et al. (2019) used ultrasound-assisted extraction with different percentages of ethanol and showed that the antioxidant activity increased with the increasing time of the ultrasound-assisted extraction and the increasing percentage of ethanol in the extraction solution. These differences could be due to the phenolic composition of each extract, which varies according to the geographic region in which the propolis was produced, the climatic conditions, the harvesting period, and the type of extraction (CAVALARO et al., 2019).

5.3.2 Characterization of starch nanoparticles loaded with the phenolic compounds from propolis extract

5.3.2.1 Loading Efficiency (LE)

In the current research, LE values oscillating between 65.45 ± 2.53% and 73.32 ± 1.61% for SNPs produced with CS and PS, respectively. LE values had statistical difference ($p < 0.05$) and could be due to the differences in the starch composition, structure, and surface charge (ALVES; MONTEIRO; VALENCIA, 2022; ZHU, 2015). Similar LE results were informed in SNPs loaded the phenolic compounds from brown propolis extract (ALVES; MONTEIRO; VALENCIA, 2022). However, LE values were higher when compared with those informed in succinylated starch nanomaterials (LE ≈ 17%) loaded with the polyphenolic extract from Arugula (*Eruca sativa*) leaves and obtained by antisolvent precipitation (GARCÍA-GURROLA et al., 2021).

5.3.2.2 Particle size distribution, surface charge and water contact angle

Starch nanoparticles displayed bimodal distribution with particle size between 8 and 23 nm and from 189 to 340 nm (Fig. 5.4a). No difference was observed between samples added or not with PE, suggesting that the phenolic compounds stabilized did not alter the particle size of starch nanomaterials. In general, the peak of small particle size has been attributed to free nanoparticles, whereas the peak of large particle size could be caused by the aggregation of starch nanoparticles during the antisolvent precipitation (SADEGHI et al., 2017).

Fig. 5.4. (a) Particle size distribution of potato starch nanoparticles (PSNPs); cassava starch nanoparticles (CSNPs); potato starch nanoparticles (PSNPs-PE) and cassava starch nanoparticles (CSNPs-PE) loading the phenolic compounds from propolis extracts (PE). (b) Surface charge of PSNPs, CSNPs, PSNPs-PE, and CSNPs-PE. (c) Water contact angle of (i) PSNPs, (ii) CSNPs, (iii) PSNPs-PE, and (iv) CSNPs-PE.

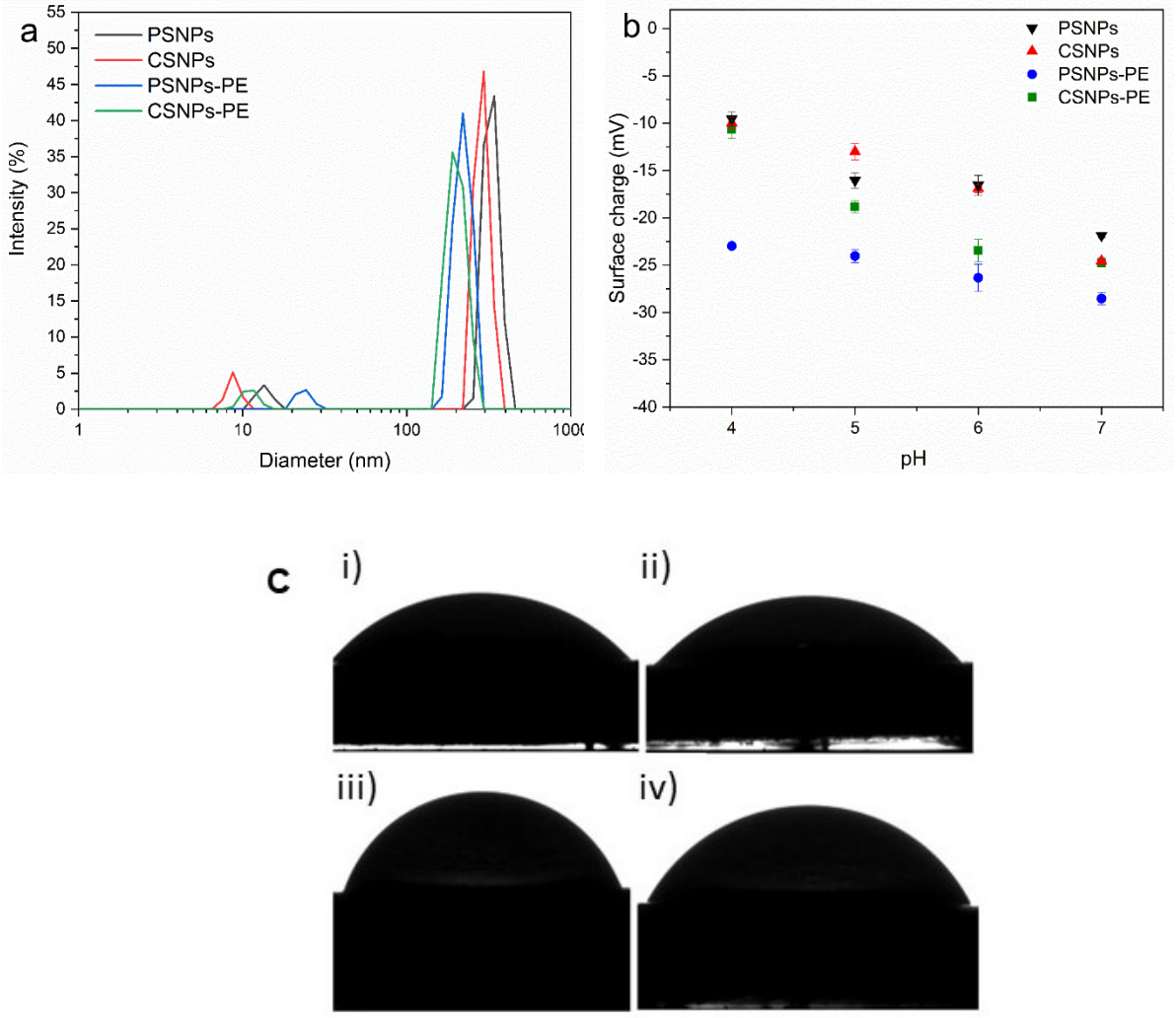

Source: Author.

In the literature, several research studies have informed comparable particle sizes. In this way, particle size of starch nanoparticles obtained through antisolvent precipitation were ranged between 207.9 nm and 475.6 nm, 16.7 nm, and 2750 nm, and 16.7 nm and 2750 nm using corn, lotus seed, and maize starches, respectively (LIN et al., 2020; SADEGHI et al., 2017; WU et al., 2016).

With respect to surface charge, it was observed that the SNPs containing the phenolic compounds from PE had higher surface charge values when compared with control samples (Fig. 5.4b), indicating that the phenolic compounds from PE increased the hydrophobicity of

the nanoparticles, which can be indicate that there was an incorporation of functional groups of the PE. Furthermore, it is concluded that these nanomaterials can be considered moderately stable (BANERJEE et al., 2016). The increase in hydrophobicity after the addition of PE can be attributed to the hydrogen bonding interaction between the molecular chains of starch and PE through the hydroxyl groups. The hydrogen bonding interaction reduced the free hydroxyl groups in the water-absorbing starch molecules, thereby increasing the hydrophobicity of the SNPs (WANG; ZHOU, 2022). The surface charge results can explain the changes in wettability observed by the contact angle analysis (WCA), in which the WCA of CSNPs and PSNPs remained constant in 41.05° ± 0.17 and 41.40° ± 0.13, respectively. With the incorporation of the phenolic compounds, it was observed an increase in the WCA, hence, starch nanoparticles loaded the phenolic compounds from PE had a WCA ranged between 66.80° ± 1.21 (CSNPs-PE) and 75.70° ± 0.75 (PSNPs-PE) (Fig. 5.4c).

5.3.2.3 Release behavior under simulated gastro-intestinal conditions and starch hydrolysis

Release and starch hydrolysis results revealed that the percentage of hydrolysis increased significantly ($p < 0.05$) in the first 80 min of the simulation in the intestinal phase (Fig. 5.5). This increase was due to the addition of the enzyme pancreatin, which is a mixture of amylase, proteases, and lipases, which has its activity optimized at the pH used in the simulation of intestinal digestion (pH = 7.0) (FERNANDES et al., 2020). After this period (80 min), the percentage of hydrolysis increased more slowly. According to Kim, Park and Lim (2008), starch hydrolysis follows two phases: an initial phase of rapid hydrolysis and a slower phase of digestion. The first phase corresponds to the hydrolysis of the amorphous region, whose amylase accessibility is greater due to the disorder of the starch chains (KIM; PARK; LIM, 2008; NAYAK; DE J. BERRIOS; TANG, 2014). The second phase corresponds to the hydrolysis of the crystalline region, less susceptible to enzymatic action (KIM; PARK; LIM, 2008; NAYAK; DE J. BERRIOS; TANG, 2014). For all samples hydrolysis was pronounced and it was typical of starch materials (Fig. 5.5) (KIM; PARK; LIM, 2008; NAYAK; DE J. BERRIOS; TANG, 2014).

Fig. 5.5. Starch hydrolysis of potato starch nanoparticles (PSNPs); cassava starch nanoparticles (CSNPs); potato starch nanoparticles (PSNPs-PE) and cassava starch nanoparticles (CSNPs-PE) loading the phenolic compounds from propolis extract (PE).

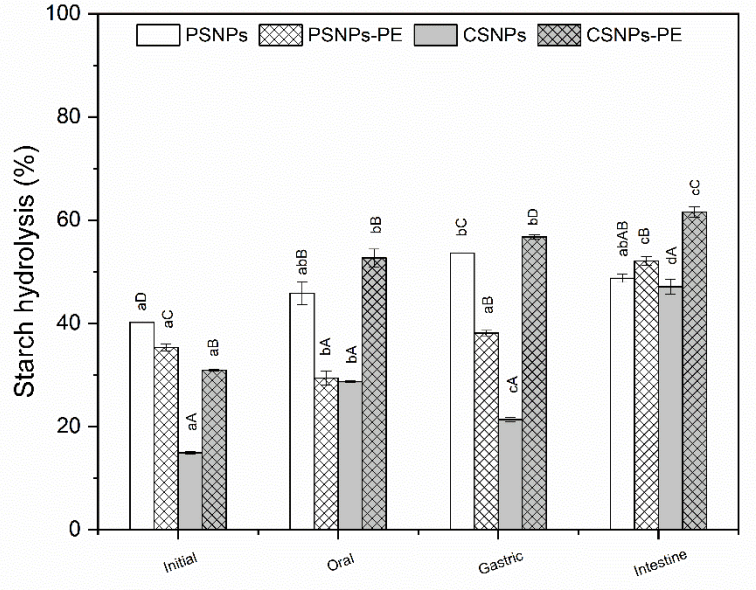

All values were expressed as mean ± standard error (n ≥ 3). Uppercase superscripts represent statistically significant differences among the samples for the same phase release, and lowercase superscripts represent statistically significant differences over phase release ($p < 0.05$).

Furthermore, PSNPs-PE and CSNPs-PE were subjected to simulated conditions intestinal digestion and the release behavior of TPC was studied (Fig. 5.6a). The initial release of phenolic compounds and antioxidants could be due to leaching and dissolution of the compounds that were free or adsorbed on the surface of the wall material. Potato and cassava SNPs showed high surface areas, as shown in the particle size results. This facilitated water absorption and contributed to the sudden release of compounds near the surfaces of starch nanoparticles (JIANG et al., 2022). After 3 h of intestinal conditions, all the trapped phenolic and antioxidant compounds were released from the nanostructures. The amount of phenolic compounds released ($p < 0.05$) after of 3h of intestinal digestion was 27.71 and, 25.48 mg of GAE/g of nanoparticles, for PSNPs-PE and CSNPs-PE, respectively.

Fig. 5.6. (a) TPC and (b) ABTS of potato starch nanoparticles (PSNPs-PE) and cassava starch nanoparticles (CSNPs-PE) loading the phenolic compounds from propolis extracts (PE).

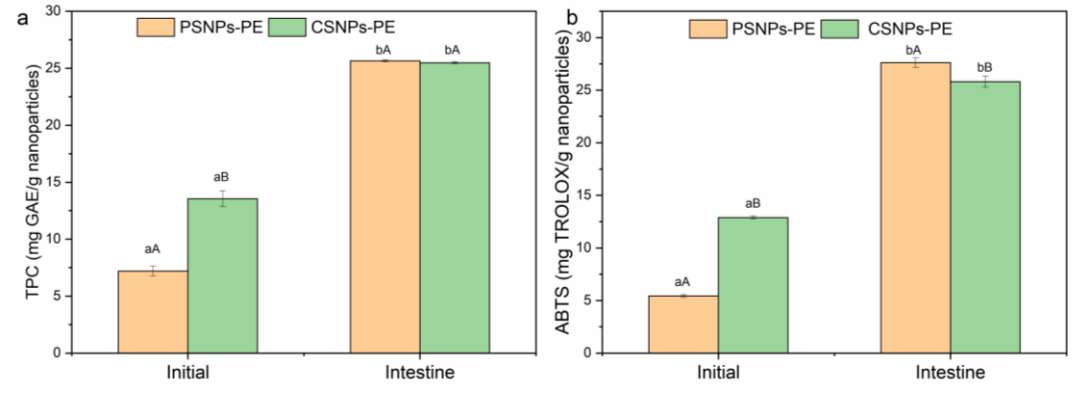

All values were expressed as mean ± standard error (n ≥ 3). Uppercase superscripts represent statistically significant differences among the samples for the same phase release, and lowercase superscripts represent statistically significant differences over phase release ($p < 0.05$).

The results of antioxidant activity by ABTS method after each digestion step is also showed in Fig. 5.6b. Antioxidant activity assessed by ABTS radical scavenging increased ($p < 0.05$) after throughout the passage through the intestinal phase for all samples. A greater release was observed in PSNPs-PE, this could be associated with the fact that this nanoparticle showed a higher LE value. PSNPs-PE and CSNPs-PE showed similar release profiles for TPC and ABTS, indicating that both NPs have similar interaction with the intestinal fluid.

Silva et al. (2019) studied the production and characterization of guarana seed extract particles obtained by spray-chilling. The authors performed the simulated release test with free extract and observed a drop in the content of phenolic compounds throughout the analysis. However, when encapsulating the extract, they observed that the release of phenolic compounds increased over time, with its maximum release in the intestinal phase of the test. Similar behavior was also observed by Salehi et al. (2023b) who used almond gum (AG) and sodium caseinate (CAS) at pH = 7 and 4.6, respectively, for encapsulation of propolis alcoholic extract. These authors observed that in the first 10 minutes, about 10% of phenolic compounds were released, and that propolis showed a sustained release at a constant rate in both gastric and intestinal conditions. The cumulative release of propolis in the gastric (after 2h) and intestinal

(after 8h) media was around 23% and 49%, respectively. In another study, Spanidi et al. (2021) evaluated the release of TPC from propolis at pH = 7.2 and indicated that the cumulative release was only 23.99% after 8 h. Protein and carbohydrate complexes have been reported to be more resistant to gastrointestinal conditions compared to a single carbohydrate or protein, resulting in less release of stabilized phenolic compounds with these macromolecules (DAJIC STEVANOVIC et al., 2020).

In the current research, stabilization of the phenolic compounds from PE using potato and cassava starches modified by antisolvent precipitation can serve as an effective protection for slow release at the absorption site of the gastrointestinal tract.

5.3.2.4 Microbial analysis

Listeria monocytogenes was chosen because it is responsible for causing listeriosis, a foodborne disease with high mortality, which makes this disease a significant concern for public health. In addition to the lack of food safety, it can also generate high economic losses (ZHANG et al., 2021). In the current research, the initial concentration (N0) was 5.7 ± 0.07 UFC/mL, and the concentrations after 48h are shown in Table 5.2. It was observed that PE has antibacterial effect against *L. monocytogenes*, with minimum inhibitory concentration (MIC) at a concentration of 0.5 mg/mL and minimum bactericidal concentration (MBC) 1.0 mg/mL, which has already been reported by other authors (DA CRUZ ALMEIDA et al., 2017; JANSEN-ALVES et al., 2019). Studies report that the antimicrobial activity of PE has been attributed to both hydrophilic and hydrophobic phenolic compounds, including flavonoids, acids, and aromatic esters, which possibly act on the cell wall of this bacterium (PATEL et al., 2015). Pernin et al. (2019) evaluated the inhibitory activity of several phenolic acids against *L. monocytogenes* as a function of their total concentration and observed that the phenolic acids (*p*-coumaric, caffeic and chlorogenic acids) inhibited the growth the *Listeria monocytogenes*. The quercetin also antimicrobial against *Listeria monocytogenes* (YONG et al., 2020).

JANSEN-ALVES et al. (2019) found superior MIC results (0.62 mg/mL) for the ethanol extract of propolis against *L. monocytogenes*. However, these authors used green propolis ethanolic extract and nanoemulsions. In another research, Seibert et al. (2019), observed that the nanoemulsion composed of corn oil (5.0% w/w) as oil phase, distilled water (84.0% w/w) as aqueous phase, nonionic surfactants sorbitan monooleate (3.0% w/w)

and polysorbate 80 (7.0% w/w) and ethanolic propolis extract (1% w/w) maintained the biological properties against *L. monocytogenes*, with a MIC value of 6.2 mg/mL.

Table 5.2. Antimicrobial activity against *Listeria monocytogenes* of propolis extract (PE), potato starch nanoparticles (PSNPs-PE) and cassava starch nanoparticles (CSNPs-PE) loading the phenolic compounds from PE.

Samples (mg/mL)	Y (UFC/mL)
PE	
0.10	*
0.25	*
0.50	5.00 ± 0.11
0.75	3.10 ± 0.07
1.00	**
PSNPs-PE	
100	*
250	6.90 ± 0.05
500	5.90 ± 0.03
750	5.20 ± 0.03
CSNPs-PE	
100	7.50 ± 0.01
250	7.60 ± 0.01
500	5.10 ± 0.01
750	4.90 ± 0.04

Y: Concentration found after 48h; *: Countless cell Count. **: Total cell inactivation.

Regarding the antimicrobial activity of the nanoparticles, it was observed that both PSNPs-PE and CSNPs-PE have action against *L. monocytogenes*, oscillating between 500 – 750 mg/mL. It can be observed that the PE showed superior antimicrobial activity than the nanoparticles, explained by the concentration of PE in the SNPs being lower than the pure extract. Therefore, the result also showed that the antisolvent process did not result in loss of these bioactive components since nanoparticles had antimicrobial activity. However, in the nanoparticles, the maximum concentration tested was 750 mg/mL and no MBC were observed,

indicating that the MBC is > 750 mg/mL. This can be explained by the difference in the cell structure and bacterial membrane (SALIM et al., 2023). Salehi et al. (2023b) obtained similar results to those of the antibacterial activity of propolis against *L. monocytogenes*.

5.4 CONCLUSIONS OF CHAPTER 5

In this study, starch nanoparticles loaded with the phenolic compounds from propolis extract (PE) were produced by the antisolvent precipitation method. Nanoparticles exhibited particle sizes between 8 - 340 nm and high loading efficiency (65 - 73%) of phenolic compounds from PE. According to the digestibility results, it was possible to verify that potato starch nanoparticles stabilizing the phenolic compounds from PE (PSNPs-PE) presented the highest release of compounds when compared to CSNPs-PE (cassava starch nanoparticles stabilizing the phenolic compounds from PE). The presence of phenolic compounds increased the hydrophobicity of the starch nanoparticles. Additionally, PSNPs-PE and CSNPs-PE showed positive results concerning the antimicrobial activity, demonstrating their effectiveness in the inhibition of *L. monocytogenes*. Starch nanomaterials loaded with the phenolic compounds from propolis extract could be used as an antimicrobial agent and as an antioxidant ingredient to manufacture functional foods.

CAPÍTULO 6

PRODUÇÃO E CARACTERIZAÇÃO DE BALAS DE GELATINA FORTIFICADAS COM NANOPARTÍCULAS DE AMIDO COM E SEM EXTRATO DE PRÓPOLIS VERDE

Apresentado na forma de artigo

6 GELATIN CANDIES ARCHITECTED WITH ACTIVE STARCH NANOPARTICLES CONTAINING PHENOLIC COMPOUNDS FROM PROPOLIS EXTRACT

Este capítulo relata a quarta fase experimental desta tese, que envolve o estudo da aplicação de nanopartículas de amido carregadas com compostos bioativos de própolis em balas de gelatina.

A partir desta etapa, foi escrito o quarto artigo experimental intitulado "Gelatin candies architected with active starch nanoparticles containing phenolic compounds from propolis extract" publicado no Starch (fator de impacto (2021): 2.741; https://doi.org/10.1002/star.202300162. acordo com as regras de assinatura da Wiley, os autores se reservam o direito de incluir o artigo em uma tese, desde que não seja publicado comercialmente.

Abstract

Gelatin candies were selected as a model food system to incorporate starch nanoparticles (SNPs) obtained by nanoprecipitation and loaded with phenolic compounds from green propolis extract (PE). The aim of this study was to use starch nanomaterials (CSNPs-PE and PSNPs-PE), honey and gelatin to develop a candy product, and to investigate their effect on physicochemical properties, texture and functional properties. Candy stability was evaluated during storage at 25°C and 30% RH for 60 days. Water activity and total soluble solids resulted in stable gelatin candies at room temperature and RH = 30% from the microbiological point of view. According to the results, the addition of SNPs in gelatin candies did not prove to be a factor that influenced texture parameters, especially hardness, gumminess and chewiness. Candies containing SNPs loaded with the phenolic compounds from PE have high total phenolic compounds (324 - 362 mg of GAE/100 g) and antioxidant activity (133 - 136 µmol TROLOX/100 g). These results indicate that SNPs loaded with the phenolic compounds from PE can be used for gelatin candies fortification.

Keywords: functional foods, natural additives, macromolecules, phenolic compounds.

Abbreviations

AP: anti-solvent precipitation; a_w: water activity; CS: cassava starch; GAE: gallic acid equivalent; PSNPs-PE: potato starch nanoparticles loading the phenolic compounds from acidified propolis extracts; CSNPs-PE: cassava starch nanoparticles loading the phenolic compounds from acidified propolis extracts PE; CSNPs: starch nanoparticles based on cassava starch; GRAS: Generally Recognized as Safe; PSNPs: starch nanoparticles based on potato starch; PE: propolis extract; PS: potato starch; S1: gelatin candy; S2: gelatin candy containing CSNPs-PE; S3: gelatin candy containing PSNPs-PE; S4: gelatin candy containing CSNPs; S5: gelatin candy containing PSNPs; SNPs: starch nanoparticles; TPA: Texture profile analysis; TPC: total phenolic content.

6.1 INTRODUCTION

Nowadays, consumers are interested in purchasing natural products and processed foods having shorter ingredient lists, familiar ingredients or minimally processed ingredients. This trend has been known as clean label (CL), being broadly explored in recent years (SÁ; CARMO; VALENCIA, 2023). In addition, ingredients such as artificial food additives (flavoring and coloring) also have negative health effects (CRUPI et al., 2018). In this sense, consumers look for natural and attractive foods that confer health benefits (LUIZA KOOP et al., 2022). Therefore, the confectionery industry has sought technological innovation, mainly by replacing some artificial ingredients present in products with healthier alternatives (ADAMS; SAVAGE, 2017; RIEDEL; BÖHME; ROHM, 2015).

In the literature, several studies have used natural ingredients to manufacture soft and gelatinous candies, among gummy candies colored with *Opuntia ficus-indica* betalains (OTÁLORA et al., 2019), gummy candies colored with a red beet extract (MOGHADDAS KIA et al., 2020), chewy candies added guava pulp in (VERGARA et al., 2020), candies added honey and fruit juices (MUTLU; TONTUL; ERBAŞ, 2018), gummy candies added beta-carotene microcapsules (CONSTANTINO; GARCIA-ROJAS, 2023).

Propolis is a GRAS (Generally Recognized as Safe) and natural product produced by bees, which has many beneficial properties (BALICA et al., 2021; CORNARA et al., 2017). Propolis is a source of antioxidant compounds, whose activity is due to its ability to scavenge free radicals (YAN et al., 2020). However, in terms of food applications of propolis, not only can it act as a natural preservative, but it also has excellent functional properties. However, the

use of propolis is limited due to its strong and unique odor, which can affect the sensory qualities of food (BODINI et al., 2013).

Recently, starch nanoparticles were used to stabilize phenolic compounds from propolis extract. These nanomaterials had showed better water-solubility when compared with native starches and propolis extract, as well as antioxidant properties (ALVES; MONTEIRO; VALENCIA, 2022). To date, no study has explored the application of these materials in foods. In this context, the application of starch nanoparticles loaded with bioactive propolis compounds in gelatin candies is a promising alternative. Therefore, the objective of this research was to produce and characterize the physicochemical properties of gelatin candies fortified with starch nanoparticles containing phenolic compounds from propolis extract, as well as to evaluate the change in these properties during storage.

6.2 MATERIALS AND METHODS

6.2.1 Materials

Native starches isolated from cassava (Juréia Food Industry, Santa Catarina, Brazil) and potato (Shambala Naturals Food Industry, Santa Catarina, Brazil) were used as macromolecules. Bovine gelatin (bloom 250, Gelnex, Brasil) was used as macromolecule in the candies. Commercial honey was purchased from the local market. Green propolis (Breyer®, Formigas – Minas Gerais, Brazil) was used as the source of bioactive compounds. Distilled water, ethanol (≥ 99.6%, Êxodo Científica, Brazil) and hydrochloric acid (37 wt%, Neon, Brazil) were used as solvents. Potassium chloride and sodium carbonate were purchased from Dinâmica (Brazil). Folin-Ciocalteu and 2,2-diphenyl-1-picrylhydrazyl (DPPH) were acquired from Sigma-Aldrich (Brazil). All reagents used were of analytical grade and they were used as received.

6.2.2 Production and characterization of the green propolis extract

The extraction of phenolic compounds from green propolis was carried out using sonication and mechanical stirring methods. Propolis extract (PE) produced by sonication was prepared by dispersing the resin (2.85 g) in a hydroethanolic solution (100 mL, 96% v/v) and then sonicated by 20 min at 30 °C using an ultrasonic probe device (4 mm diameter) (Eco-

Sonics, model QR500, Indaiatuba, SP-BR) with a digital timer, operating with a power of 500 W (100% amplitude) and a frequency of 20 kHz. In sequence, PE was stirred in a shaker at 30 °C for 24 h, stirring at 120 rpm.

PE was centrifuged at 25 ºC using a centrifuge (Kasvi, Brazil) with 1700 × g force at 4000 rpm for 15 minutes, and finally filtered using qualitative filter paper and stored in amber flasks at -24 °C under the absence of light until analysis.

Total phenolic compounds (TPC) of PE was measured using the method described by Alves et al. (2022). PE was diluted in ethanol (≥ 99.6%) in a 1:40 (% v/v) ratio. An aliquot of 100 µL of the ethanolic extract was transferred to test tubes and mixed with 7.9 mL of distilled water and 0.5 mL of Folin-Ciocalteu reagent (2N), followed by homogenization in vortex. In sequence, 1.5 mL of sodium carbonate solution 7.5% (w/v) was added and then homogenized in vortex. The test tubes were kept in dark at room temperature for 2 h. The absorbance of solutions was measured at a wavelength of 760 nm, using an UV-Vis spectrophotometer (QUIMIS, Q898U2M5, Diadema, SP, Brazil) and a blank solution with ethanol concentration of 95.6%.

TPC results were expressed as milligrams of gallic acid equivalent (GAE) per g of green propolis according to a calibration curve with concentrations varying between 0 and 750 µg of GAE/mL of extract ($y = 0.0011x + 0.0548$, $R^2 = 0.9993$).

DPPH radical scavenging was quantified according the previous study of Alves et al. (2022). In summary, 100 µL of PE was mixed with 2.9 mL of a DPPH solution (0.1 mM) at room temperature. The mixture was kept in a dark place for 30 min. Then, the same UV–Vis spectrophotometer was used to measure the absorbance of samples at 515 nm. Trolox results were expressed as µmol of Trolox per g of green propolis, according to a calibration curve with concentrations varying between 0 and 750 µmol Trolox/L ($y = -0.0006x + 0.7766$, $R^2 = 0.9753$).

6.2.3 Production of starch nanoparticles loaded with the phenolic compounds from propolis extract

Starch nanoparticles (SNPs) were produced by antisolvent precipitation as proposed by Alves et al. (2022). Starch water dispersions (5% w/w) previously prepared at 25 ºC were heated at 90 °C for 30 minutes and then cooled to 30 ºC. Gelatinizad starches were precipitated by the addition of PE (previously acidified with HCl, pH 1) using a peristaltic pump (flow of

0.7 mL/min) drop wise for the gelatinized starch in a 1:1 (% v/v) ratio. The resulting slurry was kept in magnetic agitation with constant stirring for 12 hours and then centrifuged at 25 ºC using a centrifuge (Kasvi, Brazil) with 1700 × g force at 4000 rpm for 15 minutes to separate SNPs from the solvents. SNPs were centrifuged three times with a hydroethanolic solution (80% v/v), and finally washed with absolute ethanol (99.6%). SNPs were removed by centrifugation using the same centrifuge and the ethanol in the SNPs was evaporated using a forced-air convection oven (Solidsteel, Brazil) at 60 ºC for 10 min. In sequence, SNPs were frozen at -18 ºC for 48 h, and finally lyophilized (Liotop L 101). The resulting SNPs loading the phenolic compounds from PE were finely macerated and stored in desiccators with silica gel at 25 °C for further analysis.

6.2.4 Characterization of starch nanoparticles

Particle size determination was carried out in dispersions of SNPs in ultrapure Mili-Q water (0.03% w/v, pH 4.0 to 7.0). Dispersions were sonicated for 30 min at 40 KHz, using a sonicator bath (Ultracleaner 1650, Unique, Brazil) and then analyzed with a LUMiSizer (LUM GmbH, Germany) (AHMAD et al., 2019).

The color of SNPs was evaluated using a high-resolution digital camera (Nikon AF-SDX Nikkor 18-55mm1:3.5–5.6G VR II, 0.28m/ 0.92 ft ø 52) (ALVES; MONTEIRO; VALENCIA, 2022). SNPs without the phenolic compounds from PE were used as controls.

Total phenolic compounds (TPC) and DPPH radical scavenging in SNPs loading phenolic compounds from PE were determined using the methodologies provided in **Section 6.2.2.**

6.2.5 Production and characterization of gelatin candies added of starch nanoparticles

Gelatin candies added of SNPs were prepared according to the methodology proposed by Mutlu, Tontul e Erbaş (2018), with modifications. The composition of the candies was done using a mass ratio of 60:40 (honey: hydrated gelatin with and without the addition of nanoparticles). Candies formulations are summarized in the **Table 6.1**.

Table 6.1. Gelatin candies formulations.

Ingredients	**Samples**				
(g/100 g)	**S1**	**S2**	**S3**	**S4**	**S5**
Honey	60	60	60	60	60

Gelatin	8	8	8	8	8
Water	31.5	30.5	30.5	30.5	30.5
Citric acid	0.5	0.5	0.5	0.5	0.5
Nanoparticle	0.0	1.0	1.0	1.0	1.0

Sample 1 (S1): Gelatin; Sample 2 (S2): Gelatin + CSNPs-PE; Sample 3 (S3): Gelatin + PSNPs-PE; Sample 4 (S4): Gelatin + CSNPs; Sample 5 (S5): Gelatin + PSNPs. PE: propolis extract; CSNPs: cassava starch nanoparticles; PSNPs: potato starch nanoparticles.

Firstly, gelatin was hydrated in distilled water (25 °C) for 30 min and then heated in a water bath at 60 °C for 30 min (VALENCIA et al., 2016). In sequence, pre-heated honey (60 °C) was added to the gelatin dispersion and manually homogenized for 2 min. Finally, the mixture was poured into cylindrical molds (3 x 15 mm) cooled to room temperature for 30 min, and stored for 24 h in a refrigerator at 7 °C. After the candies were taken out of the mold and cut into slices (3 x 2 mm) and they were conditioned for three days in a desiccator containing a saturated potassium carbonate solution (30% relative humidity, RH) at 25 °C.

The water activity (a_w) of gelatin candies was measured with a hygrometer (Aqualab, Decagon Devices) at 25 °C. Samples were cut into 2 mm thick circular sheets, placed in sample containers, and analyzed. The pH of the candies was measured using a pH meter to solids (Testo 205-Brazil). Soluble solids content (ºBrix) was determined in gelatin candies using a refractometer (0 – 93º, ATAGO, PAL-BY/RI, Japan). Color of gelatin candies was determined using the same methodology informed in Section 6.2.4. The color difference (ΔE^*) was calculated using Eq. (6.1):

$$\Delta E^* = \sqrt{\left(L^*_{standard} - L^*_{sample}\right)^2 + \left(a^*_{standard} - a^*_{sample}\right)^2 + \left(b^*_{standard} - b^*_{sample}\right)^2} \qquad (6.1)$$

In this study, color parameters of each sample at day zero of storage were considered as the standard (MERZ et al., 2020).

The texture profile of gelatin candies was performed using a texture analysis device (TA-XT plus; Stable Micro Systems, Surrey, UK). For each test, 10 samples were compressed twice at a compression rate 50 % with a 35 mm flat circular probe and a speed of 2 mm. s^{-1} at 25 ºC (MUTLU; TONTUL; ERBAŞ, 2018). Texture parameters such as hardness, gumminess, and chewiness were analyzed from the force-time graph.

The functional properties of candies were evaluated by TPC (total phenolic compounds) and antioxidant activity by DPPH. Samples (5 g) were added in a falcon tube with 20 mL of distilled water, after which the tube was added in a water bath at 40 °C for 5 min to dissolve the candies. The tubes were centrifuged at 4000 g for 10 min (Kasvi, Brazil) and the supernatant was collected. The quantification of TPC and DPPH were performed using the methodologies provided in Section 6.2.2.

The physicochemical properties of gelatin candies were studied during 60 days of storage at 25 ºC and 30 %RH, in absence of light.

6.2.6 Statistical analyses

All results were expressed as means ± standard deviation ($n \geq 3$). The experimental data were analyzed using Analysis of variance (ANOVA) and Tukey test with multiple comparisons, was performed with a 5% significance level using the software Statistica 10.0 (StatSoft®, USA). Pearson's correlation was performed using Excel® software.

6.3 RESULTS AND DISCUSSIONS

6.3.1 Characterization of propolis extract and starch nanoparticles

PE had TPC and DPPH values oscillating between 732.65 – 794.14 mg of GAE/g of extract and 717.52 – 737.64 μmol TROLOX/g of extract, respectively. These results revealed that PE has a high concentration of phenolic compounds, as well as antioxidant activity. Similar results have been informed in PE using resins from different regions of Brazil (TIVERON et al., 2016).

SNPS had particle size lower than 340 nm and the presence of phenolic compounds from PE did not alter the particle size in SNPs. Similar results regarding the particle size of SNPs and the effect of PE on the particle size of these nanomaterials were informed in the literature (ALVES et al., 2021; ALVES; MONTEIRO; VALENCIA, 2022).

Cassava starch nanoparticles (CSNPs) and potato starch nanoparticles (PSNPs) had light gray color, whereas nanoparticles loaded with the phenolic compounds from PE (CSNPs-PE and PSNPs-PE) displayed light green/brown color (Fig. 6.1a). It was observed that the

presence of phenolic compounds from PE reduced the L^* values of SNPs when compared with control samples (Table 6.2). This alteration was due to the green/brown color of PE. Similar behavior was observed by Soleimanifard et al. (2021) who studied the encapsulation of different concentrations of PE with proteins.

Fig. 6.1. (a) Visual aspect of: (a) cassava starch nanoparticles loaded with the phenolic compounds from propolis extract (CSNPs-PE); cassava starch nanoparticles (CSNPs),), potato starch nanoparticles loaded with the phenolic compounds from propolis extract (PSNPs-PE) and potato starch nanoparticles (PSNPs); (b) gelatin candy (S1), gelatin candy containing CSNPs-PE (S2), gelatin candy containing PSNPs-PE (S3), gelatin candy containing CSNPs (S4), gelatin candy containing PSNPs (S5).

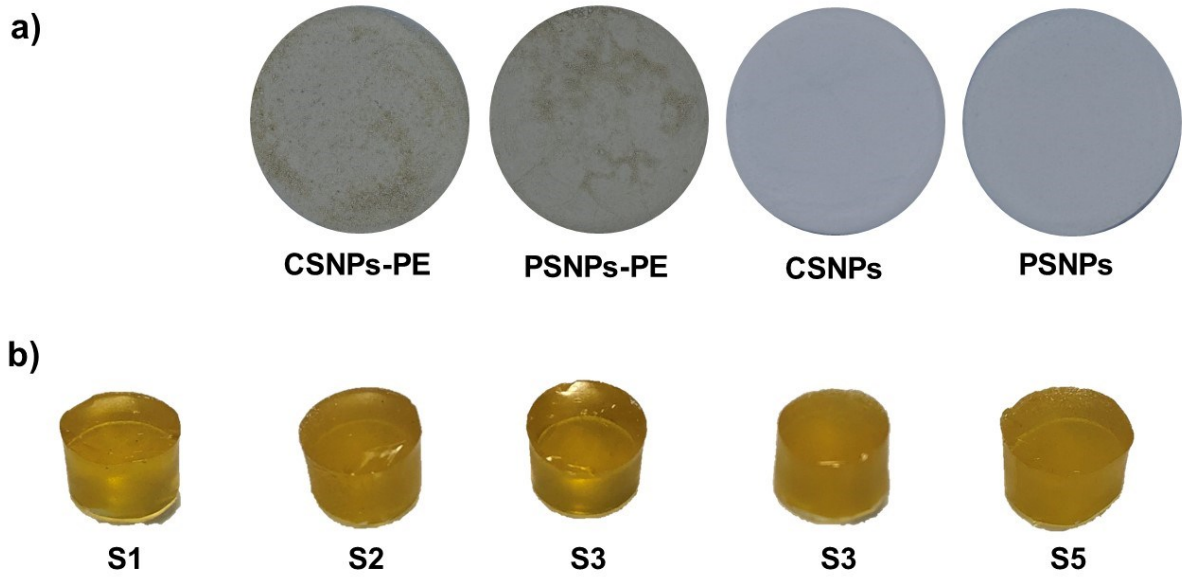

CSNPs-PE: cassava starch nanoparticles loaded with the phenolic compounds from propolis extract (PE); CSNPs: cassava starch nanoparticles; PSNPs-PE: potato starch nanoparticles loaded with the phenolic compounds from PE; PSNPs: potato starch nanoparticles.
Sample 1 (S1): Gelatin; Sample 2 (S2): Gelatin + CSNPs-PE; Sample 3 (S3): Gelatin + PSNPs-PE; Sample 4 (S4): Gelatin + CSNPs; Sample 5 (S5): Gelatin + PSNPs.

Regarding the a^* coordinate, a^* values decreased with the addition of PE ($p < 0.05$) (Table 6.2), indicating that there was a reduction in the intensity of red and a tendency towards green, confirming the retention of the phenolic compound in these nanomaterials. For the b^* parameter, a significant increase ($p < 0.05$) was observed in SNPs containing the phenolic compounds from PE (Table 6.2). These results corroborate with those informed in co-crystallized sucrose with PE (IRIGOITI; YAMUL; NAVARRO, 2021), and crystallized

powders containing compounds from yerba mate and marjoram extracts with sucrose (LÓPEZ-CÓRDOBA et al., 2014; SARABANDI; MAHOONAK; AKBARI, 2019).

Table 6.2. Color parameters (L^*, a^* and b^*) of starch nanoparticles.

Color parameter	CSNPs-PE	CSNPs	PSNPs-PE	PSNPs
L*	87.43 ± 0.21^{B}	93.69 ± 0.13^{A}	84.85 ± 0.03^{C}	93.74 ± 0.08^{A}
a*	-0.33 ± 0.02^{B}	1.10 ± 0.07^{A}	-0.66 ± 0.03^{C}	1.07 ± 0.06^{A}
b*	7.30 ± 0.16^{B}	-2.17 ± 0.05^{A}	12.01 ± 0.07^{C}	-2.43 ± 0.22^{A}

CSNPs-PE: cassava starch nanoparticles loaded with the phenolic compounds from propolis extract (PE); CSNPs: cassava starch nanoparticles; PSNPs-PE: potato starch nanoparticles loaded with the phenolic compounds from PE; PSNPs: potato starch nanoparticles.

All values were expressed as mean ± standard error ($n \geq 3$). Means in the same row followed by different capital letter are significantly different ($p < 0.05$).

6.3.2 Characterization of gelatin candies added of starch nanoparticles

6.3.2.1 Physicochemical analysis

Gelatin candies with the addition of starch nanoparticles showed a uniform appearance and attractive color (Fig. 6.1b). Water activity (a_w) values were significantly reduced with storage, probably due to the loss of moisture (Table 6.3). A_w values of the candies are in agreement with those reported (a_w = 0.54 – 0.68) by Amjadi et al. (2018) in gelatin candies added with betalains from fruits, and lower than those informed by Mutlu et al. (2018) in candies containing honey and fruit juice and also b(Yan et al., 2021) in gelatin candies added of vitamin C. Based on a_w results, these candies can be considered as safe for confectionery products (a_w = 0.48 - 0.59) (Table 6.3). At values of $a_w > 0.6$, there may be fungal growth during storage (ERGUN; LIETHA; HARTEL, 2010), so citric acid was added to the candies formulation as a

Table 6.3. Water activity (a_w) and total soluble solids content (ºBrix) of gelatin candies during storage.

Parameter	Time (days)	Gelatin candies				
		S1	**S2**	**S3**	**S4**	**S5**
a_w	0	0.592 ± 0.01^{Aa}	0.592 ± 0.00^{Aa}	0.588 ± 0.01^{Aa}	0.592 ± 0.01^{Aa}	0.586 ± 0.00^{Aa}
	20	0.561 ± 0.01^{Bab}	0.571 ± 0.01^{Ba}	0.549 ± 0.01^{Bab}	0.577 ± 0.01^{Aa}	0.561 ± 0.02^{Aa}
	40	0.475 ± 0.01^{Ca}	0.476 ± 0.01^{Ca}	0.498 ± 0.01^{Cb}	0.500 ± 0.00^{Bb}	0.481 ± 0.01^{Bab}
	60	0.488 ± 0.02^{Ca}	0.485 ± 0.01^{Ca}	0.482 ± 0.01^{Ca}	0.489 ± 0.01^{Ba}	0.487 ± 0.01^{Ba}
ºBrix	0	86.70 ± 0.69^{Aa}	84.00 ± 0.42^{ABb}	83.93 ± 0.55^{Ab}	83.10 ± 0.50^{Ab}	83.63 ± 0.25^{Ab}
	20	87.33 ± 1.40^{ABa}	82.29 ± 1.84^{Ab}	87.73 ± 1.52^{Ba}	85.88 ± 2.67^{ABa}	87.70 ± 1.32^{BCa}
	40	86.52 ± 0.41^{Aa}	87.25 ± 1.05^{BCa}	86.26 ± 1.19^{Ba}	87.58 ± 0.63^{BCa}	86.12 ± 1.00^{Ca}
	60	89.07 ± 1.01^{Ba}	88.77 ± 0.32^{Ca}	88.13 ± 0.31^{Ba}	90.17 ± 1.35^{Ca}	89.50 ± 0.82^{Ba}

Sample 1 (S1): Gelatin; Sample 2 (S2): Gelatin + CSNPs-PE; Sample 3 (S3): Gelatin + PSNPs-PE; Sample 4 (S4): Gelatin + CSNPs; Sample 5 (S5): Gelatin + PSNPs.

CSNPs-PE: cassava starch nanoparticles loaded with the phenolic compounds from propolis extract (PE); CSNPs: cassava starch nanoparticles; PSNPs-PE: potato starch nanoparticles loaded with the phenolic compounds from PE; PSNPs: potato starch nanoparticles.

All values were expressed as mean ± standard error ($n \geq 3$). Means in the same column followed by different superscripts are significantly different ($p < 0.05$). In a row, results with a different superscript letter indicate a statistically significant difference between each other ($p < 0.05$).

preservative. Rivero et al. (2021) also added citric acid and propolis extract to prevent fungal development in jelly candies.

Gelatin candies had a pH value ranging from 4.65 to 5.93 during storage, above the values reported in the literature for hibiscus candies (3.42 and 3.54) (DE MOURA et al., 2019) and vitamin C candies (3.01 to 3.12) (YAN et al., 2021). The pH value is in line with other studies that produced gelatin candies with the addition of fruit extract and citric acid and obtained pH values between 3.0 to 5.0 (ÇOBAN et al., 2021). Differences in the values are associated with the fact that in the current research a lower citric acid concentration (0.5 %w/w) was used when compared with the literature (1 %w/w) (CANO-LAMADRID et al., 2020).

The high content of total soluble solids (TSS = 82.29 – 90.17 °Brix) resulted in stable jelly candies at room temperature and RH = 30 % from the microbiological point of view. Similar values were reported for pectin candies containing hibiscus (TSS = 82.83 - 84.87) (DE MOURA et al., 2019).

Food color (L, a* and b*) is an important factor that impacts sensory acceptability of the products (SANT'ANNA et al., 2022). The effect of storage time, temperature (25 °C) and relative humidity (30% RH) on the color of gelatin candies was investigated and the values are shown in Fig. 6.2.

On day 0 of storage, the parameter L*, for candies S1, S2, S3, S4 and S5 was +15.32, +15.72, +15.90, +16.14 and +16.72, respectively. It was observed that the L* parameter of the candies did not present a significant difference ($p > 0.05\%$), showing that the incorporation of SNPs did not interfere in this parameter when compared with the control candy (S1) (Fig. 6.1b and 6.2a).

Fig. 6.2. Color of gelatin candies during storage.

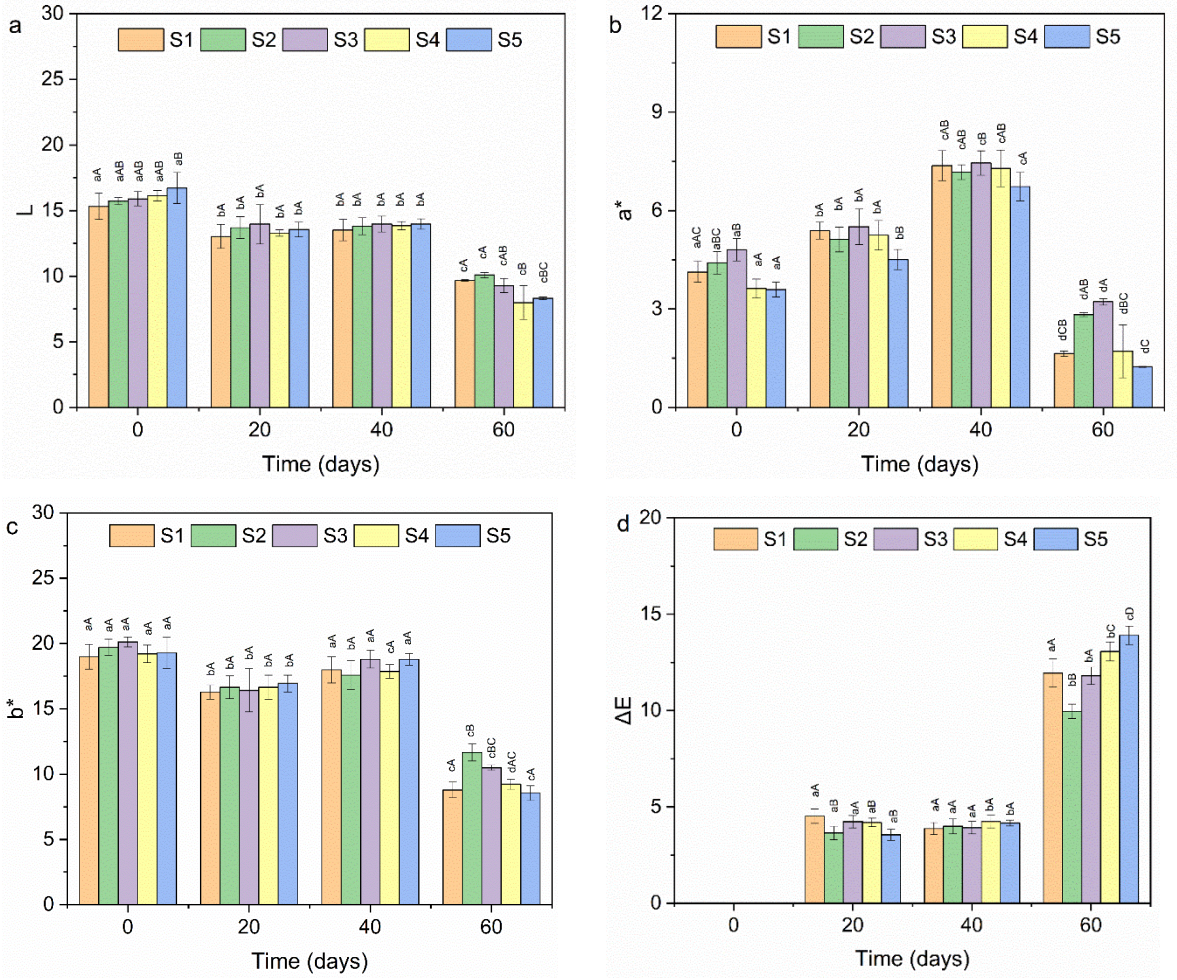

Sample 1 (S1): Gelatin; Sample 2 (S2): Gelatin + CSNPs-PE; Sample 3 (S3): Gelatin + PSNPs-PE; Sample 4 (S4): Gelatin + CSNPs; Sample 5 (S5): Gelatin + PSNPs. CSNPs-PE: cassava starch nanoparticles loaded with the phenolic compounds from propolis extract (PE); CSNPs: cassava starch nanoparticles; PSNPs-PE: potato starch nanoparticles loaded with the phenolic compounds from PE; PSNPs: potato starch nanoparticles. Uppercase superscripts represent statistically significant differences among the samples for the same time of storage, and lowercase superscripts represent statistically significant differences over times of storage ($p < 0.05$).

However, this parameter showed a significant reduction with storage time for all samples. Thus, at 60 days, the candy S2 showed a statistically different value from the candy S4, and the same behavior was observed when comparing candies S3 and S5. Therefore, it was observed that the addition of propolis had an influence only when comparing samples S2 and S4, and also when comparing samples S3 and S5. While S1, S4 and S5 candies that did not contain propolis did not differ after 60 days of storage. The reduction in the luminosity of the candies with storage time can be attributed to the lipid oxidation of the candies (MOGHADDAS KIA et al., 2020).

Positive values of a* and b* showed that the gelatin candies and the candies with the incorporation of SNPs were similar to each other, presenting a yellowish-red color, due to the natural color of honey and propolis being similar, thus not presenting a significant color modification.

For the a* parameter on day 0 of storage, it was observed that S2 and S4 candies were statistically different ($p < 0.05\%$) and S3 and S5 candies, showing that the addition of CSNPs-PE and PSNPs-PE did not affects this parameter. Furthermore, it is shown that after 60 days, the color sample changed, by decrease of a* values, indicating that the samples are less red than those at time zero (Fig. 6.2b).

Since candies S2 and S4, when compared, showed no statistical difference, while candies S3 and S5 were significantly different. Therefore, it was observed that candies S1, S4 and S5 did not present a significant difference. This result was expected since there was no addition of CSNPs-PE and PSNPs-PE. It was also observed that S2 and S3 candies, with the addition of CSNPs-PE and PSNPs-PE, respectively, showed smaller reductions in the value of a* and b*, due to the presence of propolis compounds that were efficient in maintaining the color of the candies (Fig. 6.2b-c).

The total color change (ΔE) (Fig. 6.2d) was clearly dependent on the addition of CSNPs-PE and PSNPs-PE in the gelatin candies and it was due to the decrease in a* and b* values. In this way, ΔE* were higher in samples without the addition of CSNPs-PE and PSNPs-PE, suggesting that S2 and S3 candies, due to the addition of CSNPs-PE and PSNPs-PE, presented greater color stability of the candies.

6.3.2.2 Texture profile analysis (TPA) of gelatin candies

Relevant texture descriptors for confections candies are hardness, chewiness and gumminess. The maximum force needed to distort candies on the first bite is directly related to hardness. Gumminess comes from the multiplication of hardness and cohesiveness, while chewiness comes from the multiplication of hardness, cohesiveness and elasticity (DELGADO; BAÑÓN, 2015).

On day 0 of storage, it was observed that the S2, S3, S4 and S5 candies did not show statistical difference for the hardness parameter when compared with the S1 candies. Furthermore, there was no significant difference when comparing candies S2 with candies S4,

and candies S3 with candies S5, showing that the addition of SNPs did not interfere this parameter (Fig. 6.3a).

During the storage of candies at 25 °C and 30% RH for 60 days, it was verified that the candies showed an increase in hardness ($p < 0.05$). This behavior could be due to the decrease in a_w, leading to a harder layer on the surface of the samples (Table 6.3).

Since at 60 days, the S2 candy (gelatin + CSNPs-PE) had the highest hardness value, and it was statistically different when compared with the S4 candy (gelatin + CSNPs). Similar behavior was observed between candies S3 (gelatin + PSNPs-PE) and S5 (gelatin + PSNPs). Finally, candies S5 showed no significant difference when compared with candies S1.

Fig. 6.3. Texture parameters of gelatin candies during storage.

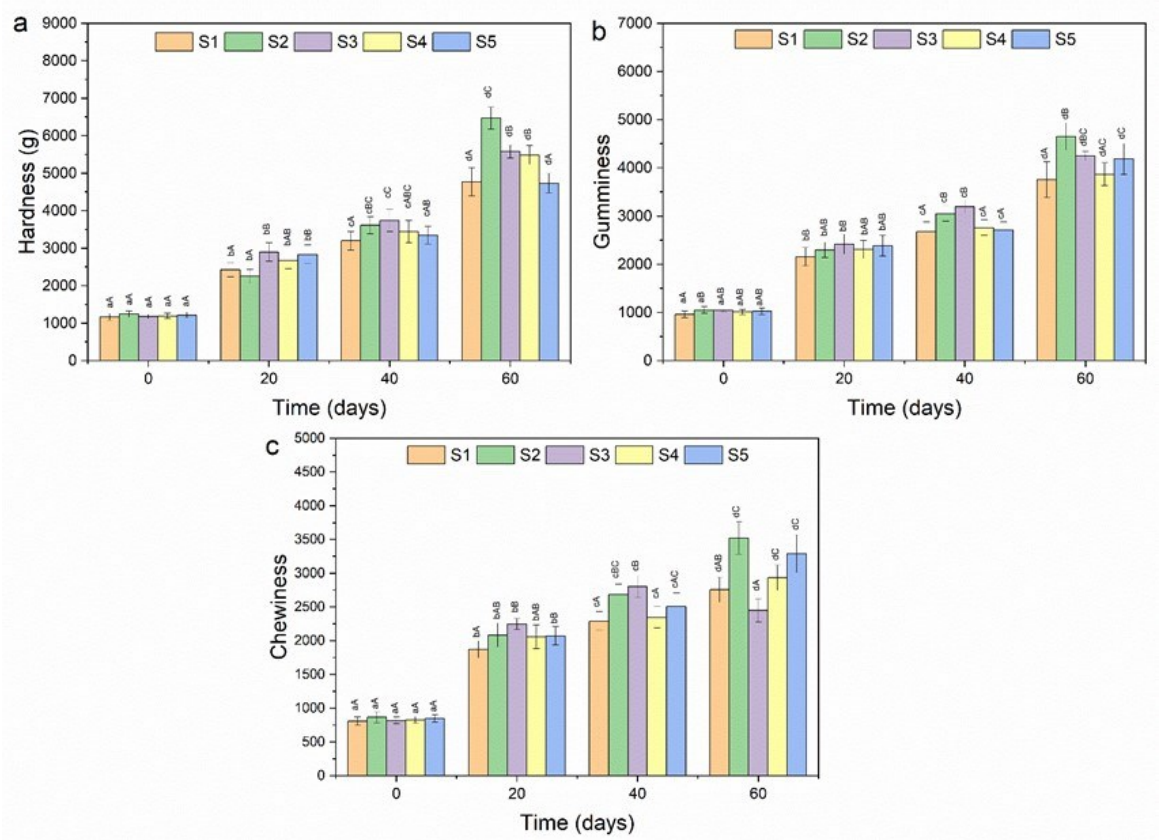

Sample 1 (S1): Gelatin; Sample 2 (S2): Gelatin + CSNPs-PE; Sample 3 (S3): Gelatin + PSNPs-PE; Sample 4 (S4): Gelatin + CSNPs; Sample 5 (S5): Gelatin + PSNPs. CSNPs-PE: cassava starch nanoparticles loaded with the phenolic compounds from propolis extract (PE); CSNPs: cassava starch nanoparticles; PSNPs-PE: potato starch nanoparticles loaded with the phenolic compounds from PE; PSNPs: potato starch nanoparticles. Uppercase superscripts represent statistically significant differences among the samples for the same time of storage, and lowercase superscripts represent statistically significant differences over times of storage ($p < 0.05$).

On the other hand, candies S2 (Fig. 6.3b) showed a statistical difference when compared to the candies S1, while the candies S3, S4 and S5 showed values similar to the candies S1. It was also observed that the effect of incorporating propolis extract and starch nanoparticles was similar. Furthermore, at 60 days, it was observed that the gumminess values increased with the increase in hardness values, and these results were compatible with those found by Periche et al. (2014) using alternative sweeteners in confectionery candies.

It was also verified that the chewiness (Fig. 6.3c) was not influenced by the addition of SNPs when compared S2, S3, S4 and S5 candies with S1 candies. Behavior similar to that found for gumminess, where at 60 days of storage it was observed that chewiness values increased with increasing hardness values.

6.3.2.3 Functional properties of gelatin candies

Potential health benefits of functional candies are an outcome of the bioactive presence in appropriate quantity and, more importantly, its stability during storage (KOOP et al., 2022). On day 0, it was observed that candies S2 (CSNPs-PE) and S3 (PSNPs-PE) had levels of phenolic compounds of 267.25 and 275.40 mg of GAE/100 g, respectively, being higher ($p < 0.05$) than the values found for candies S4 (CSNPs) and S5 (PSNPs), with values of 221.58 and 186.67 mg of GAE/100 g, respectively (Fig. 6.4a).

Candies S2 and S3 had higher values due to the presence of nanoparticles loaded with propolis extract. After 60 days of storage, the S2 and S3 candies continued to show the same behavior when compared to the S4 and S5 candies, respectively, confirming the release of these compounds present in the candies.

TPC values this word were higher than those found by Archaina et al. (2019) in freeze-dried currant and yogurt sweets using alternative sweeteners. These authors observed a total phenolic compound content of 53.64 and 52.93 mg of GAE/100 g of dry matter), sweetened with honey and stevia, respectively.

Regarding the antioxidant capacity, the same behavior was observed in the results of phenolic compounds. Initially, the candies with the addition of propolis nanoparticles, S2 and S3, presented values of 116.40 and 120.20 μmol TROLOX/100 g, respectively, being superior to the control candies, S3 and S5, with values of 53.40 and 44.37 μmol TROLOX/100 g, respectively (Fig. 6.4b).

And after 60 days of storage, the candies with the addition of propolis nanoparticles, S2 and S3, showed values of 133.02 and 136.45 µmol TROLOX/ 100 g, respectively, being superior to the control candies, S4 and S5, with values of 110.09 and 110.12 µmol TROLOX/100 g, respectively. Also, a slight increase in the levels of phenolic compounds and antioxidant activity was observed during storage, which may be related to the lack of homogenization in the samples or to the bioactive compounds showing low release in the medium.

Fig. 6.4. Total phenolic compounds (TPC) and antioxidant capacity (DPPH) of gelatin candies during storage.

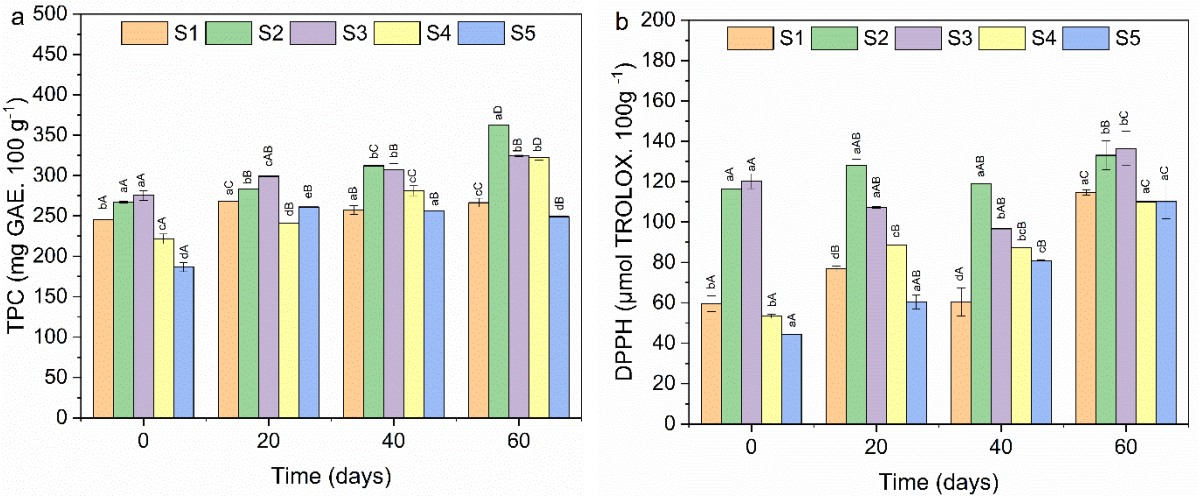

Sample 1 (S1): Gelatin; Sample 2 (S2): Gelatin + CSNPs-PE; Sample 3 (S3): Gelatin + PSNPs-PE; Sample 4 (S4): Gelatin + CSNPs; Sample 5 (S5): Gelatin + PSNPs. CSNPs-PE: cassava starch nanoparticles loaded with the phenolic compounds from propolis extract (PE); CSNPs: cassava starch nanoparticles; PSNPs-PE: potato starch nanoparticles loaded with the phenolic compounds from PE; PSNPs: potato starch nanoparticles. Uppercase superscripts represent statistically significant differences among the samples for the same time of storage, and lowercase superscripts represent statistically significant differences over times of storage ($p < 0.05$).

Cano-Lamadrid et al. (2020) reported TPC values ranging from 72–159 mg GAE/100 g for pomegranate juice-based sweets, while Šeremet et al. (2020) showed TPC of 170–180 mg EAG/100 g for white tea-based sweets. Rivero et al. (2021) obtained 550.8 mg EAG/100 g and 1820 µmol of Trolox/100 g for candies added with propolis extract and raspberry powder as a natural dye.

This behavior could be related to the difference in formulations and concentrations of ingredients. Therefore, it is important to point out that the functional properties of the gelatin candies in our formulation were associated with the presence of honey and propolis

nanoparticles. Propolis extract is rich in bioactive compounds, as previously demonstrated. And honey is a functional food produced by bees (Apis mellifera) that contains a variety of bioactive substances and enzymes that give it antioxidant properties, among these compounds we can highlight the flavonoides (such as apigenin, pinocembrin, kaempferol, quercetin, galangin, chrysin and hesperetin), phenolic acids (such as ellagic, caffeic, p-coumaric and ferulic acids, among others (ETERAF-OSKOUEI; NAJAFI, 2013).

6.4 CONCLUSIONS OF CHAPTER 6

Gelatin candies with the addition of starch nanoparticles showed a uniform appearance and attractive color. All formulations showed physicochemical characteristics expected for gelatin candies. Furthermore, fractions of bioactive compounds remained available after 60 days of storage and could exert their bioactivity. In general, the use of starch nanoparticles loaded with the phenolic compounds from propolis extract in gelatin candies is feasible and it is an innovative and promising alternative for the food industry in the fortification of gelatin candies.

CAPÍTULO 7

CONCLUSÃO GERAL E SUGESTÃO DE TRABALHOS FUTUROS

7 CONCLUSÃO GERAL E SUGESTÃO DE TRABALHOS FUTUROS

Este capítulo final apresenta as conclusões mais relevantes com base nos resultados relatados nos capítulos anteriores e sugestões para trabalhos futuros.

7.1 CONCLUSÃO GERAL

O uso da técnica de nanoprecipitação antissolvente foi eficiente para produção de nanopartículas de amidos, de batata e de mandioca, e para estabilizar os compostos bioativos dos extratos da própolis. A técnica de nanoprecitação antissolvente possibilitou a obtenção de nanopartículas de amido estabilizando os compostos de própolis pela primeira vez.

As técnicas de FTIR e DRX possibilitaram a confirmação da estabilização do extrato de própolis nos amidos, de batata e de mandioca. Independente do amido (mandioca e batata) utilizado como material estabilizante obteve-se nanopartículas com estrutura cristalina tipo V, baixo teor de umidade e atividade de água.

Em ambos os amidos, a estabilização possibilitou que os materiais apresentassem atividades biológicas. Essas atividades foram observadas em análises de digestão *in vitro*, o que possibilita a aplicação dos nanomateriais tanto na área alimentícia como farmacêutica.

Os resultados microbiológicos, expressos em CIM e CBM demonstraram que a atividade antibacteriana do extrato de própolis puro foi superior quando comparada com a as nanopartículas de amido de batata e de mandioca na concentração de 750 mg de nanopartículas/mL para a bactéria gram positiva, *Listeria monocytogenes*.

Após a aplicação das nanopartículas de amido com os compostos da própolis em balas de gelatina, apresentou coloração marrom estável, uniforme e visualmente atrativa por 60 dias de armazenamento a 25 °C e 30 UR. Os compostos fenólicos e a atividade antioxidante das formulações de balas com fortificadas com nanopartículas de amido contendo os compostos bioativos da própolis (S2 e S3) foram superiores quando comparados com a bala de gelatina (S1) e balas adicionadas de nanopartículas de amido sem os compostos bioativos da própolis (S4 e S5); este é um aspecto positivo se for considerado que as balas convencionais possuem propriedades funcionais pobres ou nulas.

Por fim, as nanopartículas obtidas nesta tese podem ser aplicadas como aditivo alimentar na indústria de alimentos.

7.2 SUGESTÃO DE TRABALHOS FUTUROS

- Identificar e quantificar os compostos bioativos após a digestão *in vitro* das nanopartículas de amido contendo compostos bioativos da própolis;
- Avaliar a citotoxidade do extrato de própolis e das nanopartículas de amido contendo compostos bioativos da própolis;
- Avaliar a aceitação e intenção de compra das balas de gelatina por análise sensorial;
- Estudar a liberação digestibilidade in vitro das balas de gelatina fortificadas com nano nanopartículas de amido contendo compostos bioativos da própolis;

REFERÊNCIAS

ABDUL MUDALIP, S. K. et al. A short review on encapsulation of bioactive compounds using different drying techniques. **Materials Today: Proceedings**, 26 fev. 2021.

ABDULLAH, N. A. et al. Physicochemical analyses, antioxidant, antibacterial, and toxicity of propolis particles produced by stingless bee Heterotrigona itama found in Brunei Darussalam. **Heliyon**, v. 5, n. 9, p. e02476, 1 set. 2019.

ACEVEDO-GUEVARA, L. et al. Development of native and modified banana starch nanoparticles as vehicles for curcumin. **International Journal of Biological Macromolecules**, v. 111, p. 498–504, 1 maio 2018.

ACOSTA-ESTRADA, B. A.; GUTIÉRREZ-URIBE, J. A.; SERNA-SALDÍVAR, S. O. **Bound phenolics in foods, a reviewFood Chemistry**Elsevier Ltd, , 1 jun. 2014.

ADAMS, E. L.; SAVAGE, J. S. From the children's perspective: What are candy, snacks, and meals? **Appetite**, v. 116, p. 215–222, 1 set. 2017.

AGI, A. et al. Influence of nanoprecipitation on crystalline starch nanoparticle formed by ultrasonic assisted weak-acid hydrolysis of cassava starch and the rheology of their solutions. **Chemical Engineering and Processing - Process Intensification**, v. 142, n. December 2018, 2019.

AHMAD, M. et al. Nano-encapsulation of catechin in starch nanoparticles: Characterization, release behavior and bioactivity retention during simulated in-vitro digestion. **Food Chemistry**, v. 270, n. April 2018, p. 95–104, 2019.

AHMAD, M. et al. Production and characterization of starch nanoparticles by mild alkali hydrolysis and ultra-sonication process. **Scientific Reports**, v. 10, n. 1, p. 1–11, 2020.

AHMAD, M.; GANI, A. Ultrasonicated resveratrol loaded starch nanocapsules: Characterization, bioactivity and release behaviour under in-vitro digestion. **Carbohydrate Polymers**, v. 251, n. June 2020, p. 117111, 2021.

AL-MUHTASEB, A. H.; MCMINN, W. A. M.; MAGEE, T. R. A. Moisture sorption isotherm characteristics of food products: A review. **Food and Bioproducts Processing**, v. 80, 2002.

ALENCAR, S. M. DE et al. Dynamic gastrointestinal digestion/intestinal permeability of encapsulated and nonencapsulated Brazilian red propolis: Active compounds stability and bioactivity. **Food Chemistry**, v. 411, n. December 2022, p. 135469, 2023.

ALMUHAYAWI, M. S. Propolis as a novel antibacterial agent. **Saudi Journal of Biological Sciences**, 14 set. 2020.

ALVARENGA, L. et al. **To bee or not to bee? The bee extract propolis as a bioactive compound in the burden of lifestyle diseasesNutrition**Elsevier Inc., , 1 mar. 2021.

ALVES, M. J. DOS S. et al. Food Applications of Starch Nanomaterials: A Review.

Starch/Staerke, v. 2100046, 2021.

AMIRABADI, S.; MILANI, J. M.; SOHBATZADEH, F. Application of dielectric barrier discharge plasma to hydrophobically modification of gum arabic with enhanced surface properties. **Food Hydrocolloids**, v. 104, p. 105724, 1 jul. 2020.

AMJADI, S. et al. Improvement in the stability of betanin by liposomal nanocarriers: Its application in gummy candy as a food model. **Food Chemistry**, v. 256, p. 156–162, 1 ago. 2018.

ANDRADE-MAHECHA, M. M.; TAPIA-BLÁCIDO, D. R.; MENEGALLI, F. C. Physical-chemical, thermal, and functional properties of achira (Canna indica L.) flour and starch from different geographical origin. **Starch/Staerke**, v. 64, n. 5, p. 348–358, 2012.

ANDRADE, I. H. P. et al. Ultrasound-assisted extraction of starch nanoparticles from breadfruit (Artocarpus altilis (Parkinson) Fosberg). **Colloids and Surfaces A: Physicochemical and Engineering Aspects**, v. 586, n. November 2019, p. 124277, 2020.

ANDRADE, J. K. S. et al. Evaluation of bioactive compounds potential and antioxidant activity of brown, green and red propolis from Brazilian northeast region. **Food Research International**, v. 101, n. July, p. 129–138, 2017.

ANDRADE, J. K. S. et al. Development and characterization of microencapsules containing spray dried powder obtained from Brazilian brown, green and red propolis. **Food Research International**, v. 109, p. 278–287, 1 jul. 2018.

ANJUM, S. I. et al. **Composition and functional properties of propolis (bee glue): A reviewSaudi Journal of Biological Sciences**Elsevier B.V., , 1 nov. 2019.

ARCHAINA, D. et al. Freeze-dried candies from blackcurrant (Ribes nigrum L.) and yoghurt. Physicochemical and sensorial characterization. **LWT**, v. 100, p. 444–449, 1 fev. 2019.

ASCHENBRENNER, E. et al. Using the polymeric ouzo effect for the preparation of polysaccharide-based nanoparticles. **Langmuir**, v. 29, n. 28, p. 8845–8855, 2013.

ASHRAF, R. et al. Recent Trends in the Fabrication of Starch Nanofibers: Electrospinning and Non-electrospinning Routes and Their Applications in Biotechnology. **Applied Biochemistry and Biotechnology**, v. 187, n. 1, p. 47–74, 2019.

AUGUSTO-OBARA, T. R. et al. Benefits of superfine grinding method on antioxidant and antifungal characteristic of Brazilian green propolis extract. **Scientia Agricola**, v. 76, n. 5, p. 398–404, 1 set. 2019.

AZEVEDO, L. F. et al. Polymeric nanoparticle systems loaded with red propolis extract: a comparative study of the encapsulating systems, PCL-Pluronic versus Eudragit®E100-Pluronic Eudragit®E100-Pluronic. **Journal of Apicultural Research**, v. 57, n. 2, p. 255–270, 2018.
BALICA, G. et al. Metabolic Diseases. p. 1–14, 2021.

BANERJEE, A. et al. Role of nanoparticle size, shape and surface chemistry in oral drug delivery. **Journal of Controlled Release**, v. 238, p. 176–185, 28 set. 2016.

BARROS, M. P. DE et al. Evaluation of antiulcer activity of the main phenolic acids found in Brazilian Green Propolis. **Journal of Ethnopharmacology**, v. 120, n. 3, p. 372–377, 8 dez. 2008.

BARTHOLD, S. et al. Preparation of maltodextrin nanoparticles and encapsulation of bovine serum albumin – Influence of formulation parameters. **European Journal of Pharmaceutics and Biopharmaceutics**, v. 142, n. June, p. 405–410, 2019.

BAYSAN, U.; ELMAS, F.; KOÇ, M. The effect of spray drying conditions on physicochemical properties of encapsulated propolis powder. **Journal of Food Process Engineering**, v. 42, n. 4, p. 1–11, 2019.

BEMILLER, J. N. Pasting, paste, and gel properties of starch–hydrocolloid combinations. **Carbohydrate Polymers**, v. 86, n. 2, p. 386–423, 15 ago. 2011.

BEMILLER, J. N. Corn starch modification. In: **Corn: Chemistry and Technology, 3rd Edition**. [s.l.] Elsevier, 2018. p. 537–549.

BERGO, P.; SOBRAL, P. J. A.; PRISON, J. M. EFFECT OF GLYCEROL ON PHYSICAL PROPERTIES OF CASSAVA STARCH FILMS. **Journal of Food Processing and Preservation**, v. 34, n. SUPPL. 2, p. 401–410, maio 2010.

BERNARDI, S. et al. Italian -type salami with propolis as antioxidant. **Italian Journal of Food Science**, v. 25, n. 4, p. 433–440, 2013a.

BERNARDI, S. et al. Italian -type salami with propolis as antioxidant. **Italian Journal of Food Science**, v. 25, p. 433–440, 1 jan. 2013b.

BHATIA, M.; ROHILLA, S. Formulation and optimization of quinoa starch nanoparticles: Quality by design approach for solubility enhancement of piroxicam. **Saudi Pharmaceutical Journal**, v. 28, n. 8, p. 927–935, 2020.

BISCAIA, D.; FERREIRA, S. R. S. Propolis extracts obtained by low pressure methods and supercritical fluid extraction. **The Journal of Supercritical Fluids**, v. 51, n. 1, p. 17–23, 1 nov. 2009.

BITTENCOURT, M. L. F. et al. Metabolite profiling, antioxidant and antibacterial activities of Brazilian propolis: Use of correlation and multivariate analyses to identify potential bioactive compounds. **Food Research International**, v. 76, p. 449–457, 1 out. 2015.

BODINI, R. B. et al. Properties of gelatin-based films with added ethanol-propolis extract. **LWT - Food Science and Technology**, v. 51, n. 1, p. 104–110, 1 abr. 2013.

BRAND-WILLIAMS, W.; CUVELIER, M. E.; BERSET, C. Use of a free radical method to evaluate antioxidant activity. **LWT - Food Science and Technology**, v. 28, n. 1, p. 25–30, 1995.

BRASIL. Ministério da Saúde/Agência Nacional de Vigilância Sanitária/Diretoria Colegiada. **Instrução Normativa - IN n° 28, de 26 de julho de 2018**. Estabelece as listas de constituintes, de limites de uso, de alegações e de rotulagem complementar dos suplementos alimentares.. Brasil, 2018. Disponível em: http://antigo.anvisa.gov.br/documents/10181/3898888/%287%29IN_28_2018_COMP.pdf/59fd99ad-1c35-4835-b5a3-abf61d145937. Acesso em: 27 jul. 2023.

BREUNINGER, W. F.; PIYACHOMKWAN, K.; SRIROTH, K. **Tapioca/Cassava Starch: Production and Use**. Third Edit ed. [s.l.] Elsevier Inc., 2009.

BRODKORB, A. et al. INFOGEST static in vitro simulation of gastrointestinal food digestion. **Nature Protocols 2019 14:4**, v. 14, n. 4, p. 991–1014, 18 mar. 2019.

BROWN, R. Hive products: Pollen, propolis and royal jelly. **Bee World**, v. 70, n. 3, p. 109–117, 1989.

BRYAN, J.; REDDEN, P.; TRABA, C. The mechanism of action of Russian propolis ethanol extracts against two antibiotic-resistant biofilm-forming bacteria. **Letters in Applied Microbiology**, v. 62, n. 2, p. 192–198, 1 fev. 2016.

BUSCH, V. M. et al. Propolis encapsulation by spray drying: Characterization and stability. **LWT - Food Science and Technology**, v. 75, p. 227–235, 1 jan. 2017.

CAICEDO CHACON, W. D. et al. The mechanism, biopolymers and active compounds for the production of nanoparticles by anti-solvent precipitation: A review. **Food Research International**, v. 168, p. 112728, 1 jun. 2023b.

CAMPELO, P. H.; SANT'ANA, A. S.; PEDROSA SILVA CLERICI, M. T. Starch nanoparticles: production methods, structure, and properties for food applications. **Current Opinion in Food Science**, v. 33, n. i, p. 136–140, 2020.

CANO-LAMADRID, M. et al. Quality Parameters and Consumer Acceptance of Jelly Candies Based on Pomegranate Juice "Mollar de Elche". **Foods**, v. 9, n. 4, 2020.

CANO, A. et al. Development and characterization of active films based on starch-PVA, containing silver nanoparticles. **Food Packaging and Shelf Life**, v. 10, p. 16–24, 2016.

CAPELLO, C. et al. Adsorption and desorption of eggplant peel anthocyanins on a synthetic layered silicate. **Journal of Food Engineering**, v. 262, p. 162–169, 2019.

CAPPA, C.; LAVELLI, V.; MARIOTTI, M. Fruit candies enriched with grape skin powders: Physicochemical properties. **LWT**, v. 62, n. 1, p. 569–575, 1 jun. 2015.

CÁRDENAS-PÉREZ, S. et al. Evaluation of the ripening stages of apple (Golden Delicious) by means of computer vision system. **Biosystems Engineering**, v. 159, p. 46–58, 1 jul. 2017.

CATCHPOLE, O. et al. Anti-gastrointestinal cancer activity of cyclodextrin-encapsulated propolis. **Journal of Functional Foods**, v. 41, p. 1–8, 1 fev. 2018.

CAUICH-KUMUL, R.; CAMPOS, M. R. S. **Bee Propolis: Properties, Chemical Composition, Applications, and Potential Health Effects**. [s.l.] Elsevier Inc., 2018.

CAVALARO, R. I. et al. In vitro and in vivo antioxidant properties of bioactive compounds from green propolis obtained by ultrasound-assisted extraction. **Food Chemistry: X**, v. 4, p. 100054, 30 dez. 2019.

CHACON, W. D. C. et al. Mathematical Models for Prediction of Water Evaporation and Thermal Degradation Kinetics of Potato Starch Nanoparticles Obtained by Nanoprecipitation. **Starch/Stärke**, v. 1800081, p. 1–7, 2019.

CHACON, W. D. C. et al. Physicochemical Properties of Potato Starch Nanoparticles Produced by Anti-Solvent Precipitation. **Starch/Staerke**, 2020a.

CHACON, W. D. C. et al. Drying and Pyrolysis of Lulo Peel: Non-Isothermal Analysis of Physicochemical, Kinetics, and Master Plots. **Bioenergy Research**, v. 13, n. 3, p. 927–938, 2020b.

CHANDNA, P. et al. Complementary and Alternative Medicine (CAM): A Review of Propolis in Dentistry. **American Journal of Phytomedicine and Clinical Therapeutics**, v. 2, n. 6, p. 670–685, 2014.

CHEN, Y. et al. Structural changes of cassava starch granules hydrolyzed by a mixture of α-amylase and glucoamylase. **Carbohydrate Polymers**, v. 85, n. 1, p. 272–275, 2011.

CHEN, Y. Y. et al. Encapsulation of luteolin using oxidized lotus root starch nanoparticles prepared by anti-solvent precipitation. **Carbohydrate Polymers**, v. 273, n. April, p. 118552, 2021.

CHIN, S. F.; PANG, S. C.; TAY, S. H. Size controlled synthesis of starch nanoparticles by a simple nanoprecipitation method. **Carbohydrate Polymers**, v. 86, n. 4, p. 1817–1819, 2011.

CHIRIFE, J.; MARÍA DEL PILAR, B. Water Activity, Glass Transition and Microbial Stability in Concentrated/Semimoist Food Systems. **Journal of Food Science**, v. 59, n. 5, p. 921–927, 1994.

ÇOBAN, B. et al. Utilization of the barberry extract in the confectionery products. **LWT**, v. 145, p. 111362, 1 jun. 2021.

CONSTANTINO, A. B. T.; GARCIA-ROJAS, E. E. Microencapsulation of beta-carotene by complex coacervation using amaranth carboxymethyl starch and lactoferrin for application in gummy candies. **Food Hydrocolloids**, v. 139, p. 108488, 1 maio 2023.

CORNARA, L. et al. Therapeutic Properties of Bioactive Compounds from Different Honeybee Products. v. 8, n. June, p. 1–20, 2017.

CORTÉS-MORALES, E. A.; MENDEZ-MONTEALVO, G.; VELAZQUEZ, G. Polysaccharide-protein complexes as encapsulation materials: A review. **Advances in Colloid**

and Interface Science, p. 102398, 3 mar. 2021.

CRUCHO, C. I. C.; BARROS, M. T. Polymeric nanoparticles: A study on the preparation variables and characterization methods. **Materials Science and Engineering C**, v. 80, p. 771–784, 2017.

CRUPI, P. et al. Seedless table grape residues as a source of polyphenols: comparison and optimization of non-conventional extraction techniques. **European Food Research and Technology**, v. 244, n. 6, p. 1091–1100, 1 jun. 2018.

CRUZ, A. I. C. et al. A sodium alginate bilayer coating incorporated with green propolis extract as a powerful tool to extend Colossoma macropomum fillet shelf-life. **Food Chemistry**, v. 355, n. March, 2021.

DA CRUZ ALMEIDA, E. T. et al. Chemical and microbiological characterization of tinctures and microcapsules loaded with Brazilian red propolis extract. **Journal of Pharmaceutical Analysis**, v. 7, n. 5, p. 280–287, 1 out. 2017.

DA SILVA, F. C. et al. Assessment of production efficiency, physicochemical properties and storage stability of spray-dried propolis, a natural food additive, using gum Arabic and OSA starch-based carrier systems. **Food and Bioproducts Processing**, v. 91, n. 1, p. 28–36, 2013.

DA SILVA, V. M. et al. Bioactive compounds of the Opuntia monacantha fruit. **Natural Product Research**, v. 8, p. 1–4, 2022.

DAJIC STEVANOVIC, Z. et al. Natural Macromolecules as Carriers for Essential Oils: From Extraction to Biomedical Application. **Frontiers in Bioengineering and Biotechnology**, v. 8, p. 563, 25 jun. 2020.

DALLABONA, I. D. et al. Development of alginate beads with encapsulated jabuticaba peel and propolis extracts to achieve a new natural colorant antioxidant additive. **International Journal of Biological Macromolecules**, v. 163, p. 1421–1432, 2020.

DE MOURA, S. C. S. R. et al. Release of anthocyanins from the hibiscus extract encapsulated by ionic gelation and application of microparticles in jelly candy. **Food Research International**, v. 121, p. 542–552, 1 jul. 2019.

DE OLIVEIRA, N. R. et al. Acetylated Starch-Based Nanoparticles: Synthesis, Characterization, and Studies of Interaction With Antioxidants. **Starch/Staerke**, v. 70, n. 3–4, p. 1–10, 2018.

DELGADO, P.; BAÑÓN, S. Determining the minimum drying time of gummy confections based on their mechanical properties. **CYTA - Journal of Food**, v. 13, n. 3, p. 329–335, 2015.

DEMBOGURSKI, D. S. DE O. DE et al. Brown propolis-metabolomic innovative approach to determine compounds capable of killing Staphylococcus aureus biofilm and Trichomonas vaginalis. **Food Research International**, v. 111, n. February, p. 661–673, 2018.

DESAI, S. K.; MONDAL, D.; BERA, S. First-line anti-tubercutilosis drugs-loaded starch

nanocrystals for combating the threat of M. tuberculosis H37Rv strain. **Carbohydrate Research**, v. 495, n. May, p. 108070, 2020.

DI CAPUA, A. et al. Preparation and characterization of Chilean propolis coprecipitates using Supercritical Assisted Atomization. **Chemical Engineering Research and Design**, v. 136, p. 776–785, 2018.

DO NASCIMENTO, T. G. et al. Polymeric Nanoparticles of Brazilian Red Propolis Extract: Preparation, Characterization, Antioxidant and Leishmanicidal Activity. **Nanoscale Research Letters**, v. 11, n. 1, 2016.

DO NASCIMENTO, T. G. et al. Caseinates loaded with Brazilian red propolis extract: preparation, protein-flavonoids interaction, antioxidant and antibacterial activities. **Journal of Thermal Analysis and Calorimetry**, n. 0123456789, 2021.

DONG, H. et al. Optimization of processing parameters to produce nanoparticles prepared by rapid nanoprecipitation of pea starch. **Food Hydrocolloids**, v. 121, p. 106929, 1 dez. 2021.

ALVES, M. J. et al. Impact of the Acidified Hydroethanolic Solution on the Physicochemical Properties of Starch Nanoparticles Produced By Anti-Solvent Precipitation. **Starch - Stärke**, v. 2100034, p. 2100034, 2021.

DUDONNÉ, S. et al. Comparative study of antioxidant properties and total phenolic content of 30 plant extracts of industrial interest using DPPH, ABTS, FRAP, SOD, and ORAC assays. **Journal of Agricultural and Food Chemistry**, v. 57, n. 5, p. 1768–1774, 11 mar. 2009.

DUFRESNE, A. **Crystalline starch based nanoparticlesCurrent Opinion in Colloid and Interface Science**Elsevier Ltd, , 1 out. 2014.

DULARIA, C. et al. Development of starch nanoparticles based composite films from non-conventional source - Water chestnut (Trapa bispinosa). **International Journal of Biological Macromolecules**, v. 136, p. 1161–1168, 2019.

EBNER, H.; DIENSTBACH, F.; SANDRITTER, W. The Ferric Reducing Ability of Plasma (FRAP) as a Measure of "'Antioxidant Power"': The FRAP Assay. **Analytical Biochemistry**, v. 239, p. 70 – 76, 1996.

EL-GUENDOUZ, S. et al. Anti-acetylcholinesterase, antidiabetic, anti-inflammatory, antityrosinase and antixanthine oxidase activities of Moroccan propolis. **International Journal of Food Science and Technology**, v. 51, n. 8, p. 1762–1773, 2016.

ELBAZ, N. M. et al. Chitosan-based nano-in-microparticle carriers for enhanced oral delivery and anticancer activity of propolis. **International Journal of Biological Macromolecules**, v. 92, p. 254–269, 2016.

ERGUN, R.; LIETHA, R.; HARTEL, R. W. Moisture and Shelf Life in Sugar Confections. **https://doi.org/10.1080/10408390802248833**, v. 50, n. 2, p. 162–192, fev. 2010.

ESCOBAR-PUENTES, A. A. et al. Effect of amylose/amylopectin content and succinylation

on properties of corn starch nanoparticles as encapsulants of anthocyanins. **Carbohydrate Polymers**, v. 250, n. May, 2020.

ESCRICHE, I.; JUAN-BORRÁS, M. Standardizing the analysis of phenolic profile in propolis. **Food Research International**, v. 106, n. November 2017, p. 834–841, 2018.

ETERAF-OSKOUEI, T.; NAJAFI, M. Traditional and modern uses of natural honey in human diseases: A review. **Iranian Journal of Basic Medical Sciences**, v. 16, n. 6, p. 731–742, jun. 2013.

FERNANDES, J. M. et al. Rice in vitro digestion: application of INFOGEST harmonized protocol for glycemic index determination and starch morphological study. **Journal of Food Science and Technology**, v. 57, n. 4, p. 1393, 1 abr. 2020.

FESSI, H. et al. Nanocapsule formation by interfacial polymer deposition following solvent displacement. **International Journal of Pharmaceutics**, v. 55, n. 1, p. 1–4, 1989.

FLOEGEL, A. et al. Comparison of ABTS/DPPH assays to measure antioxidant capacity in popular antioxidant-rich US foods. **Journal of Food Composition and Analysis**, v. 24, n. 7, p. 1043–1048, 2011.

FONSECA, L. M. et al. Development of antimicrobial and antioxidant electrospun soluble potato starch nanofibers loaded with carvacrol. **International Journal of Biological Macromolecules**, v. 139, p. 1182–1190, 2019.

FRANCHIN, M. et al. **The use of Brazilian propolis for discovery and development of novel anti-inflammatory drugsEuropean Journal of Medicinal Chemistry.**Elsevier Masson SAS, , 10 jun. 2018.

FROST, K. et al. Crystallinity and structure of starch using wide angle X-ray scattering. **Carbohydrate Polymers**, v. 78, n. 3, p. 543–548, 2009.

FROZZA, C. O. DA S. et al. Antitumor activity of Brazilian red propolis fractions against Hep-2 cancer cell line. **Biomedicine and Pharmacotherapy**, v. 91, p. 951–963, 1 jul. 2017.

GARCÍA-CASAS, I. et al. Co-precipitation of mangiferin with cellulose acetate phthalate by Supercritical antisolvent process. **Journal of CO2 Utilization**, v. 22, n. July, p. 197–207, 2017.

GARCÍA-GURROLA, A. et al. Succinylated Starch Nanocapsules Loaded with the Polyphenolic Extract from Arugula (Eruca sativa) Leaves: Colloidal, Chemical, and Structural Properties . **Starch - Stärke**, v. 2100059, p. 2100059, 2021.

GARGOURI, W. et al. Evaluation of bioactive compounds and biological activities of Tunisian propolis. **Lwt**, v. 111, n. March, p. 328–336, 2019.

GOMES SÁ, S. H. et al. Evaluation of the release, stability and antioxidant activity of Brazilian red propolis extract encapsulated by spray-drying, spray-chilling and using the combination of both techniques. **Food Research International**, v. 164, n. April 2022, p. 112423, 2023.

GOÑI, I.; GARCIA-ALONSO, A.; SAURA-CALIXTO, F. A starch hydrolysis procedure to estimate glycemic index. **Nutrition Research**, v. 17, n. 3, p. 427–437, 1 mar. 1997.

GRANATO, D. et al. **Chemical perspective and criticism on selected analytical methods used to estimate the total content of phenolic compounds in food matricesTrAC - Trends in Analytical Chemistry**Elsevier B.V., , 1 jun. 2016.

GRECKA, K. et al. The anti-staphylococcal potential of ethanolic Polish propolis extracts. **Molecules**, v. 24, n. 9, p. 1–24, 2019.

GRZEGORZEWSKI, F. et al. Surface morphology and chemical composition of lamb's lettuce (Valerianella locusta) after exposure to a low-pressure oxygen plasma. **Food Chemistry**, v. 122, n. 4, p. 1145–1152, 15 out. 2010.

GUIAR, C. L. L. A. Propolis. p. 2502–2506, 2002.

GUTIÉRREZ, T. J.; VALENCIA, G. A. Reactive extrusion-processed native and phosphated starch-based food packaging films governed by the hierarchical structure. **International Journal of Biological Macromolecules**, v. 172, p. 439–451, 1 mar. 2021.

HAN, H. et al. Insight on the changes of cassava and potato starch granules during gelatinization. **International Journal of Biological Macromolecules**, v. 126, p. 37–43, 2019.

HASPERUÉ, J. H. et al. Use of LED light for Brussels sprouts postharvest conservation. **Scientia Horticulturae**, v. 213, n. 1974, p. 281–286, 2016.

HE, W.; WEI, C. Progress in C-type starches from different plant sources. **Food Hydrocolloids**, v. 73, p. 162–175, 2017.

HEBEISH, A. et al. Ultra-Fine Characteristics of Starch Nanoparticles Prepared Using Native Starch With and Without Surfactant. **Journal of Inorganic and Organometallic Polymers and Materials**, v. 24, n. 3, p. 515–524, 26 nov. 2014.

HEGAZI, A. G.; EL-HOUSSINY, A. S.; FOUAD, E. A. Egyptian propolis 14: Potential antibacterial activity of propolis-encapsulated alginate nanoparticles against different pathogenic bacteria strains. **Advances in Natural Sciences: Nanoscience and Nanotechnology**, v. 10, n. 4, 2019.

HELENO, S. A. et al. **Bioactivity of phenolic acids: Metabolites versus parent compounds: A reviewFood Chemistry**Elsevier Ltd, , 15 abr. 2015.

HUANG, S. et al. Recent Advances in the Chemical Composition of Propolis. **Molecules**, v. 19, n. 12, p. 19610–19632, 26 nov. 2014.

IADNUT, A. et al. In vitro antifungal and antivirulence activities of biologically synthesized ethanolic extract of propolis-loaded PLGA Nanoparticles against Candida albicans. **Evidence-based Complementary and Alternative Medicine**, v. 2019, 2019.

IRIGOITI, Y. et al. **The use of propolis as a functional food ingredient: A reviewTrends in Food Science and Technology.** Elsevier Ltd, , set. 2021.

IRIGOITI, Y.; YAMUL, D. K.; NAVARRO, A. S. Co-crystallized sucrose with propolis extract as a food ingredient: Powder characterization and antioxidant stability. **LWT**, v. 143, p. 111164, 1 maio 2021.

IZZULARAB, B. M.; MEGEED, M.; YEHIA, M. Propolis nanoparticles modulate the inflammatory and apoptotic pathways in carbon tetrachloride-induced liver fibrosis and nephropathy in rats. **Environmental Toxicology**, v. 36, n. 1, p. 55–66, 2020.

JAISON, D.; CHANDRASEKARAN, G.; MOTHILAL, M. pH-sensitive natural almond gum hydrocolloid based magnetic nanocomposites for theragnostic applications. **International Journal of Biological Macromolecules**, v. 154, p. 256–266, 2020.

ALVES, M.; RODRIGUES MONTEIRO, A.; AYALA VALENCIA, G. Antioxidant Nanoparticles Based on Starch and the Phenolic Compounds from Propolis Extract: Production and Physicochemical Properties. **Starch - Stärke**, v. 74, n. 7–8, p. 2100289, 1 jul. 2022.

JANSEN-ALVES, C. et al. Microencapsulation of Propolis in Protein Matrix Using Spray Drying for Application in Food Systems. **Food and Bioprocess Technology**, v. 11, n. 7, p. 1422–1436, 1 jul. 2018.

JANSEN-ALVES, C. et al. Propolis microparticles produced with pea protein: Characterization and evaluation of antioxidant and antimicrobial activities. **Food Hydrocolloids**, v. 87, n. September 2018, p. 703–711, 2019.

JIA, Z.; DUMONT, M. J.; ORSAT, V. **Encapsulation of phenolic compounds present in plants using protein matricesFood Bioscience**Elsevier Ltd, , 1 set. 2016.

JIANG, F. et al. Preparation and characterization of quinoa starch nanoparticles as quercetin carriers. **Food Chemistry**, v. 369, p. 130895, 1 fev. 2022.

JOYE, I. J.; MCCLEMENTS, D. J. Production of nanoparticles by anti-solvent precipitation for use in food systems. **Trends in Food Science and Technology**, v. 34, n. 2, p. 109–123, 2013.

KARLSSON, M. E.; ELIASSON, A. C. Gelatinization and retrogradation of potato (Solanum tuberosum) starch in situ as assessed by differential scanning calorimetry (DSC). **LWT - Food Science and Technology**, v. 36, n. 8, p. 735–741, 2003.

KATIYAR, D. Propolis: A natural biomaterial. **Materials Today: Proceedings**, 2 jun. 2023.
KIM, D. H. et al. Development of propolis extract-loaded nanoparticles with chitosan and hyaluronic acid for improving solubility and stability. **Lwt**, v. 181, n. March, p. 114738, 2023.

KIM, D. O. et al. Vitamin C equivalent antioxidant capacity (VCEAC) of phenolic phytochemicals. **Journal of Agricultural and Food Chemistry**, v. 50, n. 13, p. 3713–3717, 19 jun. 2002.

KIM, J. Y.; PARK, D. J.; LIM, S. T. Fragmentation of Waxy Rice Starch Granules by Enzymatic Hydrolysis. **Cereal Chemistry**, v. 85, n. 2, p. 182–187, 1 mar. 2008.

KIM, Y. H.; CHUNG, H. J. The effects of Korean propolis against foodborne pathogens and transmission electron microscopic examination. **New Biotechnology**, v. 28, n. 6, p. 713–718, 1 out. 2011.

KOU, Z. et al. Preparation, characterization, and performance analysis of starch-based nanomicelles. **International Journal of Biological Macromolecules**, v. 145, p. 655–662, 2020.

KOWACZ, M.; POLLACK, G. H. Propolis-induced exclusion of colloids: Possible new mechanism of biological action. **Colloids and Interface Science Communications**, v. 38, p. 100307, 1 set. 2020.

KUROPATNICKI, A. K.; SZLISZKA, E.; KROL, W. Historical aspects of propolis research in modern times. **Evidence-based Complementary and Alternative Medicine**, v. 2013, 2013.
LECORRE, D. et al. Enzymatic pretreatment for preparing starch nanocrystals. **Biomacromolecules**, v. 13, n. 1, p. 132–137, 2012.

LECORRE, D.; BRAS, J.; DUFRESNE, A. Influence of native starch's properties on starch nanocrystals thermal properties. **Carbohydrate Polymers**, v. 87, p. 658–666, 2012.

LEE, D. H. et al. Structural and physicochemical properties of composites between starch nanoparticles and β-carotene prepared via nanoprecipitation. **International Journal of Biological Macromolecules**, v. 214, p. 100–110, 1 ago. 2022.

LIMA, K. T. DOS SANTOS et al. Physicochemical Properties of Modified Starches Obtained by Anti-Solvent Precipitation Containing Anthocyanins from Jambolan (Syzygium cumini) Fruit. **Starch/Staerke**, v. 2000221, p. 1–10, 2021.

LIN, X. et al. Structural and physicochemical properties of lotus seed starch nanoparticles. **International Journal of Biological Macromolecules**, v. 157, p. 240–246, 15 ago. 2020.

LIU, C. et al. Properties of curcumin-loaded zein-tea saponin nanoparticles prepared by antisolvent co-precipitation and precipitation. **Food Chemistry**, v. 391, n. January, p. 133224, 2022.

LIU, G. et al. Electrospun starch nanofibers: Recent advances, challenges, and strategies for potential pharmaceutical applicationsJournal of Controlled Release**. Elsevier B.V**., , 28 abr. 2017.

LIU, Q. et al. Preparation of debranched starch nanoparticles by ionic gelation for encapsulation of epigallocatechin gallate. **International Journal of Biological Macromolecules**, v. 161, p. 481–491, 2020.

LIU, Y. et al. Gelatinization behavior of starch: Reflecting beyond the endotherm measured by differential scanning calorimetry. **Food Chemistry**, v. 284, p. 53–59, 30 jun. 2019.

LÓPEZ-CÓRDOBA, A. et al. Yerba mate antioxidant powders obtained by co-crystallization: Stability during storage. **Journal of Food Engineering**, v. 124, p. 158–165, 1 mar. 2014.

LOURDIN, D. et al. Crystalline Structure in Starch. In: NAKAMURA, Y. (Ed.). . **Starch: Metabolism and Structure**. 1. ed. [s.l.] Springer, 2015. p. 61–90.

LUCIANO, C. G. et al. Evaluation of extraction method on the structure and physicochemical properties of starch from seeds of two jackfruit varieties. **Starch/Stärke**, v. 1700078, p. 1–10, 2017.

LUIZA KOOP, B. et al. Flavonoids, anthocyanins, betalains, curcumin, and carotenoids: sources, classification and enhanced stabilization by encapsulation and adsorption. **Food Research International**, v. 153, n. January, p. 110929, 2022.

MACHADO, G. T. P. et al. Development of propolis nanoparticles for the treatment of bovine mastitis: In vitro studies on antimicrobial and cytotoxic activities. **Canadian Journal of Animal Science**, v. 99, n. 4, p. 713–723, 2019.

MAHDAVI-ROSHAN, M.; GHEIBI, S.; POURFARZAD, A. Effect of propolis extract as a natural preservative on quality and shelf life of marinated chicken breast (chicken Kebab). **LWT**, v. 155, p. 112942, 1 fev. 2022.

MARC, F. et al. **Studies of several analytical methods for antioxidant potential evaluation in foodMedecine/Sciences**Elsevier Masson SAS, , 2004. Disponível em: <https://pubmed.ncbi.nlm.nih.gov/15124120/>. Acesso em: 24 maio. 2021

MARCUCCI, M. C. Propolis: chemical composition, biological properties and therapeutic activity. **Apidologie**, v. 26, n. 2, p. 83–99, 1995.

MARTÍNEZ RIVAS, C. J. et al. **Nanoprecipitation process: From encapsulation to drug deliveryInternational Journal of Pharmaceutics**Elsevier B.V., , 30 out. 2017.

MARTINOTTI, S.; RANZATO, E. Propolis: a new frontier for wound healing? **Burns & Trauma**, v. 3, p. 1–7, 2015.

MAŠEK, T. et al. Chemical composition, antioxidant and antibacterial activity of different extracts of poplar type propolis. **Croatica Chemica Acta**, v. 91, n. 1, p. 81–88, 2018.

MELLO, B. C. B. S.; HUBINGER, M. D. Antioxidant activity and polyphenol contents in Brazilian green propolis extracts prepared with the use of ethanol and water as solvents in different pH values. **International Journal of Food Science and Technology**, v. 47, n. 12, p. 2510–2518, 2012.

MELLO, B. C. B. S.; PETRUS, J. C. C.; HUBINGER, M. D. Concentration of flavonoids and phenolic compounds in aqueous and ethanolic propolis extracts through nanofiltration. **Journal of Food Engineering**, v. 96, n. 4, p. 533–539, 2010.

MERZ, B. et al. A novel colorimetric indicator film based on chitosan, polyvinyl alcohol and anthocyanins from jambolan (Syzygium cumini) fruit for monitoring shrimp freshness.

International Journal of Biological Macromolecules, v. 153, p. 625–632, 2020.

MINEKUS, M. et al. A standardised static in vitro digestion method suitable for food – an international consensus. **Food Funct.**, v. 5, n. 6, p. 1113–1124, 2014.

MOGHADDAS KIA, E. et al. Red beet extract usage in gelatin/gellan based gummy candy formulation introducing Salix aegyptiaca distillate as a flavouring agent. **Journal of Food Science and Technology**, v. 57, n. 9, p. 3355–3362, 1 set. 2020.

MONROY, Y. M. et al. Brazilian green propolis extracts obtained by conventional processes and by processes at high pressure with supercritical carbon dioxide, ethanol and water. **Journal of Supercritical Fluids**, v. 130, n. August, p. 189–197, 2017.

MOON, J. K.; SHIBAMOTO, T. Antioxidant assays for plant and food components. **Journal of Agricultural and Food Chemistry**, v. 57, n. 5, p. 1655–1666, 11 mar. 2009.

MÜLLER, R. H.; JACOBS, C. Buparvaquone mucoadhesive nanosuspension: preparation, optimisation and long-term stability. **International Journal of Pharmaceutics**, v. 237, n. 1–2, p. 151–161, 26 abr. 2002.

MUTLU, C.; TONTUL, S. A.; ERBAŞ, M. Production of a minimally processed jelly candy for children using honey instead of sugar. **LWT**, v. 93, p. 499–505, 2018.

NARA, B. S.; KOMIYA, T. Studies on the Relationship Between Water-satured State and Crystallinity by the Diffraction Method for Moistened Potato Starch. **Starch/Stärke**, v. 35, p. 407–410, 1983.

NAYAK, B.; DE J. BERRIOS, J.; TANG, J. Impact of food processing on the glycemic index (GI) of potato products. **Food Research International**, v. 56, p. 35–46, 1 fev. 2014.

NODA, T. The preparation and food applications of divalent cation–substituted potato starch. **Journal of Biorheology**, v. 35, n. 1, p. 2–9, 2021.

NORI, M. P. et al. Microencapsulation of propolis extract by complex coacervation. **LWT - Food Science and Technology**, v. 44, n. 2, p. 429–435, 1 mar. 2011.

OBADI, M.; XU, B. Review on the physicochemical properties, modifications, and applications of starches and its common modified forms used in noodle productsFood Hydrocolloids. **Elsevier B.V**., , 1 mar. 2021.

OLEGÁRIO, L. S. et al. Chemical characterization of four Brazilian brown propolis: An insight in tracking of its geographical location of production and quality control. **Food Research International**, v. 123, p. 481–502, 1 set. 2019.

ONBAS, R. et al. Cytotoxic and Nitric Oxide Inhibition Activities of Propolis Extract along with Microencapsulation by Complex Coacervation. **Plant Foods for Human Nutrition**, v. 71, n. 3, p. 286–293, 2016.

ONG, T. H. et al. Chitosan-propolis nanoparticle formulation demonstrates anti-bacterial activity against Enterococcus faecalis biofilms. **PLOS ONE**, v. 12, n. 3, p. e0174888, 31 mar. 2017.

OROIAN, M.; URSACHI, F.; DRANCA, F. Influence of ultrasonic amplitude, temperature, time and solvent concentration on bioactive compounds extraction from propolis. **Ultrasonics Sonochemistry**, v. 64, n. November 2019, p. 105021, 2020.

OTÁLORA, M. C. et al. Encapsulated betalains (Opuntia ficus-indica) as natural colorants. Case study: Gummy candies. **LWT**, v. 103, p. 222–227, 1 abr. 2019.

PANDEY, R. P. et al. **Microbial production of natural and non-natural flavonoids: Pathway engineering, directed evolution and systems/synthetic biologyBiotechnology Advances**Elsevier Inc., , 1 set. 2016.

PANT, K. et al. Encapsulated bee propolis powder: Drying process optimization and physicochemical characterization. **Lwt**, v. 155, p. 112956, 2022.

PARK, S. J. et al. Development of nanostructured lipid carriers for the encapsulation and controlled release of vitamin D3. **Food Chemistry**, v. 225, p. 213–219, 15 jun. 2017.

PARKER, R.; RING, S. G. **Aspects of the physical chemistry of starchJournal of Cereal Science**Academic Press, , 1 jul. 2001.

PASUPULETI, V. R. et al. Honey, Propolis, and Royal Jelly: A Comprehensive Review of Their Biological Actions and Health Benefits. **Oxidative Medicine and Cellular Longevity**, v. 2017, 2017.

PATEL, J. et al. Potentiating antimicrobial efficacy of propolis through niosomal-based system for administration. **Integrative Medicine Research**, v. 4, n. 2, p. 94–101, 2015.

PEDONESE, F. et al. Effect of an Italian propolis on the growth of Listeria monocytogenes, staphylococcus aureus and bacillus cereus in milk and whey cheese. **Italian Journal of Food Safety**, v. 8, n. 4, p. 218–222, 2019.

PEI, K. et al. p-Coumaric acid and its conjugates: Dietary sources, pharmacokinetic properties and biological activities. **Journal of the Science of Food and Agriculture**, v. 96, n. 9, p. 2952–2962, 2016.

PEIXOTO, M. et al. Antioxidant and antimicrobial activity of blends of propolis samples collected in different years. **LWT**, v. 145, p. 111311, 1 jun. 2021.

PÉREZ-MASIÁ, R. et al. Encapsulation of folic acid in food hydrocolloids through nanospray drying and electrospraying for nutraceutical applications. **Food Chemistry**, v. 168, p. 124–133, 1 fev. 2015.

PÉREZ-VERGARA, L. D. et al. Development and characterization of edible films based on native cassava starch, beeswax, and propolis. **NFS Journal**, v. 21, p. 39–49, 1 nov. 2020.

PÉREZ, S.; BALDWIN, P. M.; GALLANT, D. J. Structural Features of Starch Granules I. In: **Starch**. [s.l.] Elsevier Inc., 2009. p. 149–192.

PERICHE, A. et al. Optical, mechanical and sensory properties of based-isomaltulose gummy confections. **Food Bioscience**, v. 7, p. 37–44, 1 set. 2014.

PERNIN, A.; GUILLIER, L.; DUBOIS-BRISSONNET, F. Inhibitory activity of phenolic acids against Listeria monocytogenes: Deciphering the mechanisms of action using three different models. **Food Microbiology**, v. 80, p. 18–24, 1 jun. 2019.

PETER, C. M. et al. Chemical and cytotoxic analyses of three varieties of Brazilian propolis (green propolis, jataí propolis and brown propolis) and its anti-Sporothrix brasiliensis in vitro activity. **Arquivo Brasileiro de Medicina Veterinaria e Zootecnia**, v. 71, n. 3, p. 819–827, 1 maio 2019.

PICCINELLI, A. L. et al. Cuban and Brazilian Red Propolis: Botanical Origin and Comparative Analysis by High-Performance Liquid Chromatography–Photodiode Array Detection/Electrospray Ionization Tandem Mass Spectrometry. **Journal of Agricultural and Food Chemistry**, v. 59, n. 12, p. 6484–6491, 22 jun. 2011.

PIEDRAHÍTA MÁRQUEZ, D. G.; FUENMAYOR, C. A.; SUAREZ MAHECHA, H. Effect of chitosan-propolis edible coatings on stability of refrigerated cachama (Piaractus brachypomus) vacuum-packed fish fillets. **Packaging Technology and Science**, v. 32, n. 3, p. 143–153, 1 mar. 2019.

PIETTA, P. G.; GARDANA, C.; PIETTA, A. M. Analytical methods for quality control of propolis. **Fitoterapia**, v. 73, n. SUPPL. 1, 2002.

PINTO, V. Z. et al. Physicochemical, crystallinity, pasting and thermal properties of heat-moisture-treated pinhão starch. **Starch/Staerke**, v. 64, n. 11, p. 855–863, 2012.

POBIEGA, K. et al. Growth biocontrol of foodborne pathogens and spoilage microorganisms of food by Polish propolis extracts. **Molecules**, v. 24, n. 16, 2019.

POPOVA, M. et al. Nanostructured silver silica materials as potential propolis carriers. **Microporous and Mesoporous Materials**, v. 263, n. November 2017, p. 28–33, 2018.

PRZYBYŁEK, I.; KARPIŃSKI, T. M. Antibacterial Properties of Propolis. **Molecules 2019, Vol. 24, Page 2047**, v. 24, n. 11, p. 2047, 29 maio 2019.

QIN, Y. et al. Characterization of starch nanoparticles prepared by nanoprecipitation: Influence of amylose content and starch type. **Industrial Crops and Products**, v. 87, p. 182–190, 2016.

QIU, C. et al. Novel Approach with Controlled Nucleation and Growth for Green Synthesis of Size-Controlled Cyclodextrin-Based Metal–Organic Frameworks Based on Short-Chain Starch Nanoparticles. **Journal of Agricultural and Food Chemistry**, v. 66, n. 37, p. 9785–9793, 19 set. 2018.

QIU, C. et al. A review of green techniques for the synthesis of size-controlled starch-based nanoparticles and their applications as nanodelivery systems. **Trends in Food Science & Technology**, v. 92, p. 138–151, 1 out. 2019.

QIU, C. et al. Advances in research on preparation, characterization, interaction with proteins, digestion and delivery systems of starch-based nanoparticles. **International Journal of Biological Macromolecules**, v. 152, p. 117–125, 2020.

QUIROZ, J. Q. et al. Use of plant proteins as microencapsulating agents of bioactive compounds extracted from annatto seeds (Bixa orellana L.). **Antioxidants**, v. 9, n. 4, 1 abr. 2020.

RE, R. et al. Antioxidant activity applying an improved ABTS radical cation decolorization assay. **Free Radical Biology and Medicine**, v. 26, n. 9–10, p. 1231–1237, 1 maio 1999.

REIS, A. S. DOS et al. Physico-chemical characteristics of microencapsulated propolis co-product extract and its effect on storage stability of burger meat during storage at −15 °C. **LWT - Food Science and Technology**, v. 76, p. 306–313, 1 mar. 2017.

REMANAN, M. K.; ZHU, F. Encapsulation of rutin using quinoa and maize starch nanoparticles. **Food Chemistry**, n. November 2019, p. 128534, 2020.

REYES, L. M.; LANDGRAF, M.; SOBRAL, P. J. A. Gelatin-based films activated with red propolis ethanolic extract and essential oils. **Food Packaging and Shelf Life**, v. 27, n. June 2020, p. 100607, 2021.

RIEDEL, R.; BÖHME, B.; ROHM, H. Development of formulations for reduced-sugar and sugar-free agar-based fruit jellies. **International Journal of Food Science & Technology**, v. 50, n. 6, p. 1338–1344, 1 jun. 2015.

RIMBACH, G. et al. Anti-Inflammatory Properties of Brazilian Green Propolis Encapsulated in a γ-Cyclodextrin Complex in Mice Fed a Western-Type Diet. **International Journal of Molecular Sciences**, v. 18, n. 6, p. 1141, 26 maio 2017.

RIVERO, R. et al. Development and characterization of two gelatin candies with alternative sweeteners and fruit bioactive compounds. **LWT**, v. 141, p. 110894, 1 abr. 2021.

ROVALINO-CÓRDOVA, A. M.; FOGLIANO, V.; CAPUANO, E. A closer look to cell structural barriers affecting starch digestibility in beans. **Carbohydrate Polymers**, v. 181, p. 994–1002, 1 fev. 2018.

SÁ, A. G. A.; CARMO, L. M.; VALENCIA, G. A. The influence of clean food labels on consumers ' perception. **Packaging Technology and Science**, n. December 2022, p. 1–10, 2023.

SADEGHI, R. et al. Effects of starch composition and type of non-solvent on the formation of starch nanoparticles and improvement of curcumin stability in aqueous media. **Journal of Cereal Science**, v. 76, p. 122–130, 1 jul. 2017.

SALEHI, A. et al. Almond gum-sodium caseinate complexes for loading propolis extract: Characterization, antibacterial activity, release, and in-vitro cytotoxicity. **Food Chemistry**, v. 405, n. PA, p. 134801, 2023a.

SALEHI, A. et al. Almond gum-sodium caseinate complexes for loading propolis extract: Characterization, antibacterial activity, release, and in-vitro cytotoxicity. **Food Chemistry**, v. 405, p. 134801, 30 mar. 2023b.

SALIM, A. et al. Antimicrobial and antibiofilm activities of pomegranate peel phenolic compounds: Varietal screening through a multivariate approach. **Journal of Bioresources and Bioproducts**, 14 jan. 2023.

SANT'ANNA, A. C. et al. The influence of packaging colour on consumer expectations of coffee using free word association. **Packaging Technology and Science**, n. December 2021, p. 629–639, 2022.

SANTOS, M. S. et al. Propolis as natural additive: A systematic review. **African Journal of Biotechnology**, v. 17, n. 41, p. 1282–1291, 2018.

SANTOYO-ALEMAN, D.; SANCHEZ, L. T.; VILLA, C. C. Citric-acid modified banana starch nanoparticles as a novel vehicle for β-carotene delivery. **Journal of the Science of Food and Agriculture**, v. 99, n. 14, p. 6392–6399, 2019.

SARABANDI, K.; MAHOONAK, A. S.; AKBARI, M. Physicochemical properties and antioxidant stability of microencapsulated marjoram extract prepared by co-crystallization method. **Journal of Food Process Engineering**, v. 42, n. 1, p. 1–11, 2019.

SATO, T. et al. Chitosan-based coacervate polymers for propolis encapsulation: Release and cytotoxicity studies. **International Journal of Molecular Sciences**, v. 21, n. 12, p. 1–15, 2020.

SEIBERT, J. B. et al. Development of propolis nanoemulsion with antioxidant and antimicrobial activity for use as a potential natural preservative. **Food Chemistry**, v. 287, p. 61–67, 30 jul. 2019.

SELEEM, D.; PARDI, V.; MURATA, R. M. **Review of flavonoids: A diverse group of natural compounds with anti-Candida albicans activity in vitroArchives of Oral Biology**Elsevier Ltd, , 1 abr. 2017.

ŠEREMET, D. et al. Challenges in confectionery industry: Development and storage stability of innovative white tea-based candies. **Journal of Food Science**, v. 85, n. 7, p. 2060–2068, 1 jul. 2020.

SFORCIN, J. M. Biological Properties and Therapeutic Applications of Propolis. **Phytotherapy Research**, v. 30, n. 6, p. 894–905, 2016.

SHARAF, S.; EL-NAGGAR, M. E. Eco-friendly technology for preparation, characterization and promotion of honey bee propolis extract loaded cellulose acetate nanofibers in medical domains. **Cellulose**, v. 25, n. 9, p. 5195–5204, 2018.

SHEHATA, M. G. et al. Chemical analysis, antioxidant, cytotoxic and antimicrobial properties of propolis from different geographic regions. **Annals of Agricultural Sciences**, v. 65, n. 2, p. 209–217, 1 dez. 2020.

SHI, L. et al. Starch-menthol inclusion complex: Structure and release kinetics. **Food Hydrocolloids**, v. 97, p. 105183, 1 dez. 2019.

SHISHIR, M. R. I. et al. Advances in micro and nano-encapsulation of bioactive compounds using biopolymer and lipid-based transportersTrends in Food Science and Technology. **Elsevier Ltd**, , 1 ago. 2018.

SILVA, M. P. et al. Production and characterization of solid lipid microparticles loaded with guaraná (Paullinia cupana) seed extract. **Food Research International**, v. 123, p. 144–152, 1 set. 2019.

SINGH, M.; LARA, S.; TLALI, S. Effects of size and shape on the specific heat, melting entropy and enthalpy of nanomaterials. **Journal of Taibah University for Science**, v. 11, n. 6, p. 922–929, nov. 2017.

SINGH, N. et al. **Morphological, thermal and rheological properties of starches from different botanical sourcesFood Chemistry**Elsevier, , 1 maio 2003.

SINGLETON, V. L.; ORTHOFER, R.; LAMUELA-RAVENTÓS, R. M. Analysis of total phenols and other oxidation substrates and antioxidants by means of folin-ciocalteu reagent. **Methods in Enzymology**, v. 299, p. 152–178, 1 jan. 1999.

SINTOV, A. C. AmyloLipid Nanovesicles: A self-assembled lipid-modified starch hybrid system constructed for direct nose-to-brain delivery of curcumin. **International Journal of Pharmaceutics**, v. 588, n. July, p. 119725, 2020.

SOLEIMANIFARD, M.; FEIZY, J.; MAESTRELLI, F. Nanoencapsulation of propolis extract by sodium caseinate-maltodextrin complexes. **Food and Bioproducts Processing**, v. 128, p. 177–185, 1 jul. 2021.

SPANIDI, E. et al. A New Controlled Release System for Propolis Polyphenols and Its Biochemical Activity for Skin Applications. **Plants 2021, Vol. 10, Page 420**, v. 10, n. 2, p. 420, 23 fev. 2021.

SPINELLI, S. et al. Microencapsulated Propolis to Enhance the Antioxidant Properties of Fresh Fish Burgers. **Journal of Food Process Engineering**, v. 38, n. 6, p. 527–535, 1 dez. 2015.

STEENEKEN, P. A. M.; WOORTMAN, A. J. J. Identification of the thermal transitions in potato starch at a low water content as studied by preparative DSC. **Carbohydrate Polymers**, v. 77, n. 2, p. 288–292, 10 jun. 2009.

ŠTURM, L. et al. Encapsulation of non-dewaxed propolis by freeze-drying and spray-drying using gum Arabic, maltodextrin and inulin as coating materials. **Food and Bioproducts Processing**, v. 116, p. 196–211, 1 jul. 2019.

SUN, Q. **Starch Nanoparticles**. [s.l.] Elsevier Ltd, 2018a.

SUN, Q. Starch Nanoparticles. In: **Starch in Food: Structure, Function and Applications: Second Edition**. [s.l.] Elsevier Inc., 2018b. p. 691–745.

TAVARES, J. A. O. et al. The effectiveness of propolis extract in reducing dentin hypersensitivity – A systematic review. **Archives of Oral Biology**, v. 131, n. August, p. 105248, 2021.

TEODORO, A. P. et al. Cassava starch films containing acetylated starch nanoparticles as reinforcement: Physical and mechanical characterization. **Carbohydrate Polymers**, v. 126, p. 9–16, 1 ago. 2015.

TIVERON, A. P. et al. Chemical Characterization and Antioxidant, Antimicrobial, and Anti-Inflammatory Activities of South Brazilian Organic Propolis. **PLOS ONE**, v. 11, n. 11, p. e0165588, 1 nov. 2016.

TORETI, V. C. et al. Recent progress of propolis for its biological and chemical compositions and its botanical origin. **Evidence-based Complementary and Alternative Medicine**, v. 2013, 2013.

VALENCIA, G. A. et al. Physicochemical Properties of Maranta (Maranta arundinacea L.) Starch. **International Journal of Food Properties**, v. 18, n. 9, p. 1990–2001, 2015a.

VALENCIA, G. A. et al. Physicochemical, morphological, and functional properties of flour and starch from peach palm (*Bactris gasipaes* K.) fruit. **Starch - Stärke**, v. 67, n. 1–2, p. 163–173, 1 jan. 2015b.

VALENCIA, G. A. et al. Physical and morphological properties of nanocomposite films based on gelatin and Laponite. **Applied Clay Science**, v. 124–125, p. 260–266, 2016.

VALENCIA, G. A. et al. Self-Assembled Carbohydrate Polymers for Food Applications: A Review. **Comprehensive Reviews in Food Science and Food Safety**, v. 18, n. 6, p. 2009–2024, 2019.

VALENCIA, G. A.; DJABOUROV, M.; DO AMARAL SOBRAL, P. J. Water desorption of cassava starch granules: A study based on thermogravimetric analysis of aqueous suspensions and humid powders. **Carbohydrate Polymers**, v. 147, p. 533–541, 20 ago. 2016.

VALENCIA, G. A.; HENAO, A. C. A.; ZAPATA, R. A. V. Comparative study and characterization of starches isolated from unconventional tuber sources. **Journal of Polymer Engineering**, v. 32, p. 531–537, 2012.

VAMADEVAN, V.; BERTOFT, E. Observations on the impact of amylopectin and amylose structure on the swelling of starch granules. **Food Hydrocolloids**, v. 103, p. 105663, 1 jun. 2020.

VASILAKI, A. et al. A natural approach in food preservation: Propolis extract as sorbate

alternative in non-carbonated beverage. **Food Chemistry**, v. 298, p. 125080, 15 nov. 2019.

VERGARA, L. P. et al. Stability of bioactive compounds in conventional and low-calorie sweet chewable candies prepared with red and yellow strawberry guava pulps. **International Food Research Journal**, v. 27, n. 4, p. 625–634, 2020.

WAGH, V. D. Propolis: A wonder bees product and its pharmacological potentials. **Advances in Pharmacological Sciences**, v. 2013, 2013.

WALLER, S. B. et al. Chemical and cytotoxic analyses of brown Brazilian propolis (Apis mellifera) and its in vitro activity against itraconazole-resistant Sporothrix brasiliensis. **Microbial Pathogenesis**, v. 105, p. 117–121, 1 abr. 2017.

WANG, R.; ZHOU, J. Waxy maize starch nanoparticles incorporated tea polyphenols to stabilize Pickering emulsion and inhibit oil oxidation. **Carbohydrate Polymers**, v. 296, n. April, p. 119991, 2022.

WANG, T. YANG; LI, Q.; BI, K. SHUN. **Bioactive flavonoids in medicinal plants: Structure, activity and biological fateAsian Journal of Pharmaceutical Sciences**Shenyang Pharmaceutical University, , 1 jan. 2018.

WATANABE, M. A. E. et al. Cytotoxic constituents of propolis inducing anticancer effects: a review. **Journal of Pharmacy and Pharmacology**, v. 63, n. 11, p. 1378–1386, 12 out. 2011.

WOŹNIAK, M. et al. Phenolic profile and antioxidant activity of propolis extracts from Poland. **Natural Product Communications**, v. 14, n. 5, p. 1–7, 2019.

WU, W.; WANG, L.; WANG, S. Amorphous silibinin nanoparticles loaded into porous starch to enhance remarkably its solubility and bioavailability in vivo. **Colloids and Surfaces B: Biointerfaces**, n. November, p. 111474, 2020.

WU, X. et al. Effects of non-solvent and starch solution on formation of starch nanoparticles by nanoprecipitation. **Starch - Stärke**, v. 68, n. 3–4, p. 258–263, 1 abr. 2016.

XAVIER, J. A. et al. Polyphenol profile by uhplc-ms/ms, anti-glycation, antioxidant and cytotoxic activities of several samples of propolis from the northeastern semi-arid region of brazil. **Pharmaceutical Biology**, v. 55, n. 1, p. 1884–1893, 2017.

YAN, B. et al. Improvement of vitamin C stability in vitamin gummies by encapsulation in casein gel. **Food Hydrocolloids**, v. 113, p. 106414, 1 abr. 2021.

YAN, X. et al. Influence of Precipitation Conditions on Crystallinity of Amylose Nanoparticles. **Starch**, v. 70, n. 7–8, p. 1–6, 2018.

YAN, Z. et al. Antioxidant mechanism of tea polyphenols and its impact on health benefits. **Animal Nutrition**, v. 6, n. 2, p. 115–123, 2020.

YEO, J. D.; SHAHIDI, F. **Effect of hydrothermal processing on changes of insoluble-bound phenolics of lentilsJournal of Functional Foods**Elsevier Ltd, , 1 nov. 2017.

YONG, H. et al. Synthesis, characterization, antioxidant and antimicrobial activities of starch aldehyde-quercetin conjugate. **International Journal of Biological Macromolecules**, v. 156, p. 462–470, 1 ago. 2020.

YU, X. et al. Morphological and physicochemical properties of bulb and bulbil starches from *Lilium lancifolium*. **Starch - Stärke**, v. 67, n. 5–6, p. 448–458, maio 2015.

ZHANG, H. et al. Enhanced antioxidant activity and in vitro release of propolis by acid-induced aggregation using heat-denatured zein and carboxymethyl chitosan. **Food Hydrocolloids**, v. 81, p. 104–112, 2018.

ZHANG, X. et al. Review controlling Listeria monocytogenes in ready-to-eat meat and poultry products: An overview of outbreaks, current legislations, challenges, and future prospects. **Trends in Food Science & Technology**, v. 116, p. 24–35, 1 out. 2021.

ZHU, F. Interactions between starch and phenolic compound. **Trends in Food Science & Technology**, v. 43, n. 2, p. 129–143, 1 jun. 2015.

ZOBEL, H. F. Starch Crystal Transformations and Their Industrial Importance. **Starch - Stärke**, v. 40, n. 1, p. 1–7, 1988.

ZULHENDRI, F. et al. The use of propolis in dentistry, oral health, and medicine: A review. **Journal of Oral Biosciences**, v. 63, n. 1, p. 23–34, 2021.